

DEVELOPING A CONTROL SYSTEM FOR IMPROVING SELECTIVE POLYMER LASER SINTERING BUILD SPEED AND PART INTEGRITY

JOSEPH TAYLOR - AUGUST 2019

A THESIS SUBMITTED IN ACCORDANCE WITH THE REQUIREMENTS OF LANCASTER
UNIVERSITY'S ENGINEERING DEPARTMENT FOR THE DEGREE OF MSc ENGINEERING
(BY RESEARCH)

I NOMENCLATURE

AM – Additive manufacturing

ASCII – American Standard Code for Information Interchange

CPU – Central Processing Unit

CSV – Comma Separated Variable

HMI – Human Machine Interface

IR – Infrared

LHS – Left Hand Side

LED – Light Emitting Diode

LS – Laser Sintering

PA-12 – Polyamide 12 [Also known as Nylon12]

PC – Personal Computer

PID – Proportional, Integral, Derivative

PLC – Programmable Logic Controller

RHS – Right Hand Side

RPM – Revolutions per Minute

RS232 – Recommended Standard 232

SCR – Silicon Controller Rectifier

SLS – Selective Laser Sintering

SPLS – Selective Polymer Laser Sintering

TRIAC – Triode for Alternating Current

II ABSTRACT

Designing electronic control systems specific to additive manufacturing machines is a fast evolving practice, developments in which spur continual performance improvements, which in turn improve the quality and economic viability of parts produced (Hu & Kovacevic, 2003).

Research methods used for this work comprise of; taking receipt of externally designed and built experimental rigs, recording performance data and making incremental changes in attempts to improve performance. Focus is given to the automation and speed of the processes and research is limited only by the availability of time and funding.

This work has investigated several potential significant improvements to SLS cycle times and part quality, with the wider project continuing beyond the scope of this dissertation.

Experimentation with serial data transmission protocols using ASCII (American Standard Code for Information Interchange) found it could provide a fast, robust link between central control system elements, which is critical and can be achieved this way without great monetary cost.

Distribution of temperature across the build area surface can be optimised with a single control feedback loop to a level acceptable for the use of PA-12 (Polyamide 12) powder, though methods that are more complex may yield better results.

Rapid deoxygenation of the build chamber at the beginning of each build cycle offers a slight improvement in cycle time, and proper loop feedback can assist in mitigating safety concerns.

Current, commercially available stepper motor control systems are capable of greater accuracy than is necessary in such applications but are limited by the accuracy of their mechanical linkage, which can introduce significant backlash into the system.

Powder can be loaded into the machine using augers fed from an external hopper in such a way as to minimise powder waste through uneven feeding.

Separating power systems allows individual control of sections of the machine, improving safety, monitoring possibilities and potential for recovering failed builds.

A removable build platform, comprising the build piston and associated hardware on a movable trolley frame, significantly reduces the machine cycle time by allowing part removal and cleaning to be performed concurrently with the start of the next build.

Visibility of the process status via beacon stacks allows for quick human interaction where required, potentially reducing failure rates and improving cycle times.

III CONTENTS

I	Nomenclature.....	I
II	Abstract	III
III	Contents	V
IV	List of Figures.....	X
V	List of Tables	XIV
VI	Acknowledgements	XVI
VII	Declaration	XVII
1	Introduction.....	1
1.1	Background.....	1
1.2	Research Focus	2
1.3	Research Value	4
1.4	Research Objectives	4
2	Current Manufacturing Technologies	6
2.1	PC – PLC Communication	6
2.2	Powder Bed Temperature Distribution	7
2.3	Flow Control of Inert Gasses	9
2.4	'Z' Height Resolution and Accuracy.....	9
2.5	Powder Delivery Systems	10
2.6	Process Speed and Efficiency	12
3	Materials and Methods	14
3.1	Experimental Rack.....	14
3.2	SLC 500	17
3.3	Build Dolly Simulator	18
3.4	Nylon-12	21
3.5	Software	21
3.5.1	RSLogix 500 Pro	21

3.6	Environmental Chamber.....	21
3.7	Powder Delivery Simulator.....	25
3.8	Vibration Simulator	27
4	PLC – PC Communication	28
4.1	Serial Communication Protocol.....	28
4.2	PLC Software.....	29
4.3	PC Software	31
5	Powder Bed Temperature Distribution	32
5.1	Infrared Lamp Arrangement.....	32
5.1.1	Initial Testing	32
5.1.2	Reflections of infrared heat.....	36
5.1.3	Difference in Thermal Response of two Identical Lamps.....	37
5.1.4	Effects of Moving Lamps Away from Powder Bed	41
5.2	Power Consumption of Infrared Lamps	42
5.3	PID Control Loop.....	45
6	Nitrogen Flow Control	49
7	Layer Thickness Accuracy	54
7.1	Piston Accuracy	54
7.2	Experiment 1	57
7.3	Experiment 2	57
7.4	Experiment 3	58
7.5	Experiment 4	59
7.6	Experiment 5	61
7.7	Conclusion	63
8	Powder Delivery System.....	64
8.1	Initial Testing	65
8.2	Baseline Test.....	66
8.3	Alternate Operator	67

8.4	Scraper Alterations	68
8.5	Measuring Front and Rear Halves of Bed Independently	69
8.6	Removing Guide ‘Hills’	70
8.6.1	Baseline Test	71
8.6.2	Measuring Front and Rear Halves of Bed Independently	71
8.7	Loosening Augers in Turn	72
8.7.1	Auger 1 Loose	72
8.7.2	Auger 2 Loose	73
8.7.3	Auger 3 Loose	74
8.8	Alternate Timing Wheels	75
8.8.1	Auger 1 – 20 Teeth	76
8.8.2	Auger 1 – 24 Teeth	77
8.9	Replacement Output Tray	78
8.9.1	Without Hills, Without Baffles	78
8.9.2	Without Hills, With Baffles	79
8.9.3	With Hills, Without Baffles	80
8.9.4	With Hills, With Baffles	81
8.9.5	Tilting Machine Base	81
8.10	Tall Output Tray	82
8.10.1	Baseline Test	82
8.10.2	Front and Rear Halves Measured Independently	83
8.11	New Baffle Design	84
8.12	Running Augers Individually	85
8.13	Running Auger 3 in Opposite Direction	87
8.14	Grid Baffle	88
8.14.1	No plugs	89
8.14.2	Plug Arrangement A	90
8.14.3	Plug Arrangement B	91

8.14.4	Plug Arrangement C.....	92
8.15	Results & Conclusions.....	93
9	Process Speed & Efficiency.....	96
9.1	Power Distribution System.....	96
9.2	Removable build cylinder dolly	98
9.3	Process Status Visibility	99
10	Conclusions.....	102
11	Future Project Work	105
11.1	Build Dolly Development.....	105
11.2	Thermal Imaging.....	107
11.3	Heated Roller	108
12	Appendices	109
A	PID Loop Control Experiment Parameters	109
B	PA-12 Datasheet.....	111
C	Powder Delivery Experiment Photos & Data.....	112
C.1	Photos.....	112
C.2	Baseline Test.....	115
C.3	Alternative Operator	115
C.4	Scraper Alterations.....	116
C.5	Measuring Front and Rear Halves of Bed Independently	117
C.6	Removed Hills Baseline.....	117
C.7	Removed Hills Front & Rear	118
C.8	Auger 1 Loose	118
C.9	Auger 2 Loose	119
C.10	Auger 3 Loose	119
C.11	20 Tooth Timing Wheel	120
C.12	24 Tooth Timing Wheel	121
C.13	New Output Tray – No Hills, No Baffles.....	121

C.14	New Output Tray – No Hills, Baffles	122
C.15	New Output Tray - Hills, No Baffles	123
C.16	New Output Tray – Hills, Baffles.....	123
C.17	New Output Tray – Tilted Base.....	124
C.18	Tall Output Tray Baseline	125
C.19	Tall Output Tray Front & Rear	125
C.20	New Baffle Design.....	126
C.21	Auger 1 Only	126
C.22	Auger 2 Only	127
C.23	Auger 3 Only	128
C.24	Auger 3 Opposite Direction	128
C.25	Grid Baffle No Plugs.....	129
C.26	Grid Baffle A.....	130
C.27	Grid Baffle B.....	130
C.28	Grid Baffle C.....	131
D	Power Distribution System Images	132
13	References.....	137

IV LIST OF FIGURES

Figure 3.1 - Experimental Rack.....	16
Figure 3.2 - Experimental Rack Rear.....	16
Figure 3.3 - Allen Bradley SLC 500.....	17
Figure 3.4 - Experimental Build Dolly.....	18
Figure 3.5 - Upper Limit Sensors.....	19
Figure 3.6 - Gearbox and Lower Limit Sensor.....	20
Figure 3.7 - Step Motor and Rotary Encoder.....	20
Figure 3.8 - Experimental Heat Chamber.....	22
Figure 3.9 - Zinc Selenide Window.....	23
Figure 3.10 - Pyrometer Control Unit.....	23
Figure 3.11 - Experimental Heat Chamber.....	24
Figure 3.12 - Environmental Chamber Lamp Wiring Diagram.....	24
Figure 3.13 - Powder Delivery Test System.....	25
Figure 3.14 - Powder Delivery Test System Internal View.....	26
Figure 3.15 - Powder Delivery Test System Drive Belt and Timing Wheels.....	26
Figure 5.1 - Initial Testing - Room Temperature.....	33
Figure 5.2 - Initial Testing - 70 Degrees.....	34
Figure 5.3 - Initial Testing - 1 Hour at 70 Degrees.....	34
Figure 5.4 - Initial Testing - Stitched Image.....	36
Figure 5.5 - Chamber at 70 degrees, lamps off.....	37
Figure 5.6 - Stitched Images - Pyrometer Side Lamp Only.....	38
Figure 5.7 - Stitched Images - Non-Pyrometer Side Only.....	39
Figure 5.8 - Lamp connections reversed, pyrometer side only.....	40
Figure 5.9 - Lamp connections reversed, non-pyrometer side only.....	40
Figure 5.10 - Both lamps, rotated 180°.....	41
Figure 5.11 - Stitched Images - Lamps at Uppermost Position.....	42
Figure 5.12 - Load Required to Maintain Temperature in 5 Degree Steps.....	43
Figure 5.13 - Chamber at 100°C for 20 Minutes.....	44
Figure 5.14 - Chamber at 1% Load for 4 Hours.....	44
Figure 5.15 - Chamber at 170°C for 1.5 Hours.....	45
Figure 5.16 - Results of Block Heating with Tuned PID Loop.....	47
Figure 5.17 - PID Loop Configuration from RSLogix 500 software.....	48

Figure 6.1 - OXYGEN SENSOR CONTROL UNIT.....	49
Figure 6.2 - Experimental Oxygen Sensor Chamber	50
Figure 6.3 - Nitrogen Generator	51
Figure 6.4 - Time taken to inert ETC 13/10 AM.....	52
Figure 6.5 - Time taken to inert ETC 13/10 PM	52
Figure 6.6 - Time taken to inert ETC 14/10 AM.....	53
Figure 7.1 - Step Motor Controller	55
Figure 7.2 - Build Dolly Simulator Wiring Block Diagram	56
Figure 8.1 - Auger Rig Baseline Test Results Graph 2.....	67
Figure 8.2 - Auger Rig Alternate Operator Test Results Graph 2	68
Figure 8.3 - Auger Rig Altered Scraper Test Results Graph 2	69
Figure 8.4 - Auger Rig Front/Rear Test Results Graph 1.....	70
Figure 8.5 - Auger Rig Hills Removed Test Results Graph 2	71
Figure 8.6 - Auger Rig Hills Removed Front/Rear Test Results Graph 1.....	72
Figure 8.7 - Auger 1 Loose Test Results Graph 2.....	73
Figure 8.8 - Auger 2 Loose Test Results Graph 2.....	74
Figure 8.9 - Auger 3 Loose Test Results Graph 2.....	75
Figure 8.10 - Auger 1 at 5.2 rpm Test Results Graph 2.....	76
Figure 8.11 - Auger 1 at 4.3 rpm Test Results Graph 2.....	77
Figure 8.12 - New Tray No Hills No Baffles Test Results Graph 2.....	79
Figure 8.13 - New Tray No Hills Baffles Test Results Graph 2	79
Figure 8.14 - New Tray Hills No Baffles Test Results Graph 2	80
Figure 8.15 - New Tray Hills Baffles Test Results Graph 2.....	81
Figure 8.16 - Rig Tilted 1 Degree Test Results Graph 2	82
Figure 8.17 - 300mm Collar Test Results Graph 2	83
Figure 8.18 - 300mm Collar Front/Rear Test Results Graph 1	84
Figure 8.19 - Second Baffle Design Test Results Graph 2.....	85
Figure 8.20 - Auger 1 Only Test Results Graph 2.....	86
Figure 8.21 - Auger 2 Only Test Results Graph 2.....	86
Figure 8.22 - Auger 3 Only Test Results Graph 2.....	87
Figure 8.23 - Auger 3 Anti-clockwise Test Results Graph 2.....	88
Figure 8.24 - Grid Baffle With Plugs	89
Figure 8.25 - Grid Baffle No Plugs Test Results Graph 2.....	90
Figure 8.26 - Grid Baffle Plug Arrangement A	90

Figure 8.27 - Grid Baffle Plug Arrangement A Test Results Graph 2	91
Figure 8.28 - Grid Baffle Plug Arrangement B	91
Figure 8.29 - Grid Baffle Plug Arrangement B Test Results Graph 2	92
Figure 8.30 - Grid Baffle Plug Arrangement C	92
Figure 8.31 - Grid Baffle Plug Arrangement C Test Results Graph 2	93
Figure 9.1 - Lamp Stack.....	100
Figure 12.1 - Powder Delivery Test System Control Electronics	112
Figure 12.2 - Filling Powder Delivery Test System 1.....	112
Figure 12.3 - Filling Powder Delivery Test System 2.....	113
Figure 12.4 - Filling Powder Delivery Test System 3.....	113
Figure 12.5 - Powder Delivery Test System Full and Level	114
Figure 12.6 - Powder Delivery Test System Outline of Risen Powder	114
Figure 12.7 - Auger Rig Baseline Test Results Graph 1.....	115
Figure 12.8 - Auger Rig Alternate Operator Test Results Graph 1	116
Figure 12.9 - Auger Rig Altered Scraper Test Results Graph 1	116
Figure 12.10 - Auger Rig Hills Removed Test Results Graph 1	117
Figure 12.11 - Auger 1 Loose Test Results Graph 1	118
Figure 12.12 - Auger 2 Loose Test Results Graph 1	119
Figure 12.13 - Auger 3 Loose Test Results Graph 1	120
Figure 12.14 - Auger 1 at 5.2 rpm Test Results Graph 1.....	120
Figure 12.15 - Auger 1 at 4.3 rpm Test Results Graph 1.....	121
Figure 12.16 - New Tray No Hills No Baffles Test Results Graph 1.....	122
Figure 12.17 - New Tray No Hills Baffles Test Results Graph 1	122
Figure 12.18 - New Tray Hills No Baffles Test Results Graph 1	123
Figure 12.19 - New Tray Hills Baffles Test Results Graph 1.....	124
Figure 12.20 - Rig Tilted 1 Degree Test Results Graph 1	124
Figure 12.21 - 300mm Collar Test Results Graph 1	125
Figure 12.22 - Second Baffle Design Test Results Graph 1	126
Figure 12.23 - Auger 1 Only Test Results Graph 1.....	127
Figure 12.24 - Auger 2 Only Test Results Graph 1.....	127
Figure 12.25 - Auger 3 Only Test Results Graph 1.....	128
Figure 12.26 - Auger 3 Anti-clockwise Test Results Graph 1	129
Figure 12.27 - Grid Baffle No Plugs Test Results Graph 1.....	129
Figure 12.28 - Grid Baffle Plug Arrangement A Test Results Graph 1	130

Figure 12.29 - Grid Baffle Plug Arrangement B Test Results Graph 1	131
Figure 12.30 - Grid Baffle Plug Arrangement C Test Results Graph 1	131
Figure 12.31 - Power Distribution Cabinet Input Side (left)	132
Figure 12.32 - Power Distribution Cabinet Output Side (right)	132
Figure 12.33 - Power Distribution Cabinet Interior	133
Figure 12.34 - Power Distribution Cabinet Output Wiring	133
Figure 12.35 - Power Distribution Cabinet Circuit Breaker and Relay Wiring	134
Figure 12.36 - Power Distribution Cabinet Input Wiring	134
Figure 12.37 - Control Panel Door Interior	135
Figure 12.38 - Control Panel Door Exterior	135
Figure 12.39 - Control Panel Interior Wiring	136

V LIST OF TABLES

Table 7.1 - Results of repeatedly moving build piston 10mm in either direction.....	57
Table 7.2 – Results of Moving Build Piston Varying Distances Downwards.....	58
Table 7.3 –moving build dolly simulator repeatedly at varying distances.....	59
Table 7.4 - Second Attempt Moving Piston Downwards Repeatedly At Varying Distances	60
Table 7.5 - Repeated Homing Operations At Various Speeds.....	62
Table 8.1 - Auger Driven Powder Delivery Rig Overall Results.....	94
Table 9.1 - Machine Power Requirement Calculations.....	97
Table 12.1 - PLC Parameters.....	110
Table 12.2 - Auger Rig Baseline Test Results.....	115
Table 12.3 - Auger Rig Alternate Operator Test Results.....	115
Table 12.4 - Auger Rig Altered Scraper Test Results.....	116
Table 12.5 - Auger Rig Front/Rear Test Results.....	117
Table 12.6 - Auger Rig Hills Removed Test Results.....	117
Table 12.7 - Auger Rig Hills Removed Front/Rear Test Results.....	118
Table 12.8 - Auger 1 Loose Test Results.....	118
Table 12.9 - Auger 2 Loose Test Results.....	119
Table 12.10 - Auger 3 Loose Test Results.....	119
Table 12.11 - Auger 1 at 5.2 rpm Test Results.....	120
Table 12.12 - Auger 1 at 4.3 rpm Test Results.....	121
Table 12.13 - New Tray No Hills No Baffles Test Results.....	121
Table 12.14 - New Tray No Hills Baffles Test Results.....	122
Table 12.15 - New Tray Hills No Baffles Test Results.....	123
Table 12.16 - New Tray Hills Baffles Test Results.....	123
Table 12.17 - Rig Tilted 1 Degree Test Results.....	124
Table 12.18 - 300mm Collar Test Results.....	125
Table 12.19 - 300mm Collar Front/Rear Test Results.....	125
Table 12.20 - Second Baffle Design Experiment Results.....	126
Table 12.21 - Auger 1 Only Test Results.....	126
Table 12.22 - Auger 2 Only Test Results.....	127
Table 12.23 - Auger 3 Only Test Results.....	128
Table 12.24 - Auger 3 Anti-clockwise Test Results.....	128

Table 12.25 - Grid Baffle No Plugs Test Results..... 129

Table 12.26 - Grid Baffle Plug Arrangement A Test Results 130

Table 12.27 - Grid Baffle Plug Arrangement B Test Results 130

Table 12.28 - Grid Baffle Plug Arrangement C Test Results 131

VI ACKNOWLEDGEMENTS

I submit the following dissertation with love and admiration for my amazing wife Hannah and our equally amazing children; Elliot, Rosemary & Dorothy. They are my reason for being and without them I could not have completed this. I would like to thank them for their continued support and wish for their ongoing happiness and prosperity.

I would like to thank my co-researchers Beth and Sam along with our industry partner Graham, for providing an excellent working environment, which has been productive and supportive while being sufficiently challenging.

My supervisor Allan has been a vital resource of grounding and has continually supported my work in any way that he could, especially in times when things seemed more difficult than they perhaps were. Your calmness is infectious and has saved me from a number of breakdowns.

Finally, I'd like to thank myself, as too often we fail to appreciate ourselves for the work we have done, favouring self-deprecation over self-esteem. Well done me.

VII DECLARATION

I hereby declare that this dissertation is my own original work and has not been previously submitted for the award of any other degree or diploma at this or any other institute of higher education. To the best of my knowledge, it contains no material previously written or published by another person except where due acknowledgement is made in the text.

1 INTRODUCTION

Euriscus Ltd In association with Lancaster University have collaborated in an Innovate UK funded project with the aim of examining and improving selected elements of a large-format selective laser sintering machine's control system. The work herein comprises a number of specific system elements examined as part of the wider project. It was predicted that the intellectual property produced could directly or indirectly produce monetary return for the project sponsor, while published works could advantage the area of research on the topics of additive manufacturing and potentially in some cross-disciplinary applications.

1.1 BACKGROUND

Manufacturing of plastic parts is a prolific practice of the last 50 years (Science History Institute, 2019) with 400 megatonnes being produced worldwide in 2017 (Qualman, 2019), a figure which has increased exponentially since the 1950s, hampered only by consideration for its impact on the environment. The processes by which plastic parts are produced vary depending on the type of part, material, lead time, setup cost, cost per part and number of parts to be made.

Additive manufacturing (AM) is the practice of producing parts additively from a powder or filament as opposed to subtractively from billet or melted material. Selective laser sintering (SLS) is the practice of partially melting or 'sintering' powder, layer by layer, with a laser. SLS occupies an area of the market whereby lead time and setup cost is low but cost per part is relatively high, making it most suitable for low to mid-volume applications (Formlabs, 2019).

One of the great advantages of SLS is the ability to produce a wide variety of shapes, where other plastic manufacturing methods are generally suited to a particular type of part, for example rotational moulding, which is best suited for large, hollow parts but is not usually cost effective for other types of part (Crawford & Kearns, 2012). SLS allows the manufacture of any shape that will fit in the available build volume, with the notable exception of enclosed, hollow spaces which by the nature of the SLS process will be filled

with unsintered powder. This is a limitation which can generally be addressed by adding drainage holes for excess powder, or in some cases it could be left inside the part at the expense of weight and material cost.

Euriscus Ltd in collaboration with Lancaster University, are developing a SLS machine capable of producing parts cheaply and consistently at commercially acceptable quality. A number of the proposed machines are to be installed in an industrial environment, where orders received from a purpose built website are to be prepared, built, finished and packaged for shipping. The facility will have a focus on speed, efficiency and automation of the production cycle so as to maximise its cost-effectiveness. The research herein focusses on a number of specific elements of a SLS machine's control system, as identified to potentially improve process speed and efficiency.

1.2 RESEARCH FOCUS

The proposed AM machine employs a PLC (Programmable Logic Controller), which is a type of computer with many inputs and outputs designed specifically for the task of controlling sensors and actuators, generally in an industrial environment. This is used for control of most of the system's sensors and actuators, with a PC (Personal computer, of the type with a monitor, mouse & keyboard found in most offices) providing a human interface and software interface to the laser and scanner.

A link between the PLC and PC must be established such that system information and instructions can be passed between them. As this connection is critical to the nominal operation of the machine, it must be both fast and reliable, and contain enough bandwidth to transfer all required data within required timescales. This work examines methods by which to establish and maintain this link while keeping time and monetary costs to the project as low as possible, so other aspects can be explored more thoroughly. It is not believed that the time taken during the machine cycle or part quality could be reduced through this, but a robust, reliable link between PLC and PC should assist in minimising machine downtime through system failures.

A much more prevalent factor in the quality of parts produced by sintering is the minimisation of temperature differential across the surface of the machine's build area

(Pham, Dotchev, & Yusoff, 2008). Due to the finely controlled amounts of power and speed of the scanning laser as it completes a layer of a build, any difference in temperature of the powder surface can result in parts which are not fully sintered in colder areas of the chamber or melted parts in warmer areas (Bourell, Watt, Leigh, & Fulcher, 2014). This research examines a fairly simple mechanism for providing this heat as evenly as possible, while again keeping time and monetary cost to a minimum.

Control of the oxygen content within the build chamber is an element of an SLS system which is critical to its safety without which, build media within the chamber could potentially ignite, with obvious and terminal consequences. As such, some time is given in this dissertation to the creation of a nitrogen flow control system capable of lowering the oxygen content of the chamber as quickly as possible (to the benefit of process time), monitoring it to maintain an inert atmosphere for the duration of the build, and provide safety protocols to prevent damage in the event that the chamber atmosphere becomes prematurely oxygenated.

'Z height' resolution of AM machines is a factor which continues to improve over time, limited by the accuracy of the mechanical systems used and eventually by the particle sizes of the build media used (Turner & Gold, 2015). Any machine which is intended for long term use in a commercial or industrial environment would be advantaged to have a design capable of later improvement in this area. This project is provided with a prototype build piston mechanism and tasked with controlling it through PLC code as accurately as possible.

The majority of the time spent on this dissertation examines a novel mechanism for providing powder to the machine through a hopper and augers, rather than using feed pistons or similar existing mechanisms. The most significant area of the research is ensuring enough powder is consistently delivered by the augers in an even spread, as too much powder toward the front or rear of the chamber would create waste, and likewise too little powder in any area would cause the build to fail as one layer is sintered directly on top of another without the necessary fresh layer of powder (Nan & Ghadiri, 2019).

An auxiliary aim of this dissertation is to examine the build cycle as a whole, identifying any potential elements where improvements could be made to minimise the time taken for each build cycle. An example of this being the removable build dolly which hopes to

significantly reduce the turnaround time between builds by taking the entire build platform away to be replaced by another, pre-prepared build platform.

1.3 RESEARCH VALUE

AM processes have enjoyed a recent surge in popularity, but have not developed to the point of competing with more conventional manufacturing methods (Petrick & Simpson, 2015). The enhanced design and manufacturing possibilities provided by AM serve as a motive for developing the surrounding technologies such that they may one day compete. As such, the work herein aims to take steps in this direction, improving the process in any way possible with the time and funding provided.

Perhaps the most significant value attached to this work is to Euriscus Ltd who will own the commercial rights to it on completion of the project. It is intended that they will use it, in combination with the results of the wider project, in a production environment selling custom made parts, rather than the machines themselves. With the rise of AM technologies, it is possible that ownership of such bespoke technologies may eventually provide significant monetary returns (Weller, Kleer, & Piller, 2015).

Some of the specific areas of research within this dissertation may have cross disciplinary applications, for example auger driven powder feed mechanisms are often employed in the areas of agriculture and medicinal production systems and as such may be of some benefit therein (Yang & Evans, 2007). There may also be other applications for accurate control of stepper motor mechanisms, as these are typically used in fused deposition modelling (FDM) variants of AM machines.

1.4 RESEARCH OBJECTIVES

The objectives of this research, as laid out in the research proposal were as follows:

1. Altering the arrangement of infrared lamps to create a more even powder bed temperature distribution. This will provide a greater consistency of part quality and allow the use of materials which require a narrower hysteresis;

2. Control of the powder bed temperature distribution by use of a thermal imaging camera, where the image is processed to provide feedback values for the control loops of each heating element;
3. Implementation of a removable build 'dolly' allowing a much faster build turnover by removing the build 'cake' and piston (and associated heaters) from the machine to be separately processed, replacing it with an identical unit which can be prepared during the previous build;
4. More accurate control of the build and feed pistons will provide better part quality by way of layer accuracy and will allow for smaller layer thicknesses where the material is fine enough to allow it;
5. Heating the recoating 'roller' to reduce the time required to bring the powder bed back up to the desired temperature, thus reducing the process cycle time.

Unfortunately, due to time and financial restrictions the second and fifth objectives could not be completed within the scope of this dissertation. Similarly, the first objective is only explored in a preliminary sense. These elements of the research would potentially be covered by future work and are discussed in chapter 11.

2 CURRENT MANUFACTURING TECHNOLOGIES

It is widely believed that AM will constitute a significant portion of the manufacturing industry in the years to come (SME, 2019). Developments in these technologies is on the rise due to increased interest and investment, and companies are increasingly more able to use these processes in commercially viable ways. Current research shows that it may soon be possible to additively manufacture tiny, working electronic devices through printing of electrically conductive materials (Espalin, Muse, MacDonald, & Wicker, 2014). On the opposite end of the spectrum, entire buildings have been built with purpose made AM machines (Hager, Golonka, & Putanowicz, 2016).

Injection moulding is currently a hugely popular manufacturing technology which allows for affordable and reliable mass production of plastic parts. The global injection moulding industry is predicted to be worth US\$496.22 billion by 2025 (Grand View Research, 2019). If advances in AM technologies continue, it could be predicted that injection moulding may one day be replaced by one or more AM technologies (Kress, 2015). The primary candidate for this based on current evidence, would be SLS due to its ability to produce large volume, hollow bodied, intricate parts in a range of materials, including some metals.

Current, commercially available SLS systems are capable of reliably producing a vast array of small parts, where the tooling cost associated with injection moulding processes is replaced by a comparable (often lesser) cost for modelling and post-processing parts (Folgado, Peças, & Henriques, 2010). Currently high quantity part orders are best filled via injection moulding as the majority of the cost is incurred only once during tooling, low quantity part orders can be filled quicker and cheaper by SLS technologies due to only a computer aided design (CAD) model being required, which are often produced as part of the design process anyway.

2.1 PC – PLC COMMUNICATION

Every complex machine requires a control system, and every control system requires a central controller to operate the system's sensors and actuators based on its software

program. The Allen Bradley SLC 500 PLC (by Rockwell automation of Milwaukee, Wisconsin, USA) has been commonly used for industrial control systems since its launch in 1991. Testament to its effectiveness for the task is the fact that it is still being sold and used widely in 2017, though newer versions are certainly available. Those familiar with a range of programmable logic controllers often comment on how the Allen Bradley SLC500 is still one of the best choices available due to its reliability and ease of programming (Fitchett Jr, 2017).

Most machines also require an interface by which they can be controlled by a human. Industrial machines controlled by a PLC often use a human machine interface (HMI), which is a very specific kind of small computer with a screen, designed to provide the interface between the PLC and the human operating it. In the case of an SLS machine it could be argued that an HMI would not be sufficient as the interface may be required to handle resource intensive three-dimensional modelling as well as calculations for model slicing and laser movement. To this end it would be more appropriate to use a fully-fledged PC running windows or similar operating system, with a custom written interface program on top. This allows the PC to handle all complex, resource intensive calculation while the PLC remains focussed on the control system as per its original purpose.

Using a PC as the human interface for an SLS machine means that it will be required to communicate with a PLC by some means. This research has been provided with, and therefore uses, an Allen Bradley SLC500 PLC. As such the options for communication are limited to using one of Allen Bradley's proprietary, serial/Ethernet based protocols, or to use RS232 serial connection (Rockwell Automation, 2008). With the former, a cost is incurred through requiring proprietary hardware, and the need to learn a fairly complex networking protocol language. The latter option requires only a commonly available 9 pin D-type cable, and knowledge of an extremely common, well trusted serial protocol (O'Brien, 2012).

2.2 POWDER BED TEMPERATURE DISTRIBUTION

During laser sintering (LS) processes the build media being used must be kept at a temperature close enough to its melting point that it can be reliably melted using a given amount of laser energy for a given amount of time (Bourell, Watt, Leigh, & Fulcher, 2014).

The melting point of the polyamide 12 powder used throughout this research was 172-180°C (CRDM, 2019), however it has been noted that the actual environmental temperature varies from machine to machine and from media to media (Goodridge, Tuck, & Hague, 2012) and so the required range of temperatures to be maintained by the machine have to be found by trial and error, using the material's data sheet as the starting point.

Due to the nature of the environment in which sintering takes place, radiant heat is the only practical method for bringing the build area surface to the correct temperature. Heating through conduction is not possible as the area above the build area must be clear for the path of the laser, the area immediately below is occupied by the build 'cake' and piston, and the areas either side of the build area must be clear for the deposition of powder between layers. Convection cannot be used because the movement of air through the build chamber may cause the powder to become airborne, possibly affecting the critically flat profile of the build surface.

There is a myriad of different types of radiant heater, and most can be discounted for the purpose of a sintering machine. The location requirements mean the only available space for a surface heater is above the build area, surrounding the laser entry window, and only electrical heaters possess the required controllability over gas, water and oil solutions (Puravent, 2019). This leaves ceramic or infrared heating elements as the best possible solutions for this use case.

Information on the types of heating systems used in current commercial laser sintering systems, and their effectiveness in creating an even temperature profile, is sparse due to the commercial nature of these systems. The 3D Systems Sinterstation 2000 (available for access by the author, as it is located in Lancaster University Engineering Department's additive manufacturing laboratory) uses a number of different heaters throughout, but the radiant surface heating is achieved through infrared lamps, controllable with a single pyrometer.

Recent attempts at maintaining even surface temperature in SLS machines have suggested that controlling temperature in a number of 'zones', each of which has its own designated heater and temperature reading in multiple closed control loops, may provide a method by which to improve the consistency of build area temperature profile over

current, single 'zone' solutions (Statum, 2016) (China Patent No. CN102335741A, 2010) (Integra, 2019).

2.3 FLOW CONTROL OF INERT GASSES

There is a myriad of recently researched methods for super-fast and accurate control of gas flow, though this is generally not required for the SLS process, which merely requires that the atmosphere within the chamber have approximately 5% or less oxygen content to avoid combustion of the build media. The only requirement herein is that this process take as little time as possible so as not to delay the start of the build process. To this end many current SLS machines use simple solenoid valves controlled either by a PLC or other control interface.

The introduction of an inert gas into the build chamber also serves to keep the chamber at a pressure level slightly higher than the atmosphere surrounding the machine. This prevents oxygenated air 'leaking' into the chamber, another potential cause of build media combustion. This means that monitoring chamber pressure is necessary to ensure safety, so that heaters can be disabled in the event that oxygen content within the chamber reaches unsafe levels. This is generally achieved with readily available pressure sensors which continually report their reading to a central PLC or similar controller.

2.4 'Z' HEIGHT RESOLUTION AND ACCURACY

One of the major limitations to modern AM technologies is the accuracy and resolution with which parts can be made (Conner Seepersad, Govett, Kim, Lundin, & Pinero, 2012). This is clear when examining AM parts which contain tight curves, as curves have to be represented as a set of discretely stepped layers in almost any digital to real world transition. Perhaps the most prominent example of this is digital to analogue converters for the speakers and headphone jacks in most computers; smartphone or otherwise.

The prevalence of this phenomenon varies according to the type of process being used; laser based systems are typically more accurate, and work at a higher resolution than extrusion based systems due to the lack of a need to establish a 'bead' of flowing plastic

from a nozzle (V.Wong & Hernandez, 2012). This element of the research focusses on ensuring the 'Z' height or 'build piston' stepper motor is as accurate as possible at as high a resolution as possible. Stepper motors have been chosen for this application as they are much more accurate, powerful and available than the alternative; linear actuators.

When using stepper motors, near infinite accuracy and resolution can be attained, at the expense of speed, using gearboxes and micro stepping. Micro stepping a stepper motor gives the highest possible resolution without the use of a gearbox by alternating pulses in different coils within the motor, creating a number of steps between the conventional steps. Gearboxes, in the context of this project, are used to reduce the number of times an output wheel turns with respect to the motor itself. This has the added benefit of adding to the available torque, but at the expense of speed, which is relatively insignificant over the tiny distance a build piston lowers when moving from one layer to the next in an SLS system.

Stepper motors are generally controlled using one of two methods, usually a stepper motor controller will provide facilities for both; absolute moves, where a motor is moved to a specific point between its end limits, or relative moves, where a motor is moved by a specific number of steps from its current position. A third method known as 'jogging' also allows a motor to be moved in either direction until it is told to stop.

2.5 POWDER DELIVERY SYSTEMS

The majority of current SLS solutions utilise a dual feed piston material delivery system comprising of two feed pistons and a counter-rotating roller. The feed pistons begin the build process at the bottom of their available travel and the cavities above are filled with all the material for the build. This method carries the disadvantage that all the build medium must be loaded into the machine in advance of the build, restricting the possibilities for making changes during a build (Psarommatis Giannakopoulos, 2016). If more powder needs to be added, the entire build would have to be stopped and the machine cooled before opening. In almost all cases this results in a failed build due to the tolerances of the materials involved. Another disadvantage is that SLS machines are typically quite large in order to contain both of these feed pistons.

Some machines use a hopper driven system whereby material is dropped from a hopper using an accurately controller valve, and then moved onto the build area with a counter-rotating roller. This approach has the disadvantage that dropped powder tends to pile up directly below the hopper, and is not efficiently spread across the build area meaning more powder has to be fed each layer and consequently more powder is wasted through the process.

This research proposed a novel system whereby a single feed bin is fed powder from an external hopper by a set of horizontal augers. The build material is then moved onto the build area by a counter-rotating auger as in most current solutions. This allows build material to be added to the machine at any time, completely independently of the build process. Additionally, a machine using this principle can be much smaller due to the space saving from having material fed from only 1 side of the build area.

There is little research into auger driven powder delivery methods specifically pertaining to SLS systems, rather the literature comes mainly from the fields of pharmaceutical production and agricultural feed delivery systems. The specific areas of interest which transfer cross-discipline, in this case, are those which study even distribution for powder delivery systems. This is important in SLS machines as an uneven distribution will mean more waste powder due to excesses being discarded into a waste bin by the roller during the recoat cycle.

Previous work at the Queen Mary University of London (Yang & Evans, 2007) describes that there has been some success in using auger driven powder delivery systems to mix different materials precisely. Implementing such a system in an SLS machine with auger driven material feeds would potentially allow ratios of materials used to be gradated by layer or potentially for each layer to use a different material entirely, a theory discussed later in Chapter 11, Future Project Work. A notable limitation here is that with the system proposed in this research, it would not be possible to use different materials or composites in different areas of a single layer, rather the entire layer must use the same material. This addition would enable SLS technologies to more readily compete with newer processes which don't have this inherent limitation.

2.6 PROCESS SPEED AND EFFICIENCY

Advances in AM processes are happening rapidly; build time, turnaround time and level of human interaction requirement in the process are all falling as developments continue. In the ideal scenario a manufacturing process would be instantaneous, take no time to turn-around and require zero human interaction. As this is not currently possible, this can only be a theoretical target to aim for.

Most SLS processes, at time of writing, take an order of hours or days to complete a build, hours to turn-round and prepare a machine for its next build, with regular monitoring and human intervention required to ensure the successful completion of a build and perform all of the turn-round related tasks. These figures are, however beginning to improve as control systems become faster and more sophisticated, decreasing the human interaction requirement and improving the process speed generally through, for example; faster scanning speed and build 'cartridges' which can be interchanged in order to reduce to process turn-round time.

Loading powder into a LS machine takes time and with most currently available machines can only be performed between builds. Some newer machines have cartridge-based systems which mitigate the time taken for cleaning as it can be performed while a build is running with a different cartridge, but this still requires the cartridges to be exchanged between builds as part of the turn-round process. The external hopper system proposed by this research eliminates this need completely, except in the case where a different material is to be used in the next build.

It is in the interest of speed to the overall process that it takes as little time as possible to prepare the build chamber for sintering, such that the oxygen content and temperature are at suitable levels. Overall this adds little time to the build as compared with tasks such as scanning and recoating which are completed many times during a build, but in the pursuit of efficiency nothing should be overlooked. Inert gas inlets in the machine must move enough air in order to reduce the build chamber's oxygen content to below 5% within a number of minutes of the build starting. Similarly, the build chamber and particularly build surface should be able to reach a temperature close to but below the build media's melting point, again within a few minutes of a build starting. Similarly the

end of a build process should be as quick as possible from a speed and efficiency standpoint, without being so quick as to adversely affect part crystallinity, depending on the intended use of the parts (Zarringhalam, 2007).

It could be said that the bulk of time taken during the machine's cycle is attributed to scan time, recoat time and reheat time as these are repeated up to hundreds of times during a single build. As such, a saving of a few seconds per layer in any of these sub-processes add up to potentially hours of the overall process.

Most SLS machines use a build area which is fixed inside the machine, which means extrication of parts from the build 'cake' must be performed in situ, at significant detriment to the turnaround time of the machine. This is of particular concern in commercial markets, where speed often means the difference between novelty and affordability. The removable build 'dolly' proposed by this dissertation would effectively remove this delay by replacing with an identical (or similar) 'dolly', while the original is processed elsewhere.

Once parts have been extricated from the machine and build 'cake', the final barrier to their delivery and/or use is cleaning. Freshly sintered parts are generally covered in a layer of un-sintered and partially sintered powder which must be removed, generally by hand. This can take a few minutes per part but is of little consequence to machine turnaround time, as it can be performed away from the machine while it performs subsequent builds.

3 MATERIALS AND METHODS

Approaching the task of designing and building a complex control system is usually accomplished by breaking the system down into multiple, simpler control modules. In the case of this project the control system was broken down two ways; physically and conceptually. Physically the control system was separated into three steel cabinets which connected to each other and external sensors/actuators with a number of cables. The cabinet's contents were divided as follows:

- Power distribution cabinet – Converted 32A 3-phase electricity into switched and fused 230VAC for distribution throughout the system. Also housed relays for heater power and connected to a physical control panel that determined which items were powered at any given time via 2 hardware buttons;
- Control cabinet – Housed the PLC as the centre of the control system as well as AC-DC power supplies and other miscellaneous control hardware such as relays;
- Motor control cabinet – Contained motor control hardware and scanner power supply; items which were too large or produce too much heat to be in either of the other cabinets.

Conceptually the system was broken down according to its functions, many of which were repeated multiple times throughout the system:

- Heating control
- Stepper motor control
- Nitrogen flow control
- Power control
- Laser/scanner control
- Safety systems

3.1 EXPERIMENTAL RACK

In order to better enable the development of the physical systems a framework was conceived which held the three cabinets and computer in a way which was convenient

for access whilst also being mobile in the event that it needed to be moved to a different location. The frame was constructed from 45x45mm aluminium extrusion which was commonly available, reasonably priced and allowed easy reconfiguration should it have been required. Wheels were added for mobility, and a desk surface for the PC.

Figures 3.1 and 3.2 show the experimental rack (1) produced to allow wiring to be prototyped before the arrival of the machine frame. The power distribution cabinet (2), motor control cabinet (3) and control cabinet (6) were removed from the experimental rack and fitted directly to the machine frame upon completion. The computer shown (4) was used for system development and also as the control PC for the finished machine. The lamp stack (5) offered visual and audible indication of the state of the experimental rack and was also mounted on the machine frame. The control panel (7) was used to cycle through the machine's power-up stages which are discussed in Chapter 9.1.

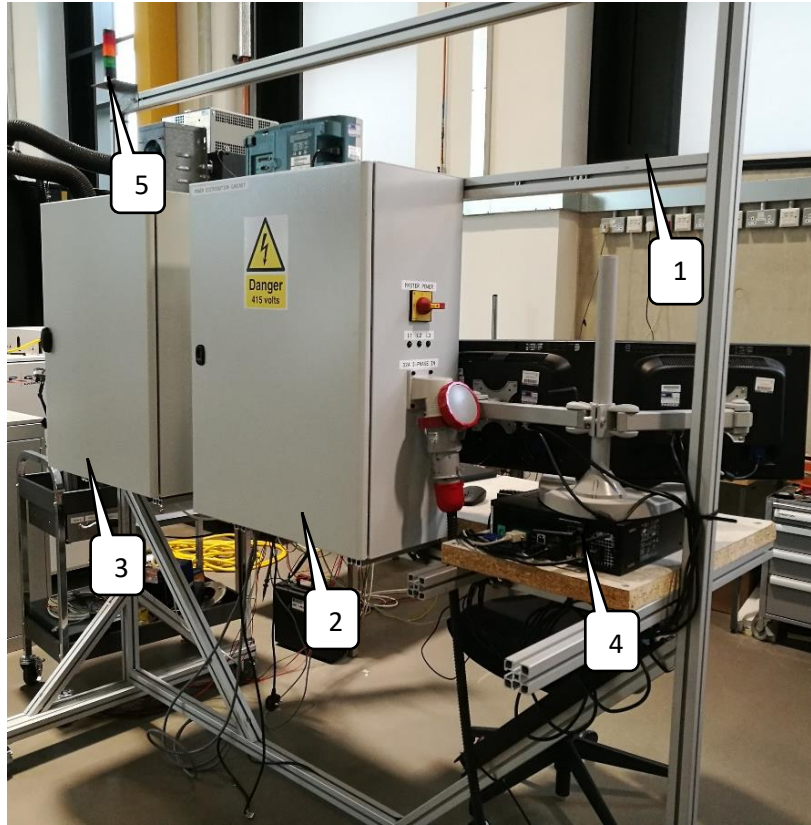


FIGURE 3.1 - EXPERIMENTAL RACK

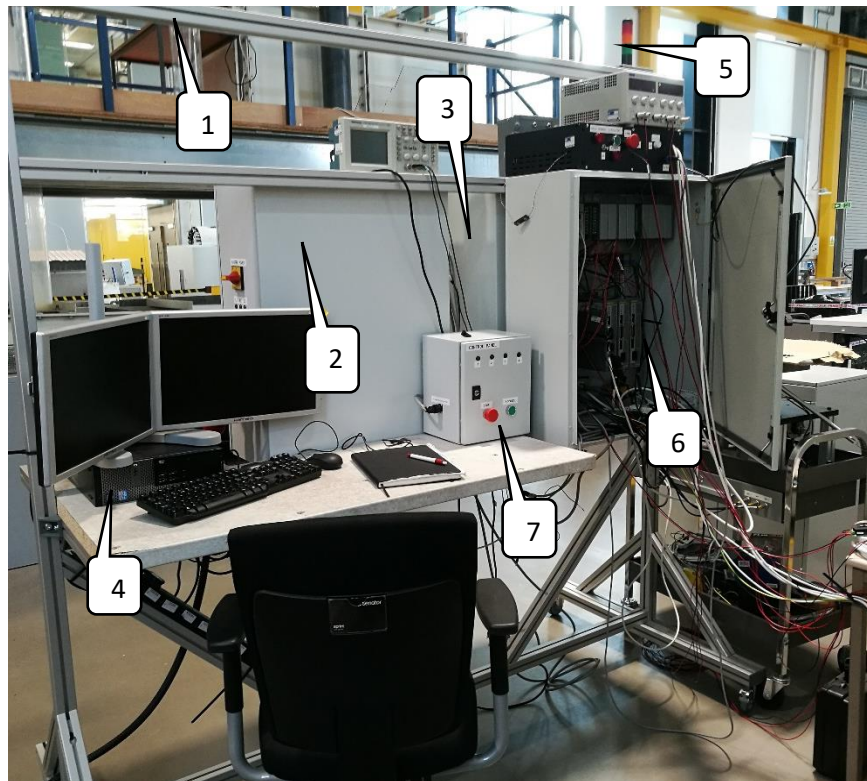


FIGURE 3.2 - EXPERIMENTAL RACK REAR

3.2 SLC 500

The Allen Bradley SLC 500 was selected as the PLC for the project due to affordability and availability. It is shown in Figure 3.3 and consisted of the following removable modules:

1. Power supply (Allen Bradley 1746-P2)
2. Processor (Allen Bradley 1746-L532)
3. Step motor controller x3 (Allen Bradley 1746-HSTP1)
4. 16 channel digital input x2 (Allen Bradley 1746-IB16)
5. 8 channel digital output (Allen Bradley 1746-OB8)
6. 16 channel digital output (Allen Bradley 1746-OB16)
7. 8 channel thermocouple (Allen Bradley 1746-NT8)
8. Analogue input and output x2 (Allen Bradley 1746-NIO4I & NIO4V)
9. Blank panel (Allen Bradley 1746-N2)
10. TRIAC (Allen Bradley 1746-OA16)

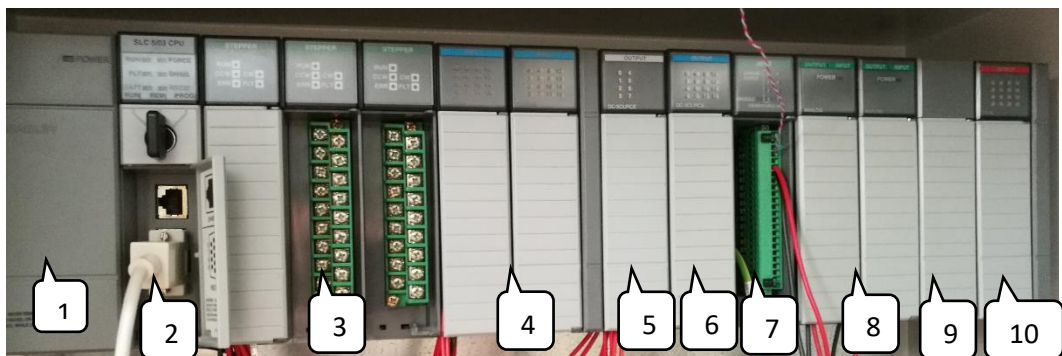


FIGURE 3.3 - ALLEN BRADLEY SLC 500

This particular unit was removed from a previously decommissioned DTM Sinterstation (DTM of Austin, Texas) and as such, it had a selection of modules applicable to its new application. A licence was acquired for RSLogix 500 (by Rockwell Automation, Milwaukee, Wisconsin, USA) which was the environment required for developing in the SLC 500's proprietary 'ladder logic' programming system.

Due to the SLC 500 processor module's limited memory (8k user program memory), care had to be taken to ensure each sub-section of the code was as small as possible, so that all sections would fit into memory.

3.3 BUILD DOLLY SIMULATOR

A significant portion of the build turnaround time for an SLS AM machine is in the removal of built parts and cleaning of the build cylinder. This dissertation aimed to reduce this time by employing a removable build 'dolly', which was to be removed from the machine as a freshly prepared one took its place for the next build. As the work required a piston assembly in order to develop piston control software and test layer height accuracy, it was convenient to place such an assembly on a 'dolly' so its effects and effectiveness could be evaluated simultaneously. Figure 3.4 shows the experiment build dolly built for the research & development phase.



FIGURE 3.4 - EXPERIMENTAL BUILD DOLLY

The dolly consisted of a vertical piston driven by a stepper motor with a rotary encoder through a gearbox, and three inductive proximity sensors, all of which was mounted on a wheeled frame. The stepper motor was driven by a Parker Digiplan PDS15-2 step motor controller which in turn was controlled by one of the PLC's 1746-HSTP1 step motor control modules. The rotary encoder and inductive proximity sensor outputs were connected directly to the same PLC module.

The two upper limit sensors shown in Figure 3.5 were slightly offset vertically giving 2 distinct limits for downward travel. The lower limit sensor shown in Figure 3.6 acted as a limit for the upward travel of the piston, preventing the end of the central threaded bar from entering the gearbox. The higher of the two acted as the main limit for downward travel, preventing damage to the mechanism by the piston platform making contact with the gearbox. The lower sensor acted as a limit to put the piston in a 'cleaning position' which allowed it to extend slightly beyond the seal between it and the enclosing cylinder so excess powder could be removed from the edges.

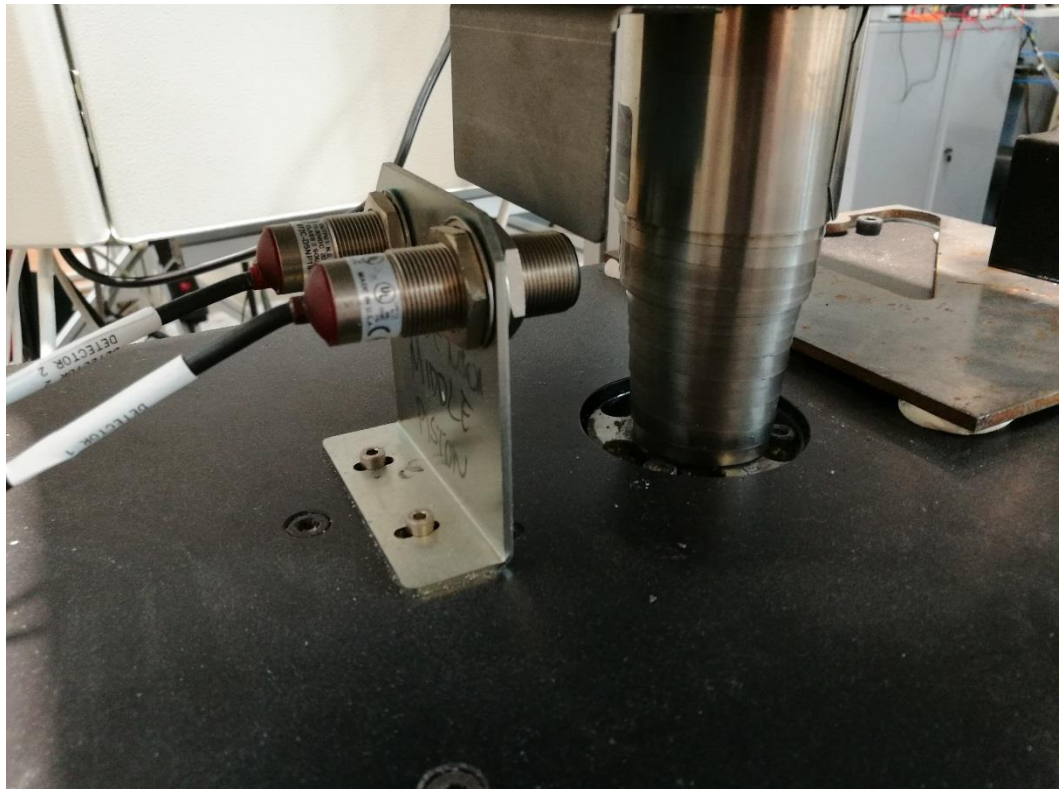


FIGURE 3.5 - UPPER LIMIT SENSORS

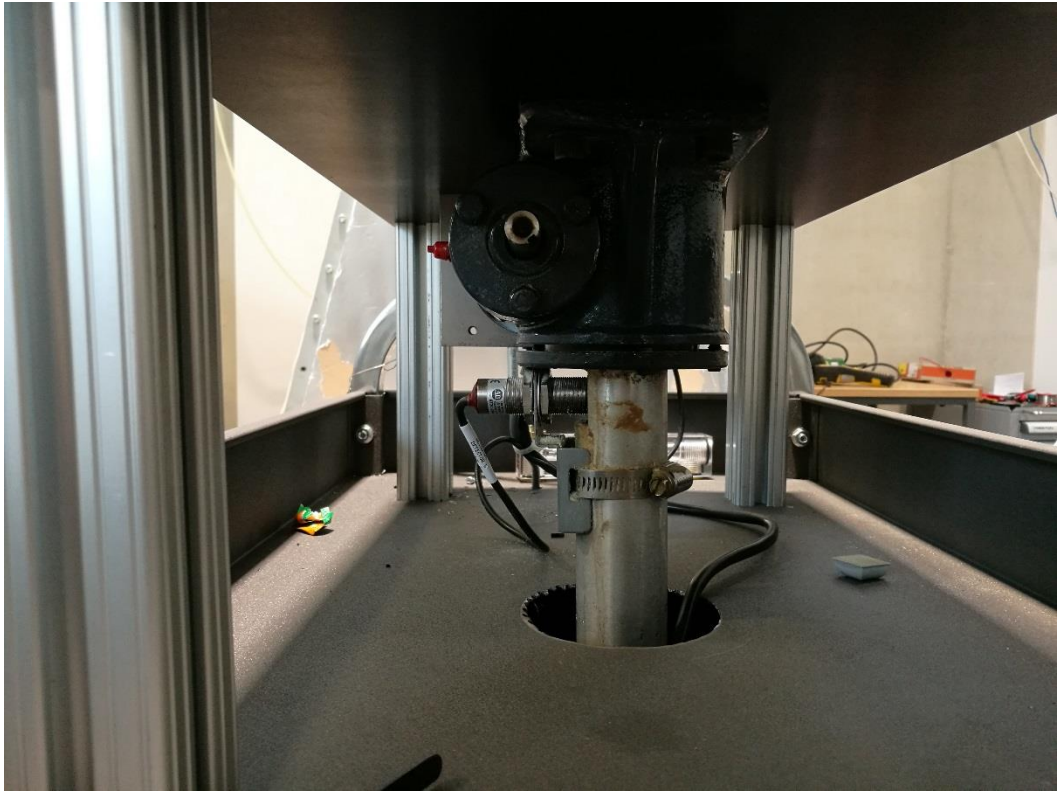


FIGURE 3.6 - GEARBOX AND LOWER LIMIT SENSOR

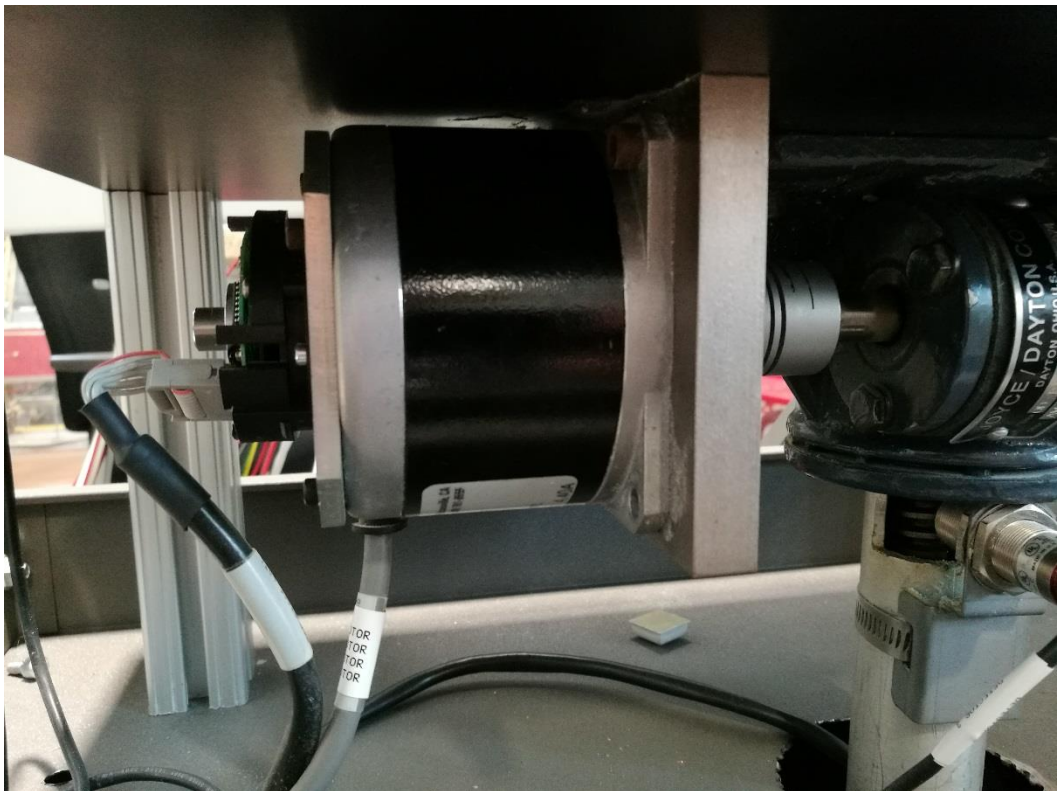


FIGURE 3.7 - STEP MOTOR AND ROTARY ENCODER

3.4 NYLON-12

At the time of undertaking this research, the materials most used in SLS systems were nylon-11 and nylon-12 (polyamide or PA-12). PA-12 was chosen for this research due to its strength, durability and finishing options (Autonomous Manufacturing Ltd, 2019). The wider project sponsor provided the powder which was used for testing and eventually part production. The datasheet is included in appendix B.

3.5 SOFTWARE

3.5.1 RSLOGIX 500 PRO

Programming of the Allen Bradley SLC 500 PLC uses a proprietary 'ladder logic' language, which is developed and uploaded to the PLC via their own RSLogix 500 software. For the purposes of this research, a copy was purchased, the license for which resided on the experimental rig development PC.

3.6 ENVIRONMENTAL CHAMBER

Due to the SLS process' requirement of an enclosed environment for purging oxygen and heating, it was useful to have an enclosed chamber with which the conditions could be replicated in order to test the heating and nitrogen control elements of the system. To this end a chamber was produced by the project sponsor and installed with the following equipment, shown in figures 3.8, 3.9, 3.10 & 3.11:

- Two 2kW GIR-2kW-530-SK15 infrared (IR) lamps (Under Control Instruments, Birmingham, England) mounted at the top of the chamber running parallel to the chamber's longest horizontal dimension, on threaded rods which allow them to be raised or lowered as required;
- A zinc selenide window through which to view the powder surface and record thermal data (1).
- One Optris CT LT pyrometer (2) (Optris GmbH, Berlin, Germany) pointed at the centre of the chamber's lower internal surface;

- Two nitrogen inlets, individually controlled by 230VAC 2 port solenoid valves;
- A shallow tray for powder heating experiments;

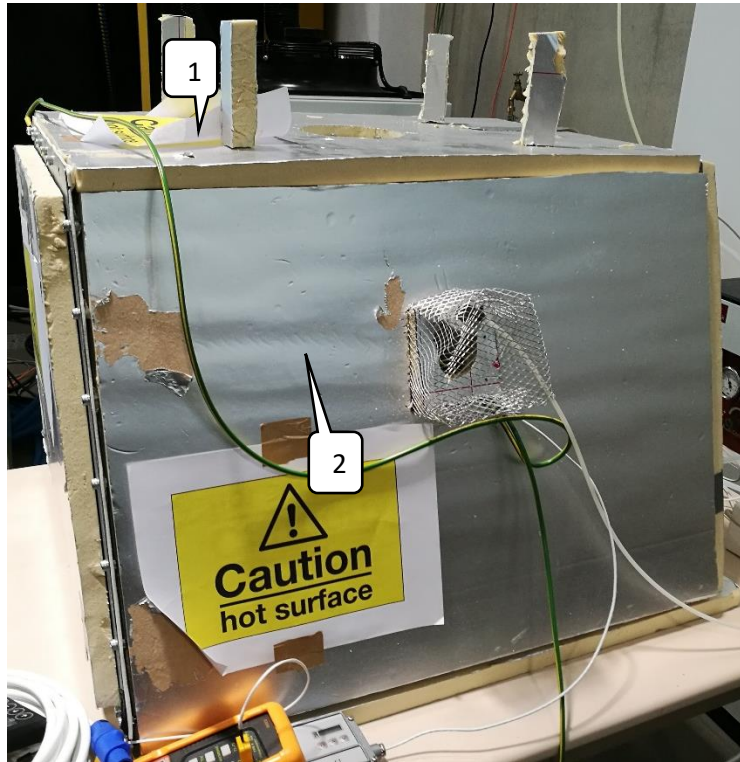


FIGURE 3.8 - EXPERIMENTAL HEAT CHAMBER

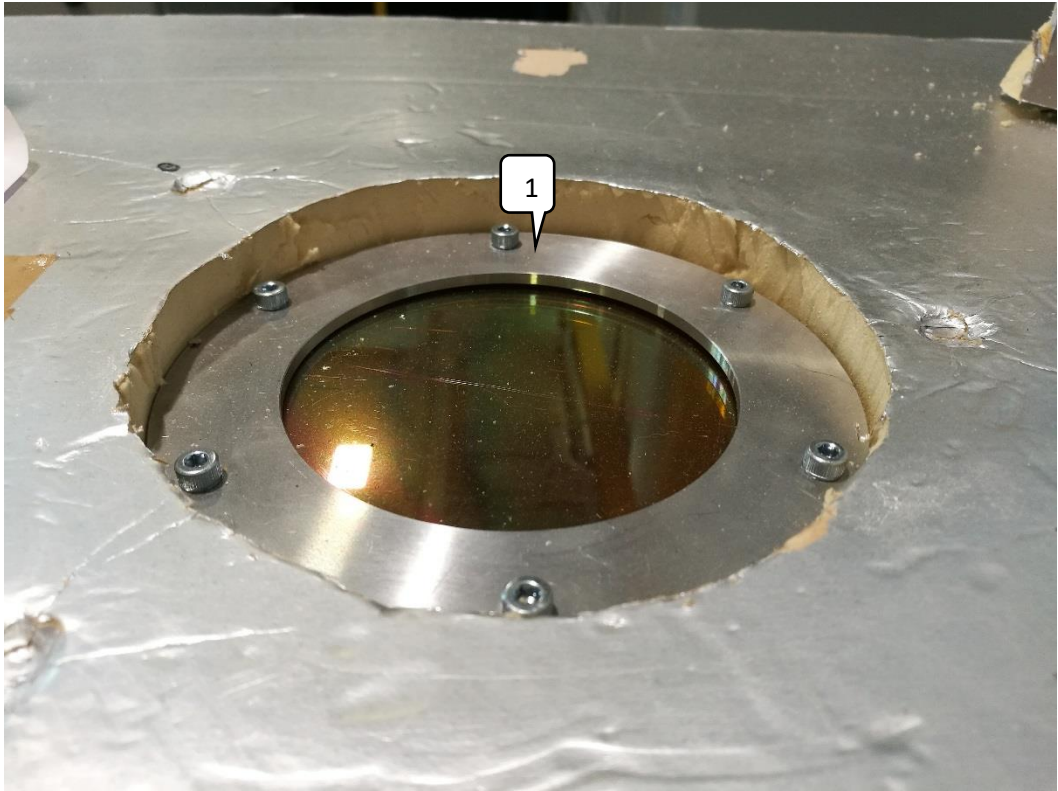


FIGURE 3.9 - ZINC SELENIDE WINDOW



FIGURE 3.10 - PYROMETER CONTROL UNIT



FIGURE 3.11 - EXPERIMENTAL HEAT CHAMBER

The two IR lamps inside the chamber were controlled from the PLC, which switched a pair of phase angle fired silicon-controlled rectifiers (SCRs). SCRs were chosen due to their suitability for the specific use case (Industrial Heating Equipment Association, 2019) of air heating with halogen infrared lamps. The configuration used is shown in Figure 3.12.

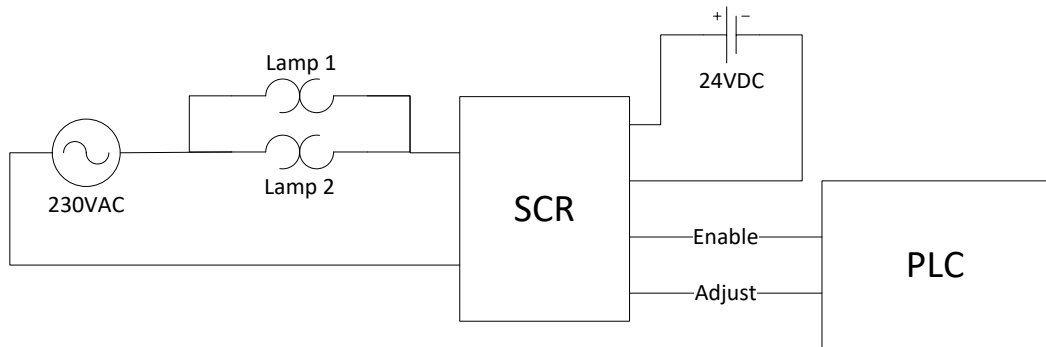


FIGURE 3.12 - ENVIRONMENTAL CHAMBER LAMP WIRING DIAGRAM

3.7 POWDER DELIVERY SIMULATOR

Delivering powder into an SLS machine using augers is not a common method and as such, a bespoke mechanism had to be designed with which to test its viability. The system employed three augers in separate tubes which connected an input hopper to an output tray. The augers were each driven by toothed pulleys and a toothed belt, connected to a step motor. This ensured the augers would rotate at the same speed which was important to create an even powder profile in the output tray. For the purposes of experimentation, the powder rising past the surface level of the output tray was moved with a flat plastic scraper into five cups, which provided a way to assess how evenly the powder was distributed in the dimension parallel with the scraper.

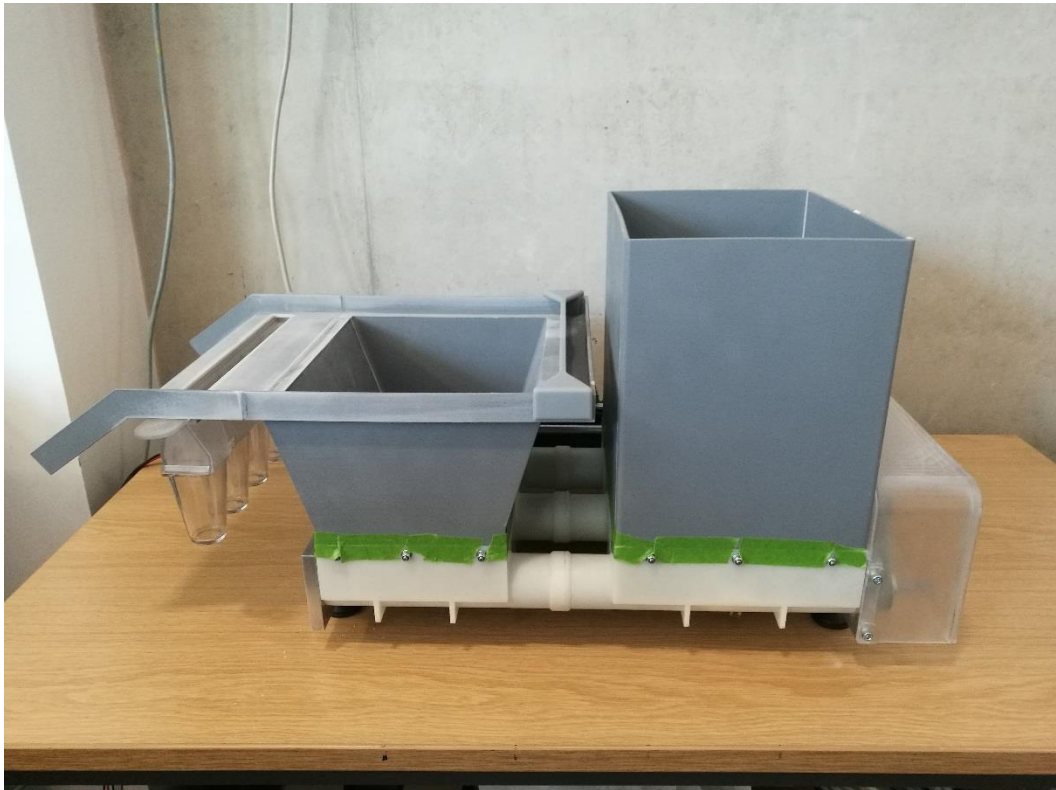


FIGURE 3.13 - POWDER DELIVERY TEST SYSTEM



FIGURE 3.14 - POWDER DELIVERY TEST SYSTEM INTERNAL VIEW

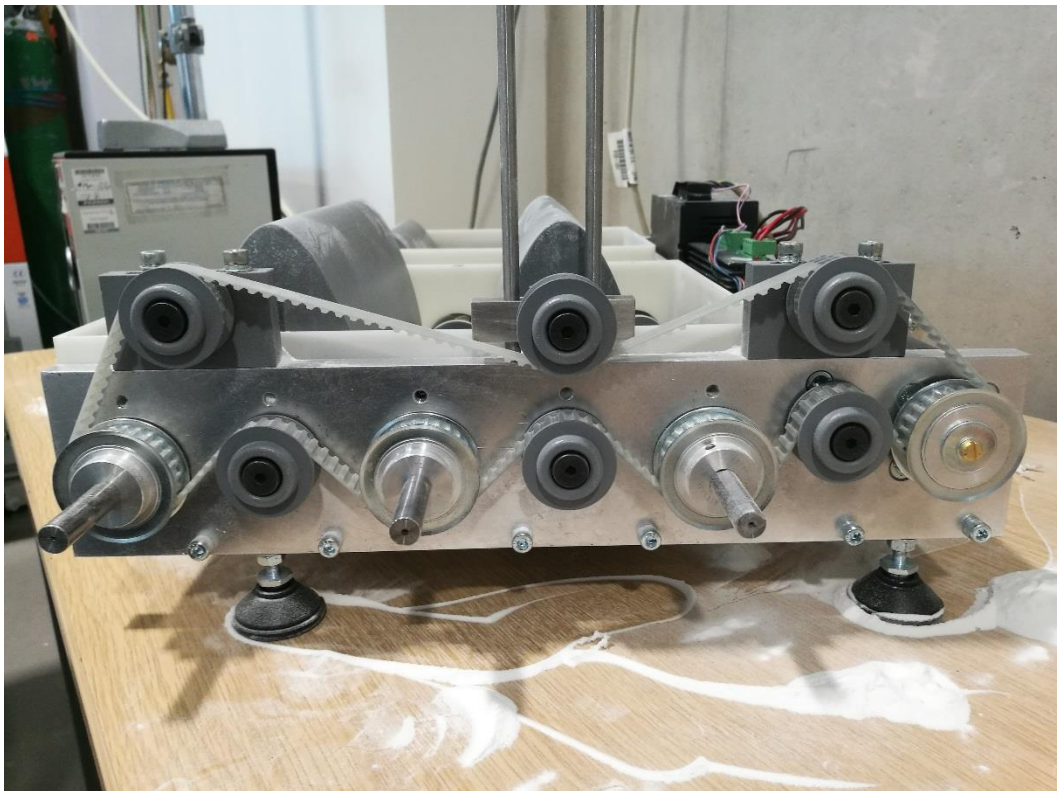


FIGURE 3.15 - POWDER DELIVERY TEST SYSTEM DRIVE BELT AND TIMING WHEELS

Additional images of the powder delivery experimental rig can be found in appendix C.

3.8 VIBRATION SIMULATOR

A need was identified to clean parts after production, so it was considered that this may occur as part of the build process as a way to improve overall process efficiency. Vibration was initially selected as the primary method for removing excess powder from built parts as it is perceivably simpler to vibrate a surface than to direct blasts of air or operate a tumbling mechanism. This required a large perforated aluminium plate attached to rubber mountings on an aluminium extrusion frame. Two pneumatic vibrators were attached horizontally to the sides of the plate in such a way that the plate would vibrate horizontally, as opposed to vertically which may have caused the parts to bounce and break on the plate. The two vibrators were both controlled by a single 230VAC 2 port solenoid valve and connected to a compressed air supply. Beneath the plate sat a collection hopper which fed excess powder into a bucket for potential re-use later.

4 PLC – PC COMMUNICATION

4.1 SERIAL COMMUNICATION PROTOCOL

In order for the PC to communicate system settings to the rest of the machine, a communication interface was required between the PC and PLC. The Allen Bradley SLC500 had two main communication interfaces located on the CPU module; serial, and a proprietary format 'DF-1' via an RJ-45 connection. As the DF-1 connection required extra proprietary hardware and software, this work used the serial connection.

As serial was a fairly old protocol and the SLC500 communicated at a maximum of 19200 baud, serial messages were kept to a minimum in order to maximise the potential number of sensors and actuators within the system, minimising use of the limited bandwidth. To this end the basic communications required were:

- PLC sends the current system status and configuration to the PC
- PC sends new system configuration to the PLC

The SLC500 limits the number of characters in a serial 'string' to 82 including the new line character. To account for this, parameters were divided into sections, each beginning with a string 'identifier' as follows:

- "C0 par1,par2,par3..."
- "S0 par1,par2,par3..."
- "C1 par1,par2,par3..."
- "S1 par1,par2,par3..."

...where 'parX' was a single parameter of one or more digits in Boolean or integer format. "C" stood for configuration; the parameters which could be set by the PC and "S" stood for status; the parameters about which the PLC informed the PC. Some parameters appeared in both "C" and "S" strings as they could be altered by both the PC and PLC. The number at the beginning of each string referred to the section of the machine as follows:

- 0 – Whole system information
- 1 – First heater block

- 2 – Build piston
- 3 – Recoat roller
- 4 – Second heater block
- 5 – Chamber inert

This allowed for simple identification of a parameter based on its location within the system and meant system logs could be saved as comma separated variable (CSV) files with minimum reconfiguration. These messages were sent as a 'block' at a regular interval, nominally set to 1 second.

Where the PC needed to know immediately about the change of a safety critical parameter (for example; when an interlock was opened) it was sent as a single, separate line with the following format:

```
PAR parameter_name new_state
```

The PC sent parameter changes to the PLC using the following format:

```
SET parameter_name new_state
```

This protocol allowed for maximised usage of the limited serial bandwidth and ensured that safety critical system components were updated in a timely fashion.

4.2 PLC SOFTWARE

The PLC's internal code had to be capable of the relatively simple task of interpreting input serial data and accessing the correct memory location for return or alteration. It must also manage the operation of all inputs and outputs, returning any significant operation back to the PC via the serial bus. A basic framework of the program required was written using Allen Bradley's RSLogix 500 software using their proprietary ladder logic programming system. It comprised eight ladder logic program files, seven called in turn from the eighth 'main' file which served as the starting point for the program. The operation of each file is as follows.

MAIN – Entry point to the program. Called each of the other seven files in turn. Some files were only called when certain logic conditions were met, for example PARSE_CMD was only called if GET_CMD had returned true, indicating that it had received a serial message which needed parsing. Similarly SEND_RPLY was only called when BLD_RPLY had returned true, indicating that it had built a reply string to be sent to the serial bus. Additionally, the main file performed some initialisation functions during the first program cycle after the PLC is powered on and set into run mode. These typically included the resetting of counters and timers.

BIT_CHANGE – Examines certain, usually safety critical parameters and if they have changed from their state in the previous program cycle, triggers a message to be sent on the serial bus.

GET_CMD – Once per program cycle, GET_CMD checks the serial input registers for a string of characters ending with a line break, which signifies a command which can be parsed. If one is found, a flag is set which triggers PARSE_CMD to run next.

PARSE_CMD – Takes the string found by GET_CMD and separates it into three sections:

1. Op code – type of instruction to execute.
2. Parameter name – which parameter should the instruction be executed upon.
3. Parameter value – In the case of received commands, only SET instructions require this. Indicates the new value which should be given to the parameter in question.

If the string found by GET_CMD does not follow the format of 3 distinct ‘words’ separated by spaces, it is discarded completely and a message is sent to the serial bus explaining that the command could not be parsed.

LUT – When PARSE_CMD successfully parses a command, LUT compares the parameter name against the list of known parameter names, then if one is found its associated memory location is either altered in the case of SET commands, or its current value converted to a string for passing to the next file, BLD_RPLY, in the case of a GET command.

BLD_RPLY – When a GET command is successfully processed by the previous program files, BLD_RPLY formats the response string to follow the conventions detailed in Chapter 4.1. In the case of a SET command, the string sent back contains the opcode “PAR” indicating a parameter, and parameter name, with the new value of that parameter, which in some cases will not be changed as the command requests, depending on various considerations mostly based around safety. For example, if one were to request “SET HEATER_LOAD 100” (%), the program would check the register for “HEATER_LOAD_MAX” and if this were set to “80” the program would set “HEATER_LOAD” to 80 and return “PAR HEATER_LOAD 80” indicating the action ultimately decided upon by the PLC.

SEND_RPLY – Checks the completed reply string for length (82 characters maximum in a single ASCII write operation) and sends it to the serial bus.

UPDATE_IO – This file forms the layer between the PLC’s internal list of current parameter values, and its input/output hardware. Simply put UPDATE_IO checks the value of a parameter, determines if its state can and/or should be changed, then alters the relevant outputs. Conversely it also takes a reading from a hardware input, compares it against the current parameter value and changes it if necessary.

4.3 PC SOFTWARE

Forming the opposite end of the communication link between the PC and PLC was a piece of software which performed much the same function as the PLC code in terms of acquiring a message, parsing it and altering its internal parameter list, or the reverse, as necessary. A simple program was coded in C# using Microsoft visual studio, a process made slightly easier than the PLC code due to availability of code libraries which would perform serial and string operations at a single function call. At this stage in the research, the parameters were simply stored in an array with their names as one purpose of the initial PC program was only to establish synchronisation of parameters between the PC and PLC. The other purpose of the initial PC program was to allow an interface to the synchronised parameter list via the keyboard, in order to examine current values or set new ones, which was accomplished with a simple text box.

5 POWDER BED TEMPERATURE DISTRIBUTION

SLS requires temperature at the surface of the build area to be maintained between the melting point and crystallisation point of the powder used (Schmid, Amado, & Wegener, 2015). For PA-12, this occurs between 146.45°C and 184.81°C (Vasquez, Haworth, & Hopkinson, 2011) for a maximum build area temperature differential of 38.36°C. However, in practice this differential needs to be much smaller due to variance within the powder and environmental differences. For this reason, target temperature differentials were set as 10°C maximum, 4°C ideal. This also allowed for the possibility for future processing of different materials with more stringent thermal requirements.

5.1 INFRARED LAMP ARRANGEMENT

An experiment was set up to investigate the effect of the position and arrangement of the lamps in physical space on the temperature distribution of the powder bed. A shallow tray of PA-12 powder with a smoothed surface was inserted into the chamber and the effects of various lamp configurations were recorded.

5.1.1 INITIAL TESTING

A grid of four thin metal bars, with the central opening measuring 50mm x 50mm, was laid over the tray of PA-12 powder in order to provide a spatial reference. This was necessary because the camera used (an E40, Flir of Wilsonville, Oregon) was fitted with a lens whose viewing angle could not capture the entirety of the tray, making spatial measurements from the data impractical.

Figures 5.1, 5.2 & 5.3 use varying temperature scales as specified on the right hand side of each figure. Figures 5.4 through 5.11 all use a fixed temperature scale of 65-75°C for reasons discussed later in this chapter.

Figure 5.1 below shows the thermal image of the centre part of the PA-12 tray at room temperature immediately before heating began. The spatial reference grid is not visible here because its temperature was not significantly different to the powder around it.

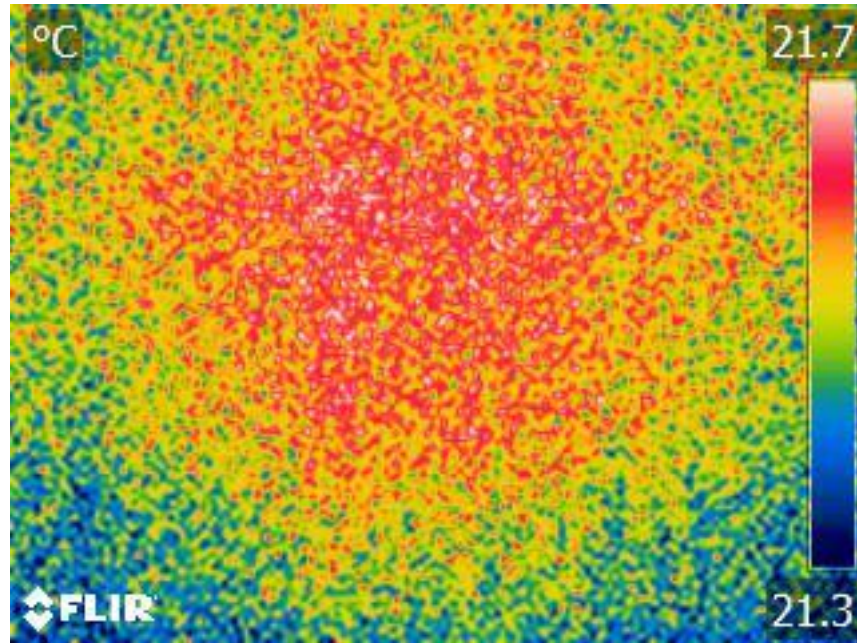


FIGURE 5.1 - INITIAL TESTING - ROOM TEMPERATURE

Figure 5.2 below shows the tray immediately after the centre reached the target temperature of 70°C as measured by the pyrometer. It can be seen that the temperature differential between the hottest (Sp1) and coldest (Sp2) points was 2.9°C, ignoring the cold blue areas immediately next to the measurement bars. This met the targets set for the experiment, however this differential was likely to increase at the much higher temperatures required for the sintering process.

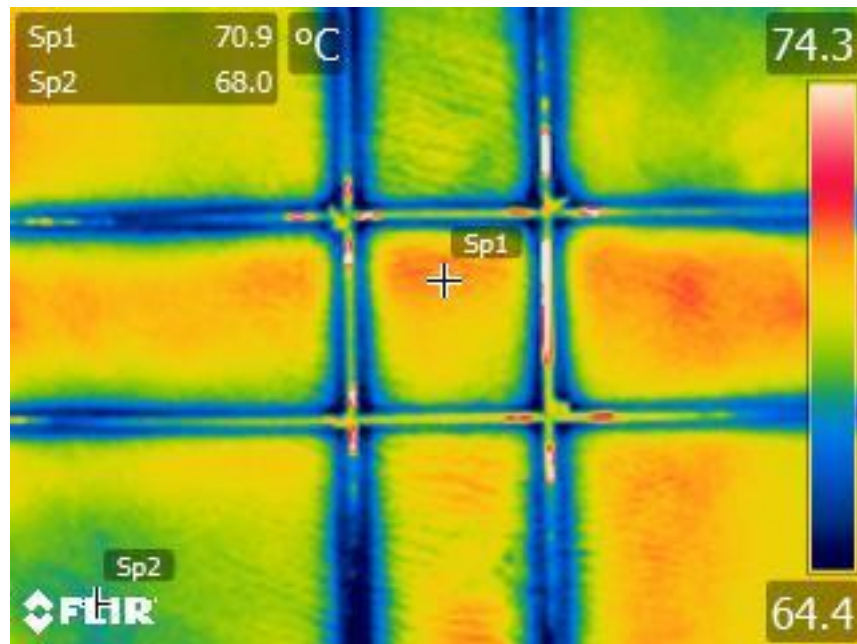


FIGURE 5.2 - INITIAL TESTING - 70 DEGREES

Figure 5.3 shows the powder tray after 1 hour maintained at 70°C. This shows the maximum differential as 3.1°C (Sp1-Sp3). Although more of the image appears to be hotter, it should be noted that this image and the previous one use different colour scales and are in fact very similar.

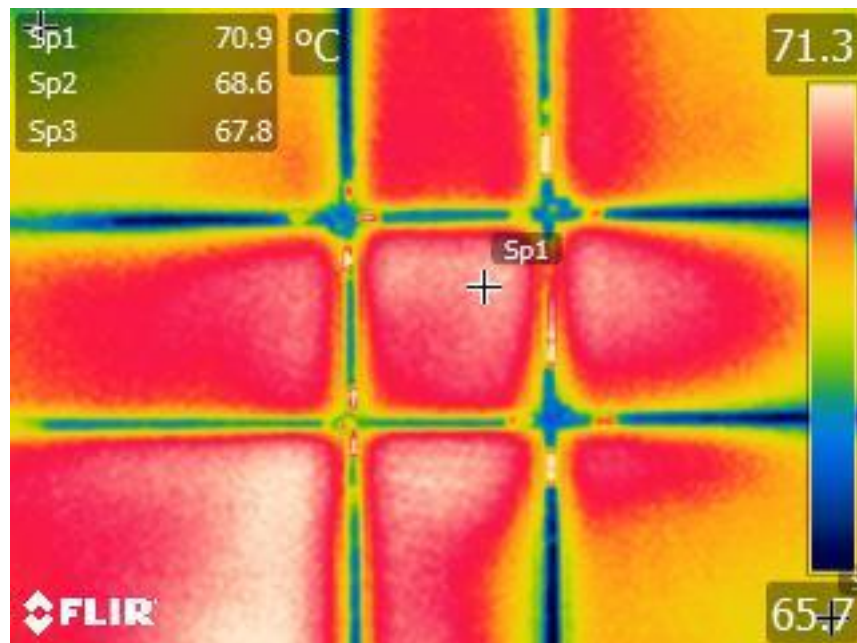


FIGURE 5.3 - INITIAL TESTING - 1 HOUR AT 70 DEGREES

At this stage it was considered that the metal grid would have a tangible effect on the temperature profile of the powder as the metal would conduct and radiate the heat more readily than the surrounding powder. For this reason, the grid was abandoned, and other options examined.

Due to time and resource restrictions it was decided that the only available option was to use the Flir E40 with a fixed colour scale, taking multiple pictures and stitching them together using image processing software. Unfortunately, the resulting stitched images contained some warping and were not spatially accurate, which limited the data available. However, the edges of the tray could be seen, and the temperature differential could be verified covering the primary aims of the experiment.

All the remaining thermal images in this chapter (Figure 5.4 onwards) are taken with a fixed temperature range of 65-75 °C, even where no scale is shown in the image, due to restrictions with the image stitching software used for some images.

Figure 5.4 shows a stitched image of the chamber at 70 °C, which shows a temperature differential of approximately 5°C, which was within the limits for effective sintering, but could be improved upon.

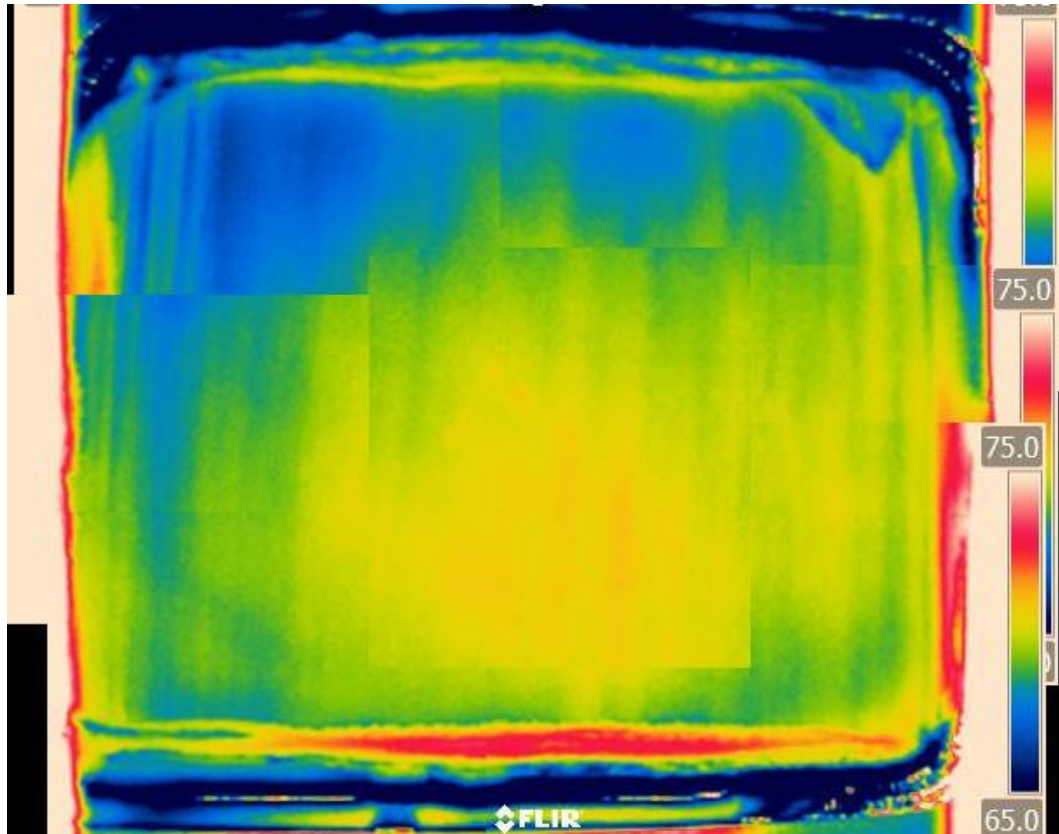


FIGURE 5.4 - INITIAL TESTING - STITCHED IMAGE

5.1.2 REFLECTIONS OF INFRARED HEAT

Due to the pulsed method by which the lamps are powered, it was noted that some of the images taken within seconds of each other seemed to show a significant difference in surface temperature. Specifically, Figure 5.4 and Figure 5.5 were taken within 2 seconds of each other with lamps on and off respectively. The logical conclusion from this was that the lit lamps cause some reflection of heat onto the powder during the 'on' portion of each cycle, making it appear to be a slightly higher temperature. In this case the difference appeared to be approximately 2°C in average surface temperature, while the temperature differential in each image remained consistent at approximately 5°C. As the aim of this specific test was to examine differentials rather than overall temperature, this factor could be ignored, but would need to be considered later when calibrating for temperature accuracy.

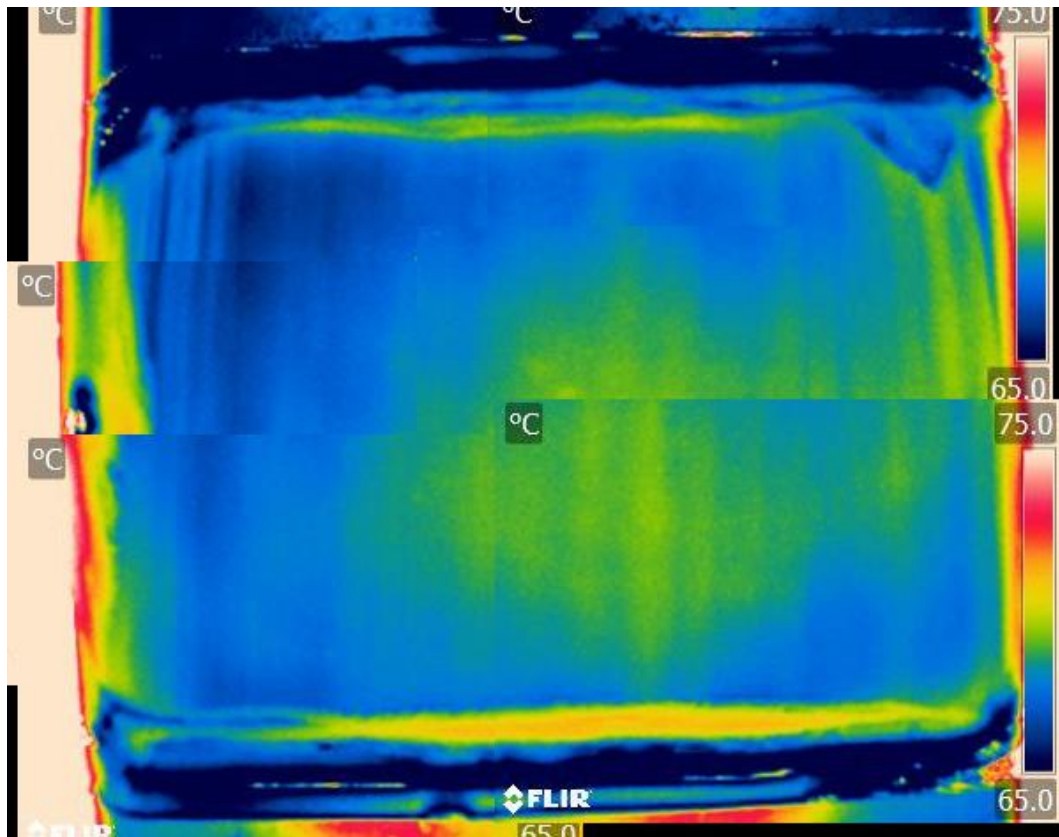


FIGURE 5.5 - CHAMBER AT 70 DEGREES, LAMPS OFF

5.1.3 DIFFERENCE IN THERMAL RESPONSE OF TWO IDENTICAL LAMPS

The two lamps used in the experimental setup were identical and placed symmetrically around the central zinc-selenide chamber window. Tests were performed in order to ensure the thermal responses from each lamp were as similar as practicable, as differences between the two lamps would have caused variances which would make future measurements inaccurate. As such, Figure 5.6 and Figure 5.7 show the thermal response with only left and right lamps powered respectively. In both images, chamber temperature target was set to 70°C as with previous tests, as measured by the pyrometer pointed at the centre of the powder surface.

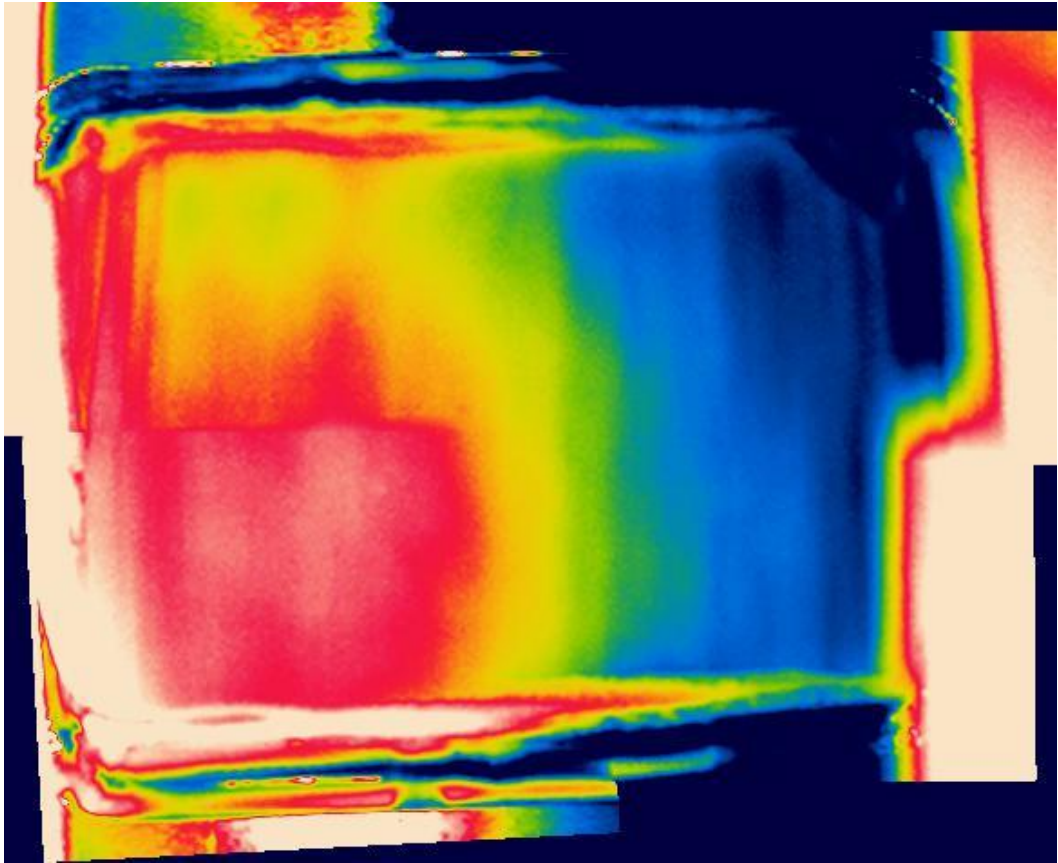


FIGURE 5.6 - STITCHED IMAGES - PYROMETER SIDE LAMP ONLY

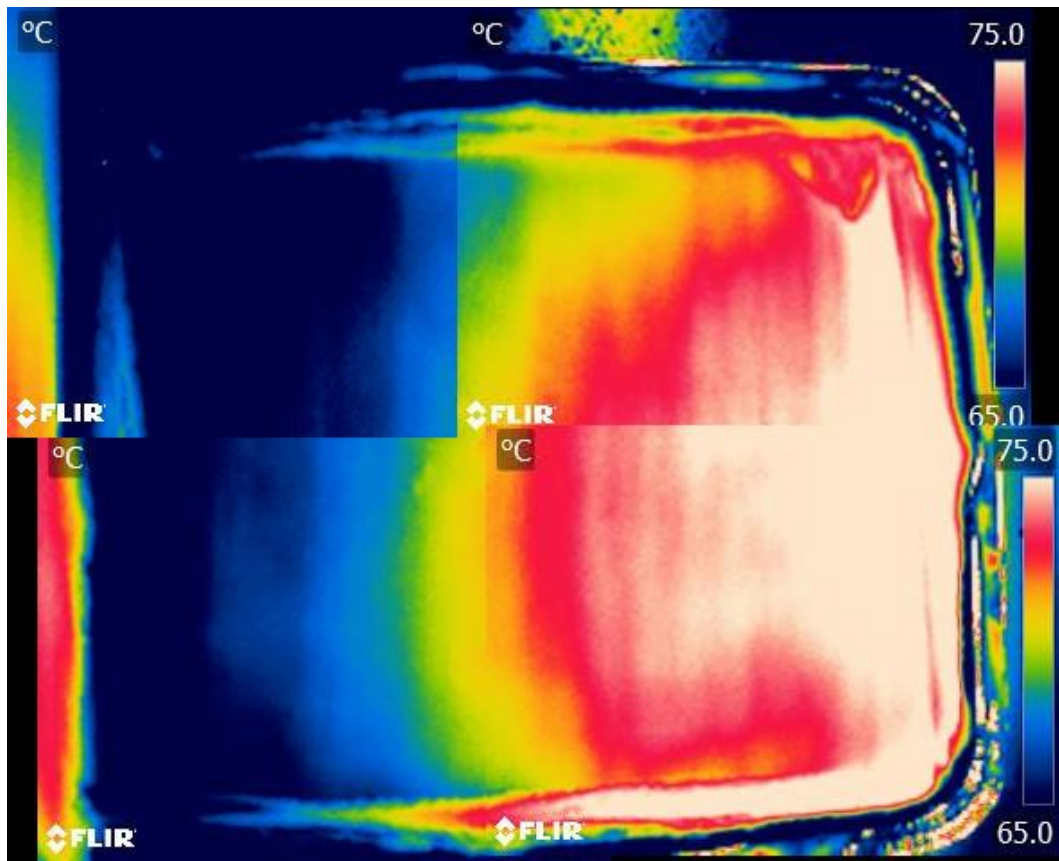


FIGURE 5.7 - STITCHED IMAGES - NON-PYROMETER SIDE ONLY

It can be seen in these images that the thermal response from the two lamps has a differential of approximately 5°C in some areas of the image, notably the pyrometer side lamp heats less in the upper left quarter of the image and the non-pyrometer side lamp heats more down the entire right hand edge of the tray. These differences could be accounted for by variances in the manufacturing of each lamp, or in the surface of the powder itself. Further tests were performed in order to examine this.

Figure 5.8 and Figure 5.9 show the effect of reversing the power connections to each lamp, which is to say that the power to the left lamp was connected to the right lamp and vice-versa. This would explore the possibility that the observed thermal asymmetry may have been due to differences in the way the lamps were powered. From this test it could be seen that, when compared with the previous test, the results were very similar, and this possibility could be discounted as the same asymmetrical feature could be seen in the top left quarter and right-hand edge.

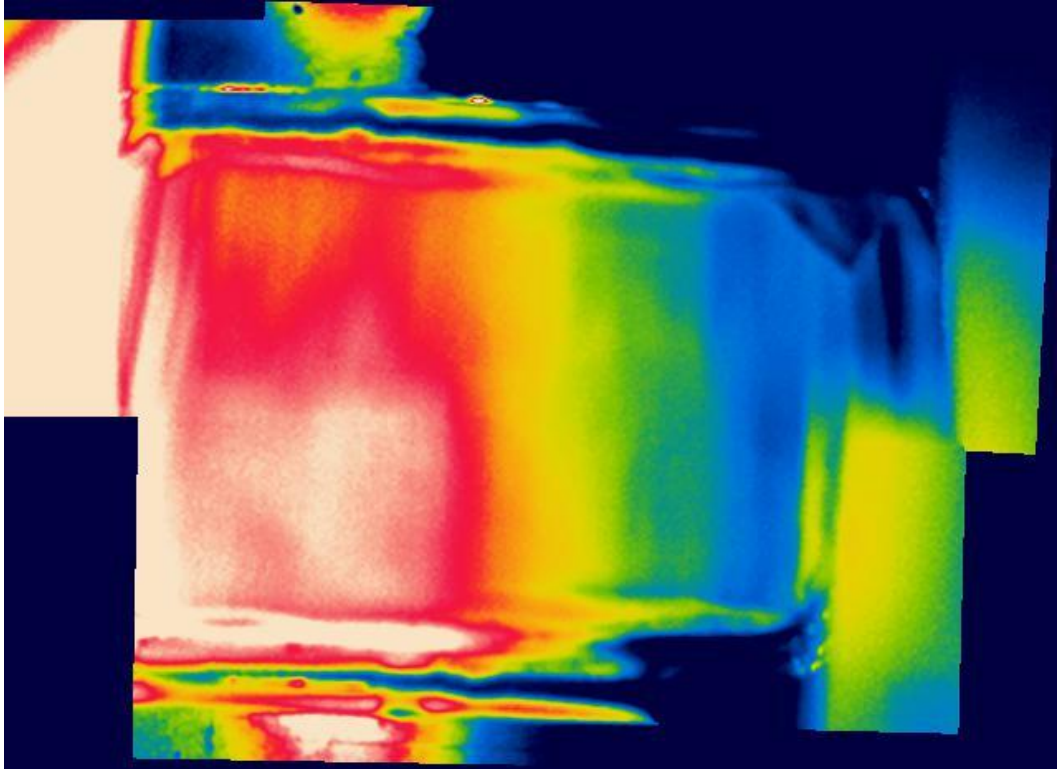


FIGURE 5.8 - LAMP CONNECTIONS REVERSED, PYROMETER SIDE ONLY

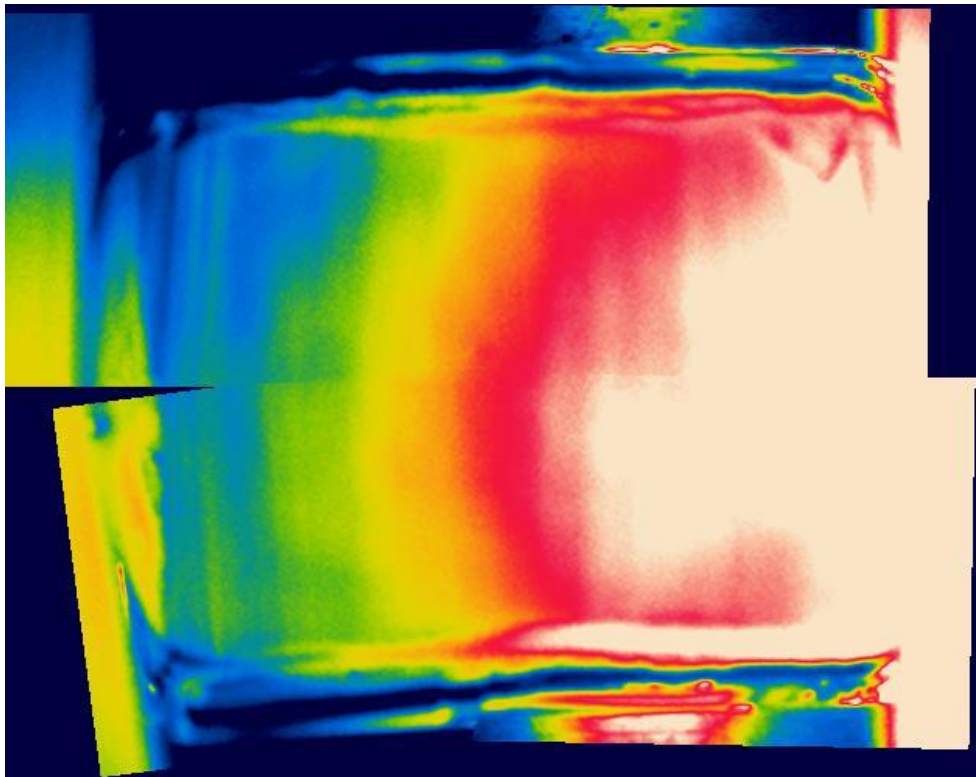


FIGURE 5.9 - LAMP CONNECTIONS REVERSED, NON-PYROMETER SIDE ONLY

Figure 5.10 shows the effect of rotating both lamps 180° within the chamber. If the lamps had had some physical difference from their manufacture, the expected result would have been a lower temperature in the lower left quarter, and a higher temperature 'stripe' near the centre of the image. Instead the thermal response in this image appears to be fairly symmetrical as with previous tests with both lamps powered. At this point it was determined that the asymmetry observed earlier was not significant enough to cause issues in achieving an even temperature profile as the experiment required.

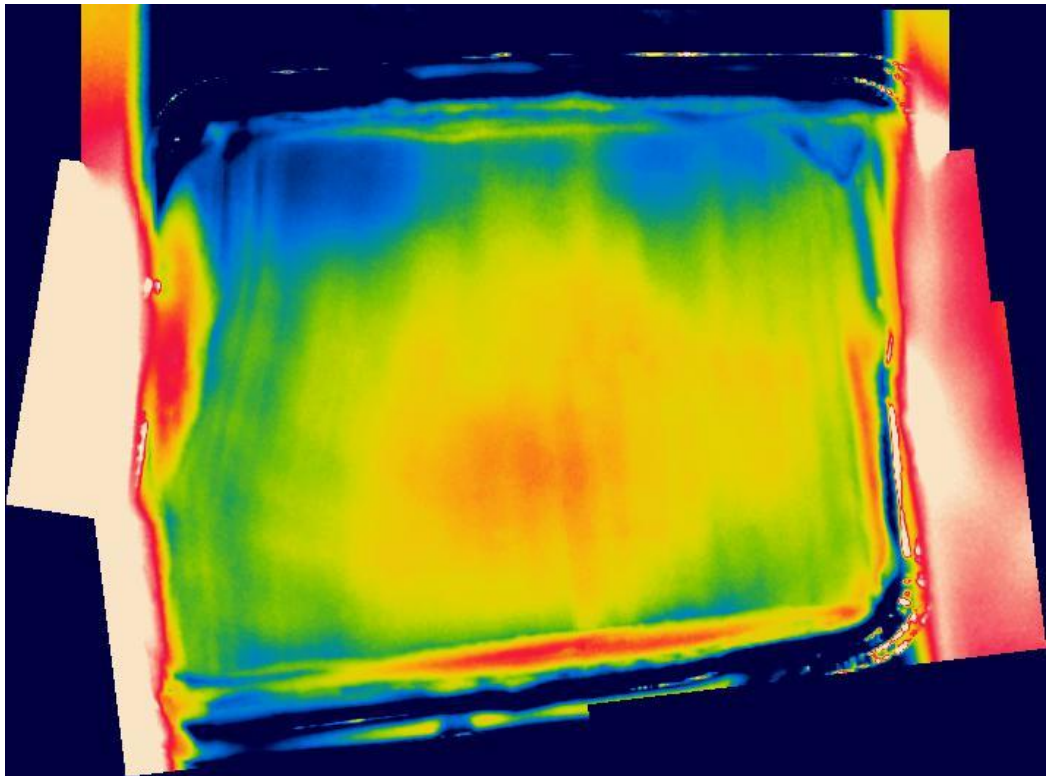


FIGURE 5.10 - BOTH LAMPS, ROTATED 180°

5.1.4 EFFECTS OF MOVING LAMPS AWAY FROM POWDER BED

The final factor examined in the pursuit of an even temperature profile was the distance from the lamps to the powder surface. It was theorised that moving the lamps further from the powder would spread the heat in such a way as to heat the powder more evenly, by diffusing the energy in the space between the two. The two lamps were adjusted to sit at the top of the chamber using the long bolts on which they were mounted. This was the highest point achievable with the current experimental setup. The chamber target was set to 70°C and images taken as previously.

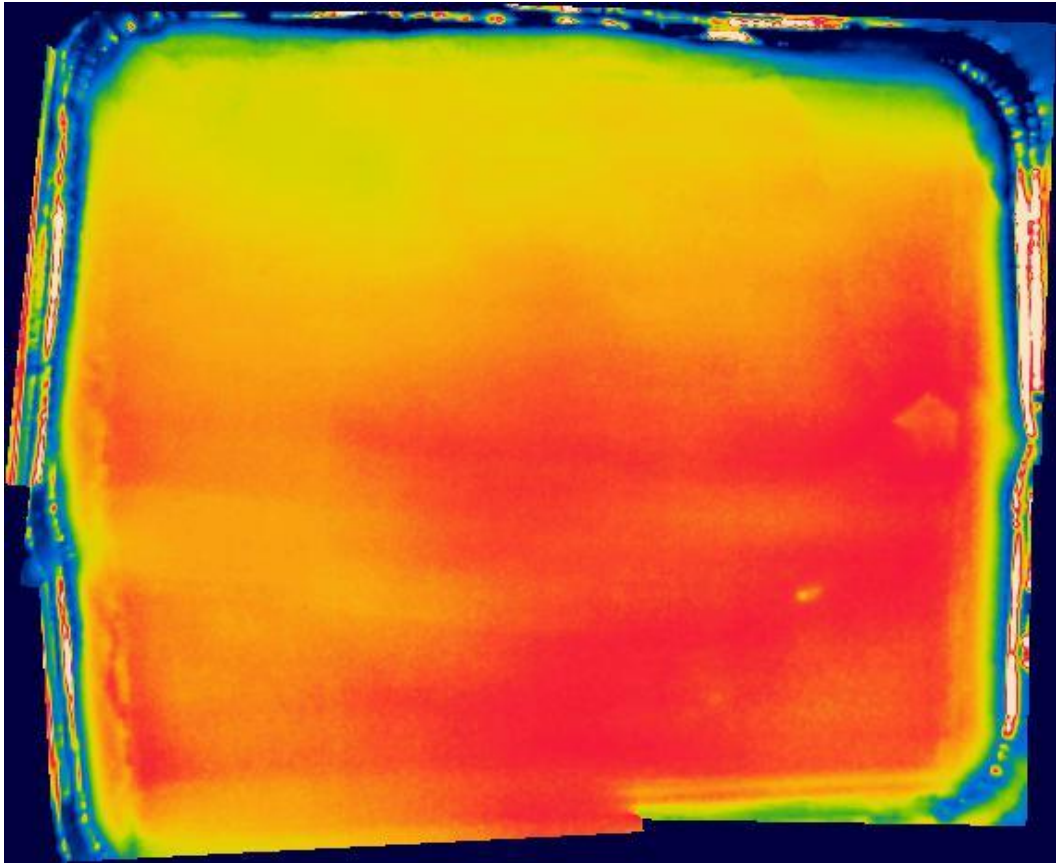


FIGURE 5.11 - STITCHED IMAGES - LAMPS AT UPPERMOST POSITION

The results of this experiment show that in Figure 5.11, as compared with Figure 5.4 where the temperature target is the same but the lamps are mounted approximately 100mm lower, the temperature differential had reduced from approximately 5°C to approximately 2.5°C, well within the aspirational targets for this experiment. This suggests that moving the lamps further from the powder bed 'defocuses' the heat & provides a lower temperature differential on the surface. The height at which the lamps can be mounted is limited by the height of the chamber, though with a taller chamber this effect could be examined further.

5.2 POWER CONSUMPTION OF INFRARED LAMPS

The amount of energy used in heating the experimental chamber is a significant factor in that it affects the amount of power required for the machine to run in an industrial environment and should be as low as possible for logistical and environmental reasons. Several experiments were performed to examine lamp power usage in various situations.

Each test was performed three times and their results averaged, giving the data shown in the following graphs.

First, the chamber target temperature was incremented in 5°C steps, waiting at each step for the chamber to reach the targeted temperature before incrementing again. Using this method, the chamber was increased from room temperature (approximately 20°C) up to 170°C. It was observed that at each step the heater load determined by the PID control loop peaked for a short time to 50% (the maximum allowed by the experimental parameters) before quickly settling to much lower values, the averages of which continued to lower the more time was spent at each step.

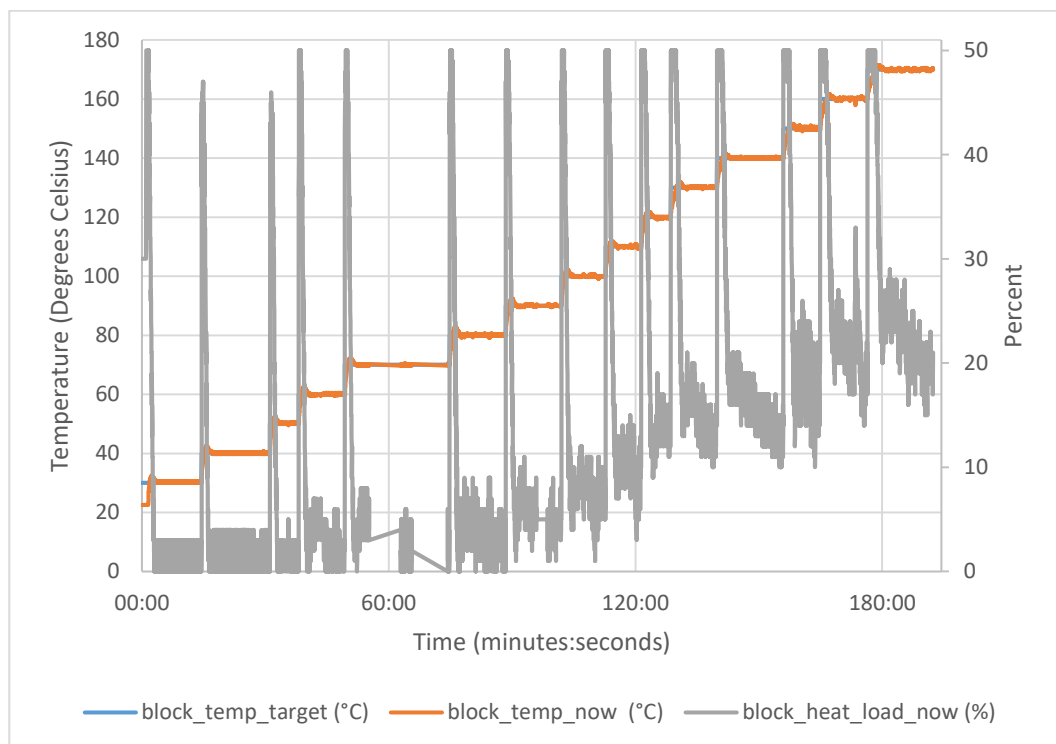


FIGURE 5.12 - LOAD REQUIRED TO MAINTAIN TEMPERATURE IN 5 DEGREE STEPS

The next experiment sought to answer the question of how long would it take for the heater load to settle at a given temperature. The target was set to 100°C and the heaters were allowed to run for an extended period. It can be seen from Figure 5.13 that after approximately 20 minutes the heater load required to maintain this temperature in the chamber settled at approximately 4%:

$$(4\text{kW}/100) * 4 = 160\text{W required to maintain chamber at } 100^{\circ}\text{C}.$$

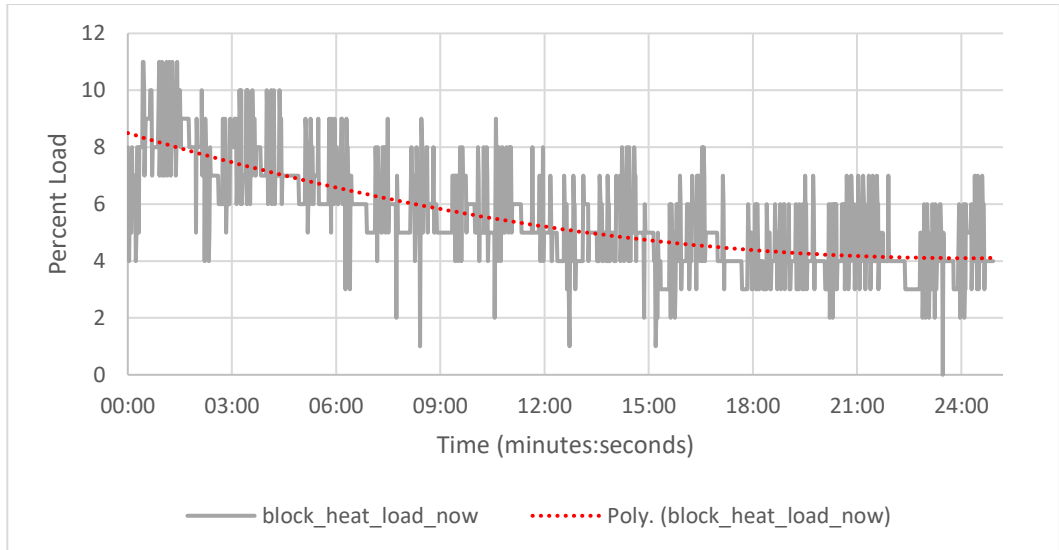


FIGURE 5.13 - CHAMBER AT 100°C FOR 20 MINUTES

In order to understand the effect of using a constant heater load, the chamber was set to heat at 1% load for 20 minutes. Figure 5.14 shows that at 1% load, temperatures approaching 85°C could be reached and maintained. This signifies that if time were no object, high temperatures could be reached with relatively little power available.

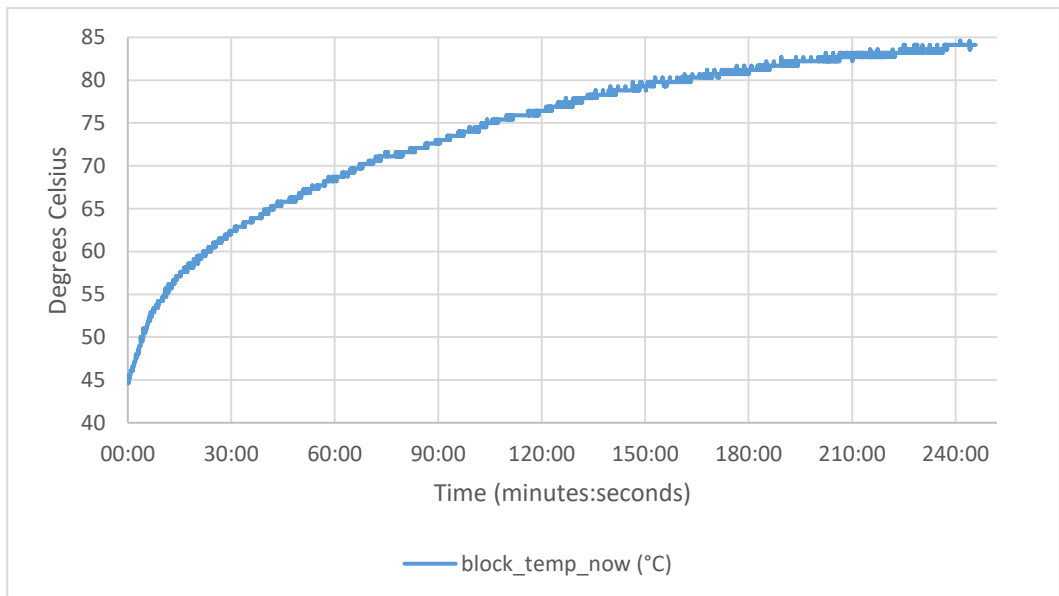


FIGURE 5.14 - CHAMBER AT 1% LOAD FOR 4 HOURS

In order to determine the approximate power usage of the machine, the chamber was set to heat to 170°C and left for 1.5 hours as shown in Figure 5.15. The load required to maintain the temperature dropped gradually until it settled at approximately 15%.

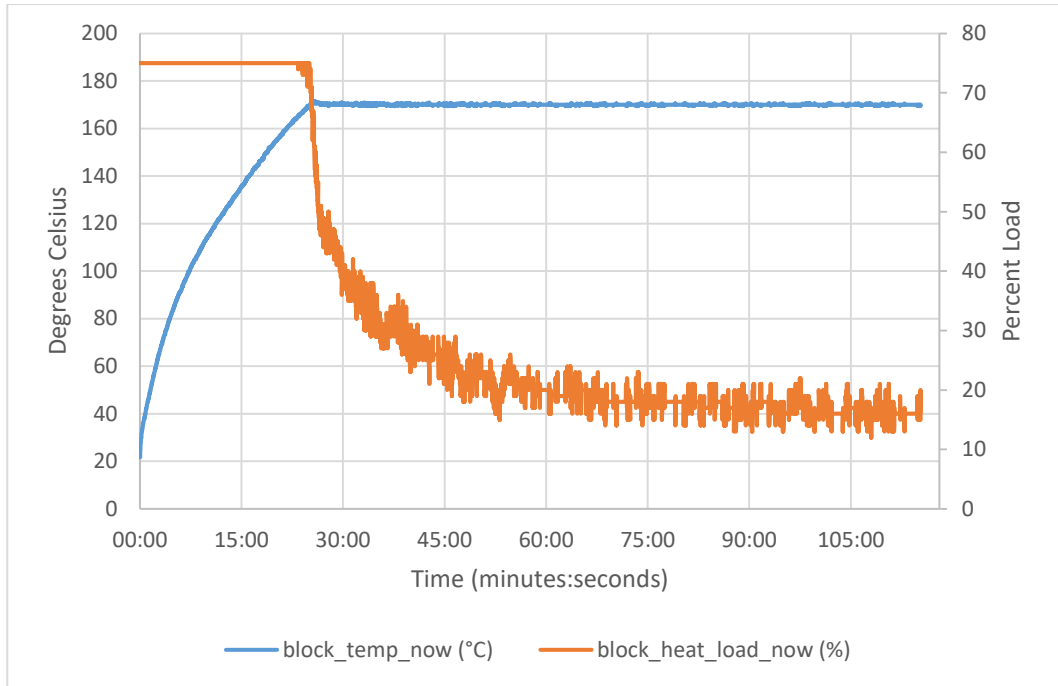


FIGURE 5.15 - CHAMBER AT 170°C FOR 1.5 HOURS

A pair of 2kW infrared lamps were used as detailed in Chapter 3.6, and wired in parallel. At 100% power the lamps were specified to dissipate a total of 4kW, so at 15%:

$$(4000/100) * 15 = 600W \text{ power dissipated at 15\% load.}$$

However, given that working versions of the build chamber were to be larger and of more complicated shape with more heaters, this should not be treated as truly indicative of potential future power dissipation. What could be learned from this experiment was that 4kW would be enough power to heat the area immediately above the build area and build surface, leaving enough load overhead to reach the desired temperature within a reasonably short amount of time.

5.3 PID CONTROL LOOP

An experiment was set up to investigate the effect of tuning PID loop parameters on the temperature control accuracy of an emulated power bed heater. This was achieved by embedding a type T thermocouple and a cartridge heater within an aluminium block. The heater was powered by 230VAC via a solid state relay, controlled by the PLC. The thermocouple readings were fed into the PLC as feedback for the PID loop. Target

temperature and safety cut off values were fed into the PLC from the PC via the serial protocol described in Chapter 2.1; these are listed in appendix A.

The theoretical ideal model for a PID controller can be mathematically defined by the following equation:

$$u(t) = k_p e(t) + k_i \int_0^t e(\tau) d\tau + k_d \frac{de}{dt}$$

The parameters of interest for this experiment were as follows:

k_p – Proportional gain

k_i – Integral gain

k_d – Derivative gain

Loop Update – Period over which control loop repeats, where time in the PID equation can be considered discrete in multiples of PLC processor cycle time.

A shorter PID loop update period allowed the system to react quicker to changes in temperature, but required more processing time from the PLC CPU. For this experiment the PID loop period was nominally set to 1 second, which gave a program cycle time of 20ms including all other parts of the program.

Figure 5.16 shows the results of tuning the PID loop with the following parameters:

$K_c = 60$

$T_i = 0.2$

$T_d = 0.02$

Loop Update = 1 second

Target temperature = 55°C

Using these figures, the experimental setup was brought up to temperature and allowed to cool to room temperature over five separate runs. These results were then averaged as shown below. During all five runs the heater overshoot the target temperature to 57.27°C, before settling between 54.94 and 44.35°C. This can be seen in the typical PID characteristic curve on Figure 5.16. The detailed loop configuration can be seen in Figure 5.17.

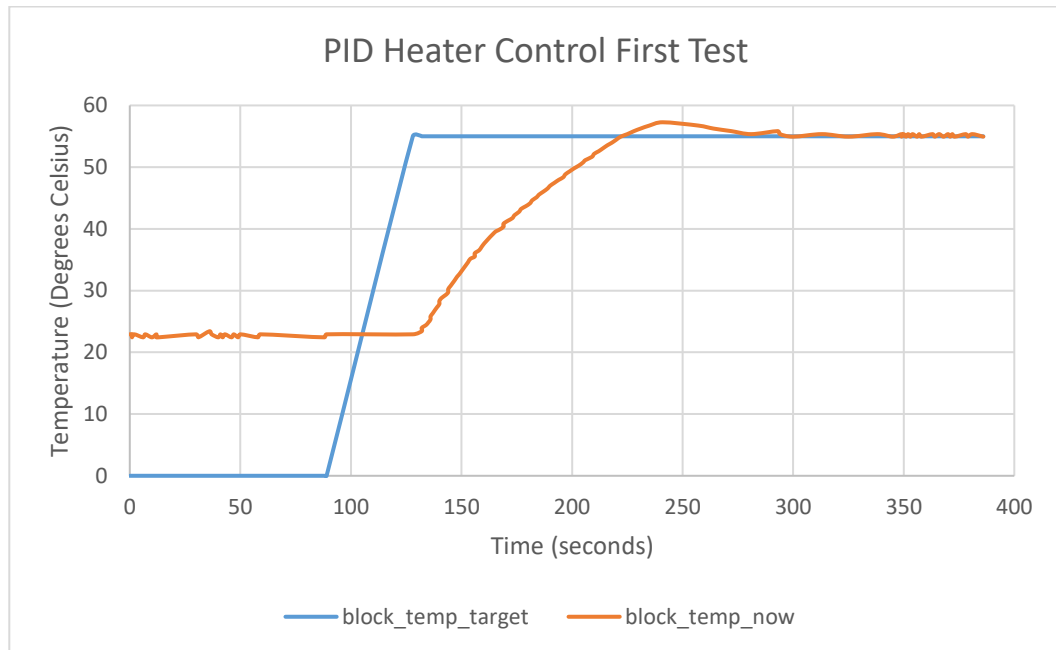


FIGURE 5.16 - RESULTS OF BLOCK HEATING WITH TUNED PID LOOP

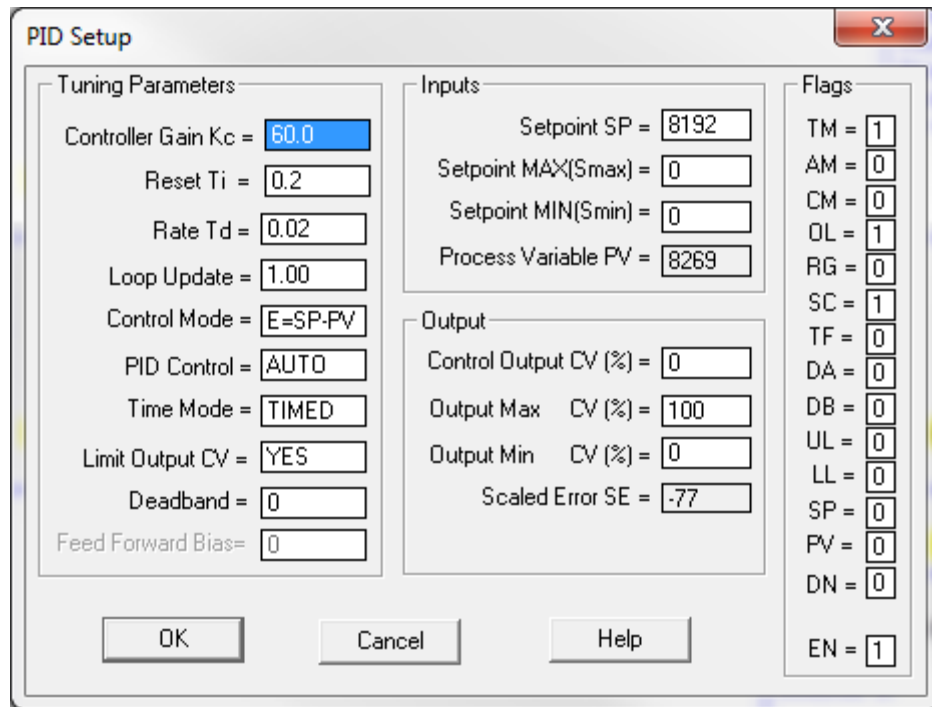


FIGURE 5.17 - PID LOOP CONFIGURATION FROM RSLOGIX 500 SOFTWARE

It is generally expected that any closed loop control system utilising PID will need ‘tuning’ to get the most accurate possible results from the setup. However on this occasion the parameters chosen for the initial tests achieved the desired temperature within an acceptable amount of time and did not suffer significantly from the characteristic oscillation which is indicative of a PID loop in need of further turning (Hardy, 2014). For this reason, and the fact that any other physical setup would require different tuning anyway, the results were accepted, and the test concluded.

6 NITROGEN FLOW CONTROL

SLS AM machines require their internal atmosphere to be inert so as to avoid oxidation or combustion of the build medium. To this end the build chamber described in Chapter 3.6 needed to be flooded with an inert gas; usually argon or nitrogen. This work used nitrogen due to its low cost and relative availability.

Figure 6.1 shows the control board of the Fujikura FCX-MW oxygen sensor which was used to measure the percentage of oxygen within the build chamber. This required a 5VDC power supply and returned a 0-5VDC analog signal representing the current value.

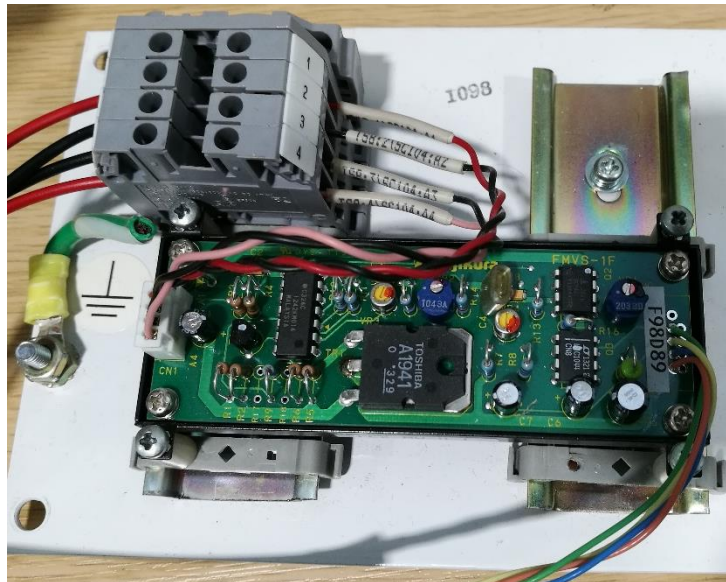


FIGURE 6.1 - OXYGEN SENSOR CONTROL UNIT

A small chamber was constructed, seen in Figure 6.2 (1), to simulate the setup needed to supply nitrogen to the chamber and measure the proportion of oxygen present. The oxygen sensor (2) was mounted on the inside of the chamber with its wire protruding from a hole and leading to the control board shown in Figure 6.1. Two solenoid operated valves (3 and 4) provided nitrogen to the chamber such that both valves open represented a 'fast' flow and one valve open represents a 'slow' or 'trickle' flow to the

chamber, though it should be noted that both valves had the same amount of gas throughput and were allocated names arbitrarily.

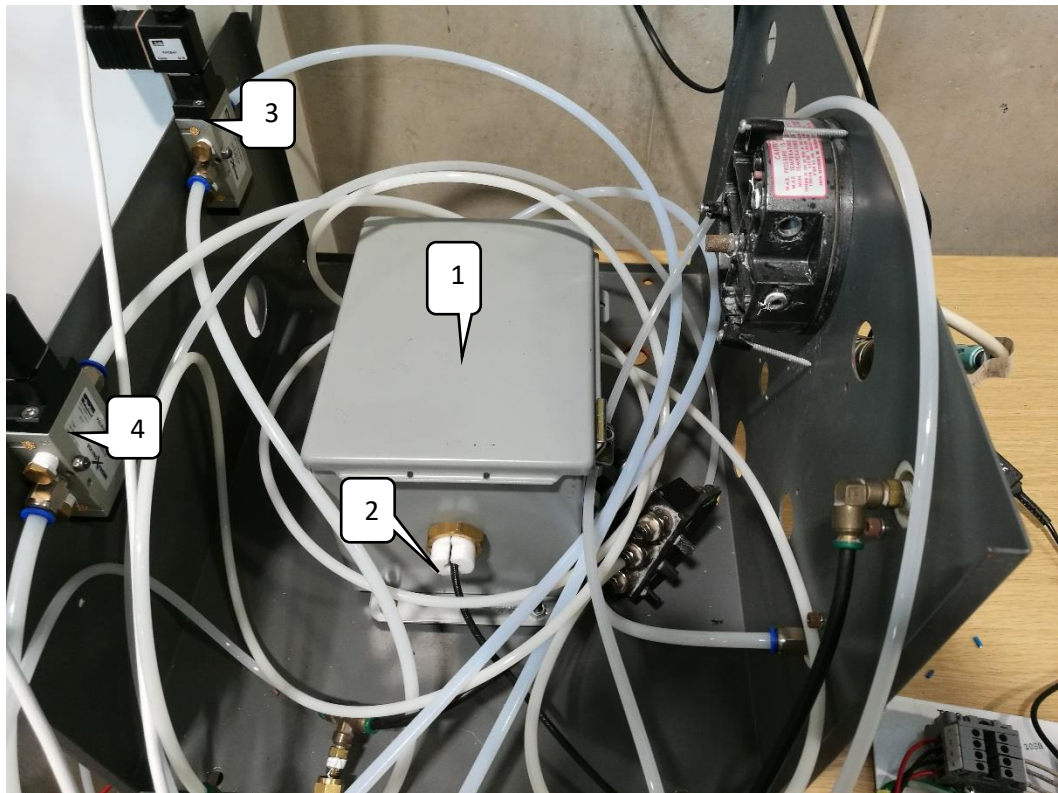


FIGURE 6.2 - EXPERIMENTAL OXYGEN SENSOR CHAMBER

As keeping an inert atmosphere within the build chamber was critical to the viability of a build, it was equally as important to have a gas delivery system which could provide the chosen gas at a rate faster than it could 'leak' from the machine's various holes and seams, effectively maintaining a positive atmospheric pressure within the build chamber. Figure 6.3 shows the nitrogen generator used during this project, for testing the nitrogen delivery system and deoxygenating the experimental heat chamber.



FIGURE 6.3 - NITROGEN GENERATOR

The two valves and the oxygen sensor worked together in a feedback loop to bring the build chamber's oxygen content down below a user specified threshold (varies by the build medium used, but usually around 5%) and keep it there for the duration of the build. The valves were controlled by the PLC's TRIAC module and the oxygen sensor's output signal was fed to one of the PLC's analog input modules. When a build is started, once the door is closed and system safety requirements are met, both valves were opened in order to inert the chamber as fast as possible. Once the threshold is reached the 'fast' valve was closed, leaving the 'slow' valve to maintain the current level. If the oxygen level reached 0.1%, which is unlikely due to the chamber's 'leakage' factor, the slow valve was then closed to allow the oxygen level to rise, because the Fujikura FCX-MW would have normally output 0% under failure conditions. This meant the PLC could treat a 0% input as a system failure and take the appropriate safety measures, making the system 'fail safe'. Under normal operation if the oxygen level rose toward the threshold, the slow valve was simply opened again.

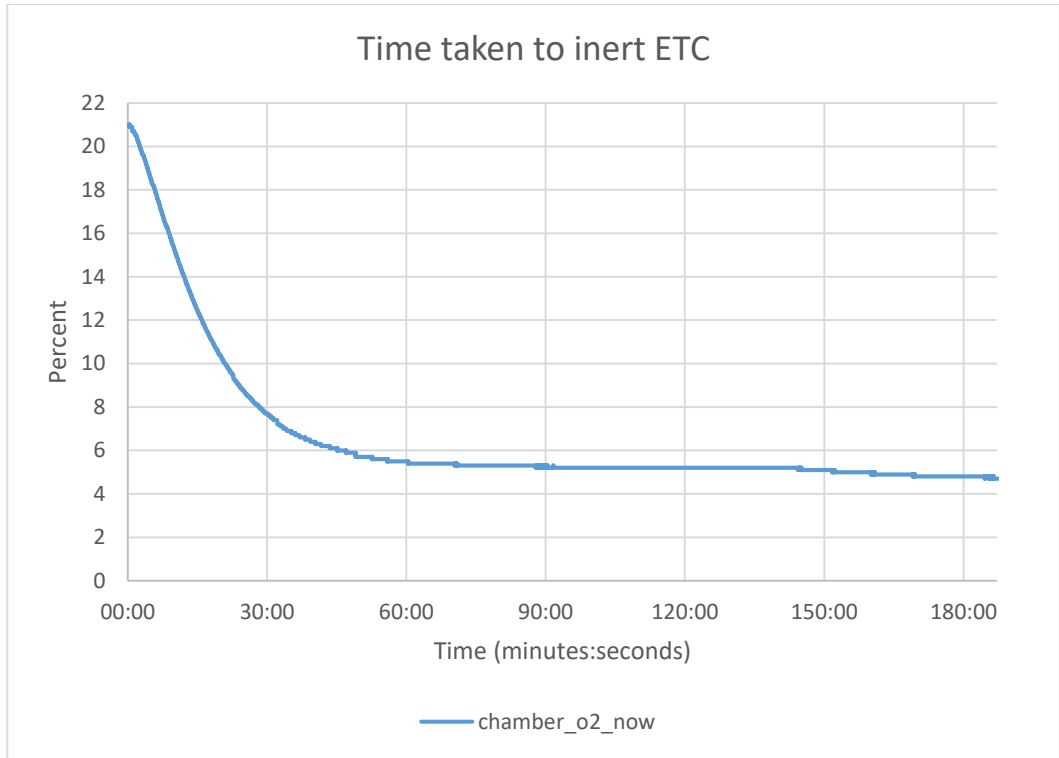


FIGURE 6.4 - TIME TAKEN TO INERT ETC 13/10 AM

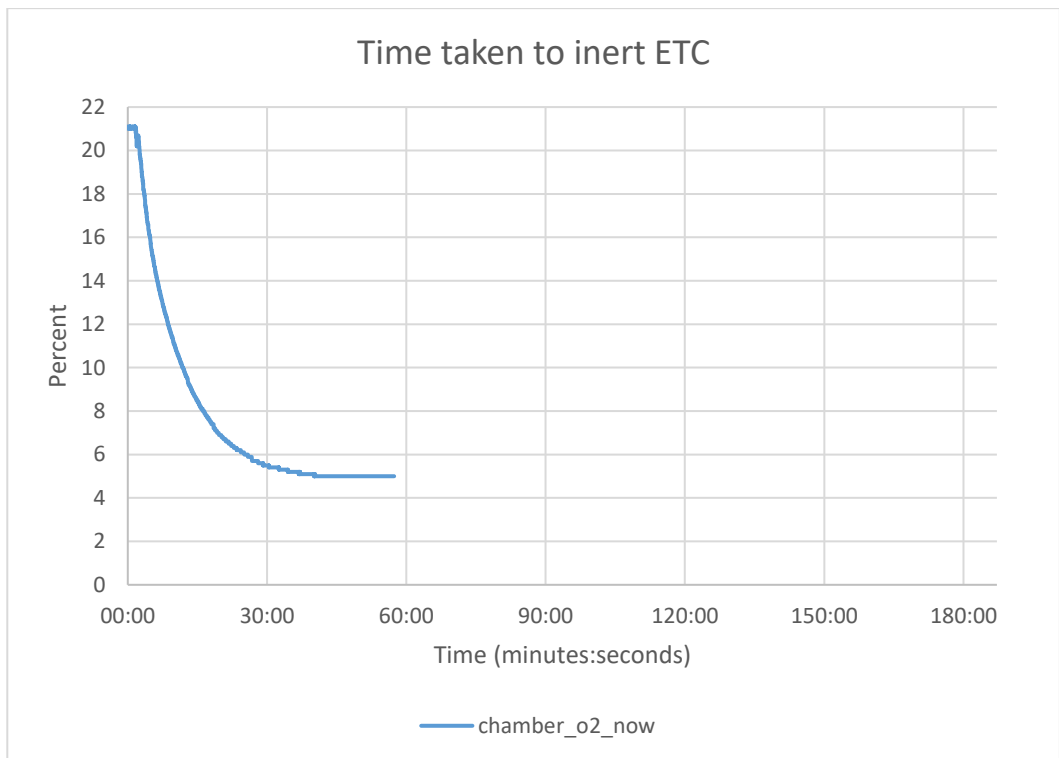


FIGURE 6.5 - TIME TAKEN TO INERT ETC 13/10 PM

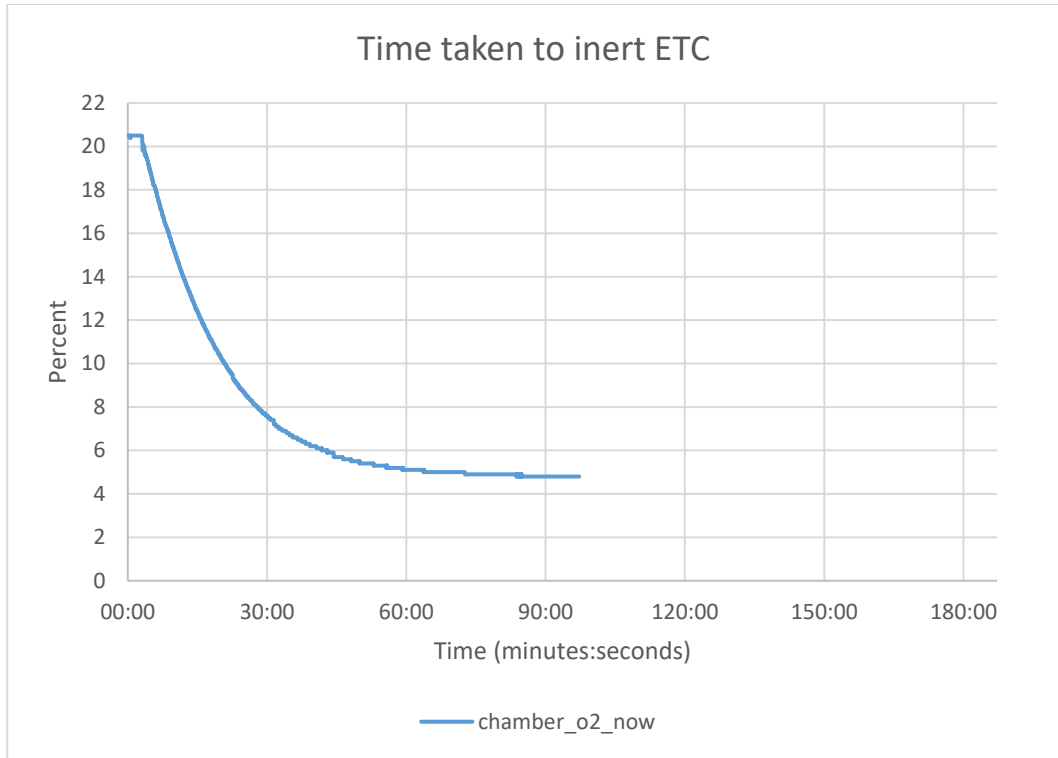


FIGURE 6.6 - TIME TAKEN TO INERT ETC 14/10 AM

Figures 6.4, 6.5 & 6.6 show the time taken to reduce the oxygen content within the environmental test chamber to 5%. The runs took approximately 1 hour, 30 minutes and 1 hour respectively. It was noted that residual nitrogen in the hoses during the second test may have caused it to be quicker as the first and third tests were run on a 'cold' system in the morning, where the second was done shortly after the first. It was also noted that the system could have been made significantly faster by employing a ballast tank, as the nitrogen generator used was not sufficient for reducing the chamber's oxygen content within an acceptable timeframe.

With the confirmation that the hardware and software setups had the capability to control the chamber oxygen content reliably, and that this could be achieved much faster with a better nitrogen source, the experiment was concluded in order to focus on other, more significant system elements.

7 LAYER THICKNESS ACCURACY

Z-height resolution of AM machines is limited by a number of factors, perhaps the most prevalent of which is the repeatable accuracy with which the build platform (or extruder head) can be moved up and down. During the work considerable time was spent investigating this as a highly accurate build piston may allow future investigation into the use of powders with smaller particle sizes, at potentially smaller z-height resolution.

7.1 PISTON ACCURACY

A number of experiments were performed using the 'build dolly simulator' described in sub-chapter 3.3. The initial aim was for the build piston to be reliably movable in 10 μ m steps for use with PA12 powder, whose particle sizes range from 10 to 50 μ m (Sigma-Aldrich, 2019).

The 'build dolly simulator' was wired into the PLC's first step motor control module through the Parker step motor controller shown in Figure 7.1. The three inductive proximity detectors were wired directly into the PLC's first step motor control module as limit switches along with the encoder, which was mounted on the rear shaft of the step motor. A full wiring 'block' diagram can be seen in Figure 7.2. A digital micrometer was mounted to the platform to accurately measure movement down to 1 μ m.



FIGURE 7.1 - STEP MOTOR CONTROLLER

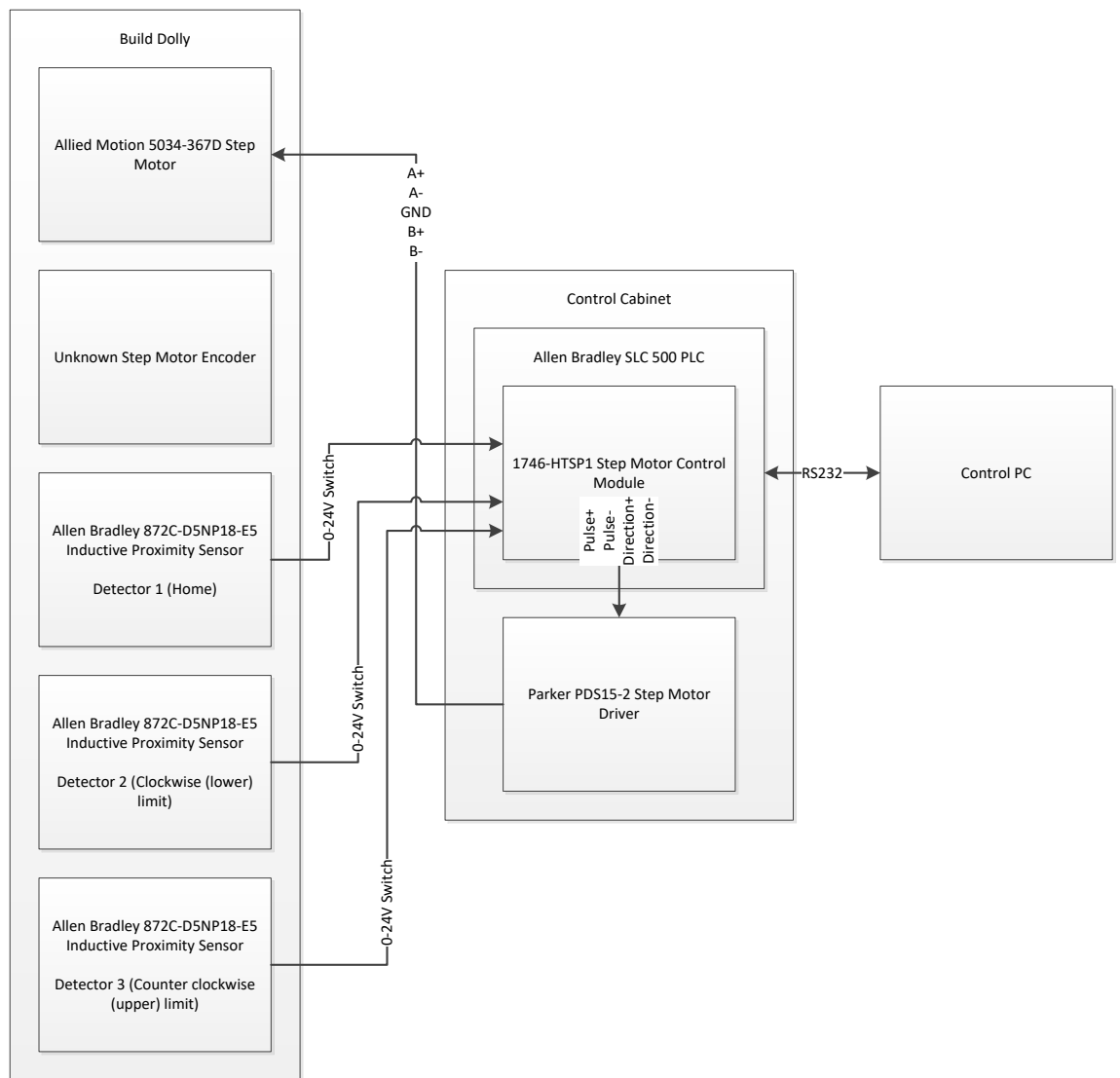


FIGURE 7.2 - BUILD DOLLY SIMULATOR WIRING BLOCK DIAGRAM

The PLC code written for these experiments was initially a simple timed loop to move the platform up and down by a fixed number of pulses. Subsequent experiments built on the code until it was fully featured and thoroughly tested, at which point it was merged with the main project PLC code file. Below are the initial parameters set on the PLC's step motor controller:

- Starting speed: 100 pulses per second
- Velocity: 125000 pulses per second
- Acceleration/deceleration: 2000 pulses per second²

7.2 EXPERIMENT 1

The PLC was programmed to move the step motor 149400 pulses (10mm), change the direction and repeat. The results can be seen in Table 7.1 below. Note that one movement represents one full cycle (up and down).

TABLE 7.1 - RESULTS OF REPEATEDLY MOVING BUILD PISTON 10MM IN EITHER DIRECTION

Number of movements	Upper measurement (mm)	Lower measurement (mm)
1	0	10
100	0.03	10
200	0.02	9.96
300	0.04	9.96
400	0.09	9.98
500	0.03	9.98
600	0.06	9.97
700	0.05	9.94
800	0.07	9.97
900	0.05	9.97
1000	0.08	9.99

It can be seen from the results that the piston was relatively accurate, but not sufficient to meet the criteria set earlier in this chapter. It should be noted that at this stage the encoder was not wired into the system and the 'build dolly simulator' suffered from a great deal of mechanical backlash, both of which had a considerable effect on accuracy.

7.3 EXPERIMENT 2

The next experiment performed was similar, but this time concentrated on movements of varying distance made in the same direction. All moves performed were downwards as this better simulated the build piston during a build. Results are shown in table 7.2 below.

TABLE 7.2 – RESULTS OF MOVING BUILD PISTON VARYING DISTANCES DOWNWARDS

Number of moves	Distance measured (by increment distance in mm (pulses))									
	1 (15200)	2 (30400)	3 (44700)	4 (59800)	5 (74900)	6 (89200)	7 (104200)	8 (121000)	9 (136600)	10 (149400)
1	1.03	1.99	3.00	3.98	5.00	5.98	7.00	8.03	9.01	9.9
2	1.97	4.04	6.00	7.88	9.88	11.87	13.85	16.07	18.1	19.82
3	3.00	6.06	8.89	11.87	14.78	17.74	20.68	24.09	n/a	n/a
4	4.02	8.01	11.86	15.81	19.8	23.66	n/a	n/a	n/a	n/a
5	5.04	10.06	14.74	19.81	24.76	n/a	n/a	n/a	n/a	n/a
6	6.06	12.1	17.75	23.7	n/a	n/a	n/a	n/a	n/a	n/a
7	7.07	14.06	20.69	n/a	n/a	n/a	n/a	n/a	n/a	n/a
8	8.00	16.09	23.67	n/a	n/a	n/a	n/a	n/a	n/a	n/a
9	9.00	18.18	n/a	n/a	n/a	n/a	n/a	n/a	n/a	n/a
10	10.03	20.17	n/a	n/a	n/a	n/a	n/a	n/a	n/a	n/a
11	11.04	22.15	n/a	n/a	n/a	n/a	n/a	n/a	n/a	n/a
12	12.07	24.23	n/a	n/a	n/a	n/a	n/a	n/a	n/a	n/a
13	13.08	n/a	n/a	n/a	n/a	n/a	n/a	n/a	n/a	n/a
14	14.04	n/a	n/a	n/a	n/a	n/a	n/a	n/a	n/a	n/a
15	15.04	n/a	n/a	n/a	n/a	n/a	n/a	n/a	n/a	n/a
16	16.08	n/a	n/a	n/a	n/a	n/a	n/a	n/a	n/a	n/a
17	17.09	n/a	n/a	n/a	n/a	n/a	n/a	n/a	n/a	n/a
18	18.12	n/a	n/a	n/a	n/a	n/a	n/a	n/a	n/a	n/a
19	19.13	n/a	n/a	n/a	n/a	n/a	n/a	n/a	n/a	n/a
20	10.12	n/a	n/a	n/a	n/a	n/a	n/a	n/a	n/a	n/a
21	21.06	n/a	n/a	n/a	n/a	n/a	n/a	n/a	n/a	n/a
22	22.08	n/a	n/a	n/a	n/a	n/a	n/a	n/a	n/a	n/a
23	23.09	n/a	n/a	n/a	n/a	n/a	n/a	n/a	n/a	n/a
24	24.11	n/a	n/a	n/a	n/a	n/a	n/a	n/a	n/a	n/a
25	25.13	n/a	n/a	n/a	n/a	n/a	n/a	n/a	n/a	n/a

It can be seen that while the piston was slightly more accurate than the previous experiment due to a small improvement in mechanical backlash by moving the piston in only one direction, the error produced accumulated over a number of movements resulting in a larger error. It should again be noted that the encoder was not present in the system for this experiment due to component availability.

7.4 EXPERIMENT 3

In order to further improve accuracy, an encoder was added to the rear shaft of the stepper motor and wired into the PLC stepper motor control module. Detector 1 then

became the home proximity sensor and home detection was provided by the marker pulse (Z) from the encoder. This provided positional feedback to the PLC which allowed for much greater accuracy. A new experiment was performed moving the platform in both directions at a distance of 10mm per move in order to assess repeatable accuracy. Note that a full up and down cycle = 2 movements of 152500 pulses each.

TABLE 7.3 –MOVING BUILD DOLLY SIMULATOR REPEATEDLY AT VARYING DISTANCES

Number of movements	Upper measurement (mm)	Lower measurement (mm)
1	0	9.85
10	0.01	9.85
20	0	9.85
30	-0.03	9.84
40	0	9.85
50	-0.01	9.86
60	0.01	9.87
70	0.01	9.87
80	0	9.87
90	0	9.86
100	0.02	9.87

This shows positional accuracy as being fairly consistent, with the maximum difference between measurements being 0.03mm. The mean average error between measurements was 0.00909mm or approximately 10 µm. This met the accuracy target required, though more testing could be performed to ensure consistency and repeatability, improving it if possible.

7.5 EXPERIMENT 4

Next, experiment 2 was repeated with a few notable changes:

- The PLC software was changed to use ‘absolute’ moves instead of the ‘relative’ moves in previous experiments. These were more accurate in theory as the platform could be freely moved to any specific position along its travel rather than up or down by a specified amount.

- An encoder had been added since the previous attempt and as such the system should have been inherently be more accurate.
- Movement was measured in encoder pulses rather than platform movement, as the experimental rig’s mechanical backlash could not be fixed electronically, and it could be assumed that a production machine would need to minimise this through mechanical design. Pulses were counted using an external pulse counting unit.
- Target distances were in multiples of 4000 pulses, which corresponded to 1 revolution of the motor, which allowed for easier monitoring of rotation via the alignment of a physical mark on the motor rear shaft and encoder casing.
- The number of moves performed at each distance was limited due to the 25mm travel of the digital micrometer used in this setup.

TABLE 7.4 - SECOND ATTEMPT MOVING PISTON DOWNWARDS REPEATEDLY AT VARYING DISTANCES

No. of moves	Distance measured (by increment distance in pulses)									
	16000	32000	48000	64000	80000	96000	112000	128000	144000	160000
1	16000	32000	48000	64000	80000	96000	112000	128000	144000	160000
2	16000	32000	48000	64000	80000	96000	112000	128000	144000	160000
3	16000	32000	48000	64000	80000	96000	112000	128000	n/a	n/a
4	16000	32000	48000	64000	80000	96000	n/a	n/a	n/a	n/a
5	16000	32000	48000	64000	80000	n/a	n/a	n/a	n/a	n/a
6	16000	32000	48000	64000	n/a	n/a	n/a	n/a	n/a	n/a
7	16000	32000	48000	n/a	n/a	n/a	n/a	n/a	n/a	n/a
8	16000	32000	48000	n/a	n/a	n/a	n/a	n/a	n/a	n/a
9	16000	32000	n/a	n/a	n/a	n/a	n/a	n/a	n/a	n/a
10	16000	32000	n/a	n/a	n/a	n/a	n/a	n/a	n/a	n/a
11	16000	32000	n/a	n/a	n/a	n/a	n/a	n/a	n/a	n/a
12	16000	32000	n/a	n/a	n/a	n/a	n/a	n/a	n/a	n/a
13	16000	n/a	n/a	n/a	n/a	n/a	n/a	n/a	n/a	n/a
14	16000	n/a	n/a	n/a	n/a	n/a	n/a	n/a	n/a	n/a
15	16000	n/a	n/a	n/a	n/a	n/a	n/a	n/a	n/a	n/a
16	16000	n/a	n/a	n/a	n/a	n/a	n/a	n/a	n/a	n/a
17	16000	n/a	n/a	n/a	n/a	n/a	n/a	n/a	n/a	n/a
18	16000	n/a	n/a	n/a	n/a	n/a	n/a	n/a	n/a	n/a
19	16000	n/a	n/a	n/a	n/a	n/a	n/a	n/a	n/a	n/a
20	16000	n/a	n/a	n/a	n/a	n/a	n/a	n/a	n/a	n/a
21	16000	n/a	n/a	n/a	n/a	n/a	n/a	n/a	n/a	n/a
22	16000	n/a	n/a	n/a	n/a	n/a	n/a	n/a	n/a	n/a
23	16000	n/a	n/a	n/a	n/a	n/a	n/a	n/a	n/a	n/a
24	16000	n/a	n/a	n/a	n/a	n/a	n/a	n/a	n/a	n/a
25	16000	n/a	n/a	n/a	n/a	n/a	n/a	n/a	n/a	n/a

These results show that the step motor achieved very good accuracy when not considering the mechanical backlash introduced by the gearbox and lead screw. This meant ultimately the system's accuracy was primarily defined by its mechanical design, as electronically the system was accurate to within $\pm 0.06\mu\text{m}$ movement of the platform (a single motor pulse).

7.6 EXPERIMENT 5

Next a test was performed in order to assess the system's capability to send the platform to the 'home' position reliably. This test was measured with a digital micrometer as with previous tests, so mechanical backlash could be assessed. Because of the previous test results, it could be assumed that the step motor moved by the exact number of pulses requested by the PLC software. The home operation was performed in a downward direction in every case.

TABLE 7.5 - REPEATED HOMING OPERATIONS AT VARIOUS SPEEDS

Move no.	Speed (Hz)	Home position (mm)	Move no.	Speed (Hz)	Home position (mm)
Benchmark	N/A	0	31	25000	-0.02
1	10000	-0.04	32	25000	-0.03
2	10000	-0.02	33	25000	-0.01
3	10000	-0.01	34	25000	-0.06
4	10000	-0.04	35	25000	-0.03
5	10000	-0.02	36	25000	-0.05
6	10000	-0.03	37	25000	-0.02
7	10000	-0.04	38	25000	-0.02
8	10000	-0.04	39	25000	-0.04
9	10000	-0.02	40	25000	-0.02
10	10000	-0.05	41	50000	-0.05
11	10000	-0.04	42	50000	-0.09
12	10000	-0.04	43	50000	-0.08
13	10000	-0.03	44	50000	-0.06
14	10000	-0.04	45	50000	-0.07
15	10000	-0.05	46	50000	-0.04
16	10000	-0.04	47	50000	-0.06
17	10000	-0.01	48	50000	-0.05
18	10000	-0.04	49	50000	-0.05
19	10000	-0.04	50	50000	-0.04
20	10000	0	51	50000	-0.07
21	25000	-0.05	52	50000	-0.04
22	25000	-0.05	53	50000	-0.05
23	25000	-0.07	54	50000	-0.05
24	25000	-0.06	55	50000	-0.06
25	25000	-0.04	56	50000	-0.05
26	25000	-0.03	57	50000	-0.04
27	25000	-0.03	58	50000	-0.05
28	25000	-0.04	59	50000	-0.05
29	25000	-0.04	60	50000	-0.05
30	25000	-0.02			

These results gave average error results at each speed tested, as follows:

- Average error at 10000 Hz = 0.032mm
- Average error at 25000 Hz = 0.0365mm
- Average error at 50000 Hz = 0.055mm

Predictably, the homing accuracy was better at slower speeds. Given that each operation was performed downwards it could be said that this was because of a slight overshoot of the target position, shown by the small negative value of most of the results. Some of the variation in these values could be attributed to the mechanical backlash discussed earlier.

7.7 CONCLUSION

In conclusion, it was clear that step motor control systems could be made to be extremely accurate due to the large number of steps per resolution on modern step motors in combination with high resolution rotary encoders and PLCs with high speed processors. It was also clear that the majority of inaccuracies in this system were introduced mechanically and must be remedied with careful design and highly accurate manufacturing methods.

8 POWDER DELIVERY SYSTEM

One major drawback of current SLS systems is that all of the required powder must be loaded into the machine prior to the build starting. This means that if an operator loads an incorrect amount of powder for a build, the build will always have to be stopped and restarted from scratch. This wastes much time and usually some powder. In an attempt to address this issue, a system was designed such that powder was fed into an internal 'feed bin' (equivalent to a 'feed piston' typically used in more established SLS processes) via several augers from an external 'feed hopper'. This meant that any amount of powder could be loaded into the machine externally while a build was running and had the added benefit that the machine could be made considerably smaller due to the lack of need for two separate feed pistons.

An experimental rig was constructed to emulate this process and assess its effectiveness. The rig contained a scaled down version of the mechanism using three augers spaced evenly across the output powder bed. A manually operated 'scraper' was used to move powder from the output bed into five plastic cups, also spaced evenly across the output powder bed. After each experiment the cups were individually weighed, and their weights recorded. Further details and figures of this setup can be found in Chapter 3.7.

A number of experiments were then conducted to test the effect of various factors on the lateral distribution of powder across the build surface, the unevenness of which causes fresh material to be wasted during each 'recoat' phase of a build.

The step motor used to turn the augers at a pre-determined speed was programmed to operate at a speed which is deemed acceptable and remained unchanged throughout testing, as follows:

Motor resolution = 1600 pulses per revolution

Chosen Motor Speed = 1600 pulses per second

Calculated Motor Output Speed = 60 revolutions per minute

Gearbox Ratio = 15:1

Gearbox output & Auger Speed = 4 revolutions per minute

8.1 INITIAL TESTING

As with a newly built car, experimental rigs often need a 'shakedown' period of running in order to discover any potential issues before they become a problem. In this case it was used to test the auger mechanism, control software, experimental procedure and to propagate powder through the system in such a way as to prepare it for beginning experiments proper.

A significant amount of torque was required to turn the augers under the weight of powder when the machine is full. This was made apparent by the fact that initially the powder in this machine did not move, despite the auger shafts visibly turning from the ends. Dismantling of the system showed that the glue bond between the auger shafts and the augers themselves had broken, causing the augers to remain stationary under the weight of the powder while the auger shafts spun. This was rectified by drilling 6 holes through each auger and shaft and inserting pins to ensure one cannot spin without the other. This proved to be an effective method of bonding the auger to its shaft.

The control software used in this instance was a simple PLC program which set the step motor speed and activated it on the change of a bit in the PLC memory. The shakedown showed that it was useful for the PLC to run the step motor for a specified number of seconds, as this provided more accuracy than a human with a stopwatch. A timer was added to the program which fulfils this function and the program was considered suitable for the remainder of the experiment.

The initial experimental procedure was as follows:

1. Empty, clean and weigh cups
2. Run machine for 10 seconds
3. Weigh cups
4. Repeat from step 2, until cups are full

The 'shakedown' results showed that this procedure could have been more thorough in that it did not take into account powder lost through removing and replacing the cups for weighing. In order to rectify this, the machine was levelled using the adjustable feet and the following procedure was used for the remainder of the experiment:

1. Empty and clean cups and funnel
2. Weigh empty cups
3. Replace cups
4. Run machine for n+10 seconds
5. Scrape powder into cups
6. Weigh cups with powder
7. Repeat until cups are full

Properly propagating powder through the system was an important step; once the machine was filled with powder and run for the first time, the powder on the output side 'sank' before rising. This was likely due to air gaps between the blades of the augers filling as it began to turn. Once these air gaps were all filled by running the motor for a short period, powder began to rise as in normal operation. If this step was not taken, initial experimental results would have been significantly different.

8.2 BASELINE TEST

The first 'proper' test used the machine in a so-called 'default' state, in order to produce a baseline by which any following tests could be compared. The machine was run as previously described and produced results as follows:

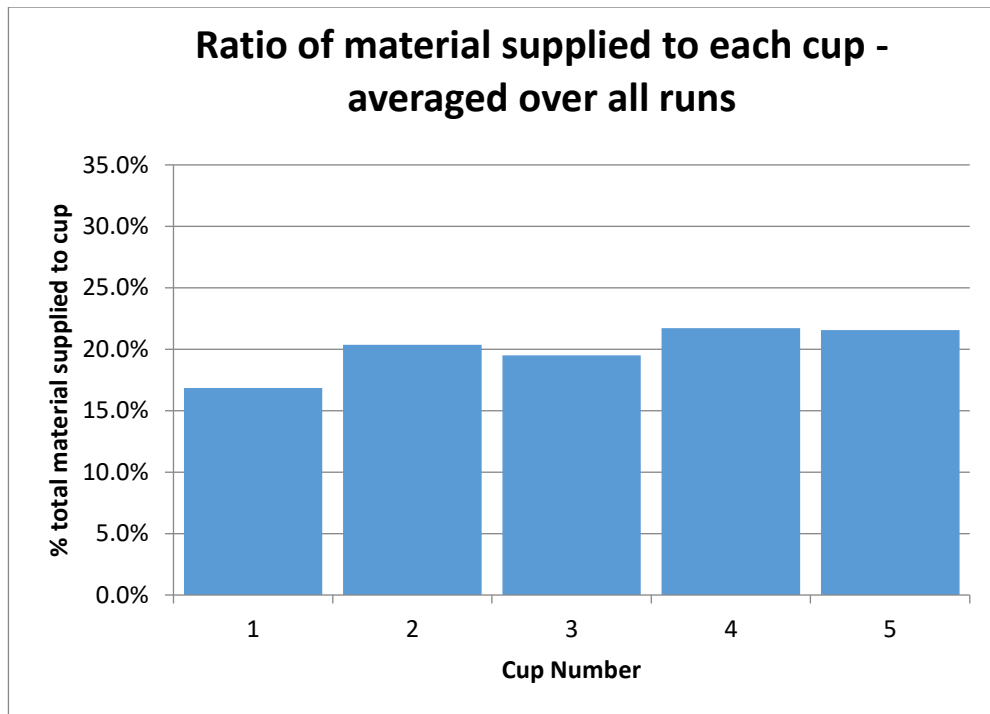


FIGURE 8.1 - AUGER RIG BASELINE TEST RESULTS GRAPH 2

In order for the auger-driven method of delivering powder to be considered a success, the percentage difference of powder delivered to each cup should have been no more than 2% ideally. In this test, Figure 8.1 showed an average difference between Cups 1 and 4 of 4.8%. It could also be seen that Cup 1 on average contained significantly less powder than the other four. This was the first observation of an effect which would continue throughout all other tests and became the main focus of the experiments.

8.3 ALTERNATE OPERATOR

It was proposed that the significant difference observed in the baseline test may have been due to the technique used to manually scrape powder from the output bed into the cups. For this reason, the next test used an alternative operator in order to determine if this was a significant factor.

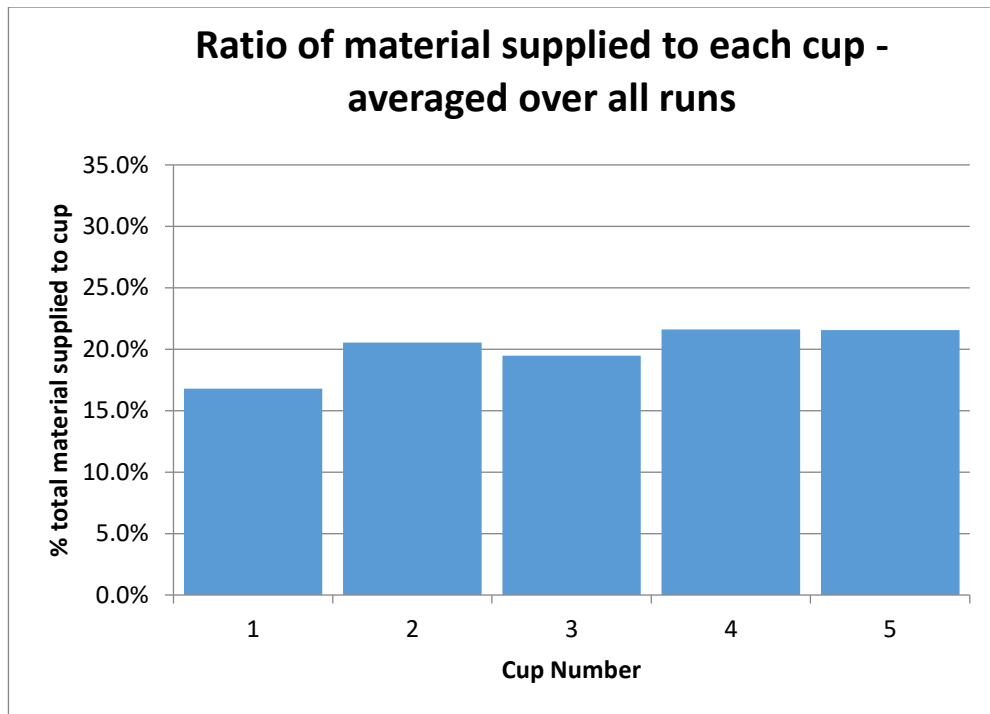


FIGURE 8.2 - AUGER RIG ALTERNATE OPERATOR TEST RESULTS GRAPH 2

The results from this test were extremely similar to the previous baseline test, with the maximum difference between average powder levels in each cup being 4.8%, the same as before. This suggested that operator ‘technique’ is not a significant factor in the results.

8.4 SCRAPER ALTERATIONS

It was observed at this point that the manual scraper used for previous tests was tight to the edges of the output tray, which caused significant friction when moving powder into the cups. As it was possible that this is the reason for the observed disparity between cups, the scraper was altered such that this friction was eliminated.

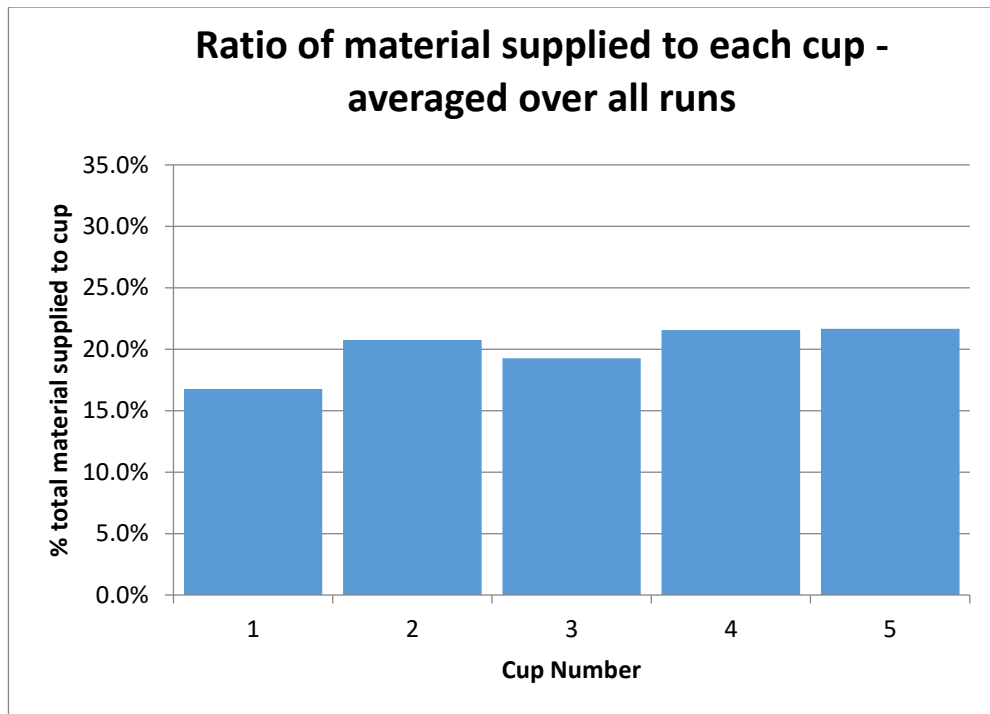


FIGURE 8.3 - AUGER RIG ALTERED SCRAPER TEST RESULTS GRAPH 2

Figure 8.3 shows no significant change in the results as compared with the previous two tests, with maximum difference between averages at 4.9%. This suggested scraper friction was likely not the cause of the irregular powder profile.

8.5 MEASURING FRONT AND REAR HALVES OF BED INDEPENDENTLY

In order to better understand the profile of powder being produced by the auger rig, the powder was next scraped and measured half a bed at a time, as follows:

1. Empty and clean cups & funnel
2. Weigh empty cups
3. Replace cups
4. Run machine for n+10 seconds
5. Scrape 'front' half of powder (nearest to cups) into cups
6. Weigh cups with powder
7. Empty and clean cups
8. Replace cups
9. Scrape 'rear' half of powder (furthest from cups) into cups

10. Weigh cups with powder

11. Repeat until cups full

This method meant that it was possible to visualise whether powder was being equally distributed across the output tray in the direction of the augers. The alternative possibilities were that the powder may have risen as soon as it entered the output tray (rear half) or clung to the augers and rose at the opposite side (front half).

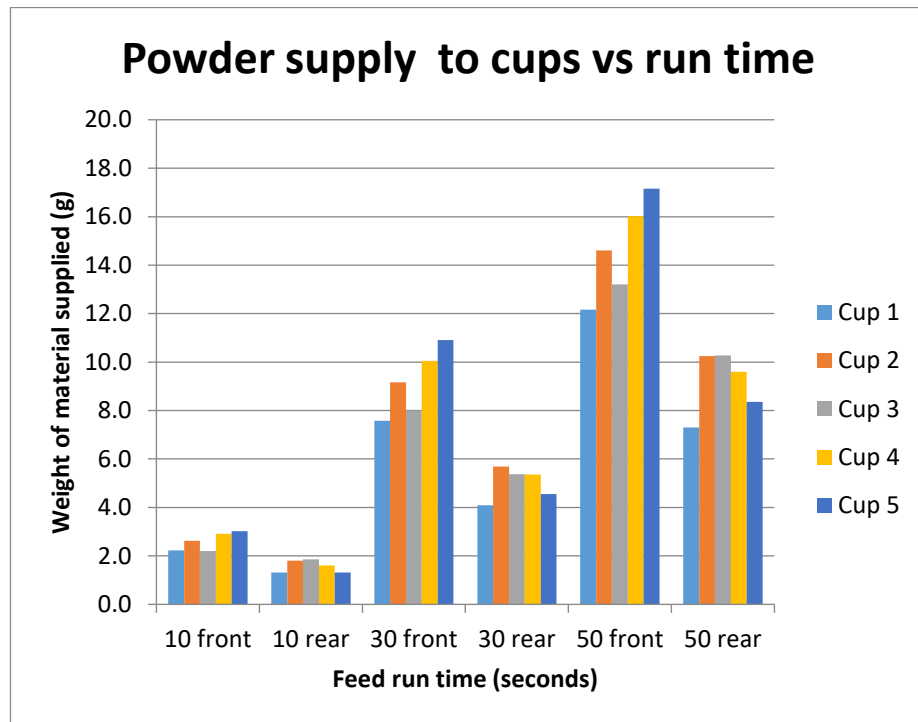


FIGURE 8.4 - AUGER RIG FRONT/REAR TEST RESULTS GRAPH 1

Figure 8.4 indicates that the powder rose through the output tray towards the front edge by a significant margin, on average the front half contained 63% of the total powder measured. This suggested that the output tray itself could have been made shorter (in the front-rear dimension spanning the path of the scraper) in order to save space and perhaps reduce the possibility of inconsistency across the cups.

8.6 REMOVING GUIDE 'HILLS'

At the bottom of the output tray were three guiding 'hills', shown earlier in Figure 3.14, which were intended to guide the powder away from the augers and reduce the total

mass of powder required to fill the output tray. As a possible contributor to the observed problem, these were removed, and two tests performed; one as normal and one with front and rear halves measured independently.

8.6.1 BASELINE TEST

In this instance removing the hills appeared to exasperate the problem as shown in Figure 8.5, with notably less powder in Cups 1 and 2, showing a general gradient of powder moving towards Cup 5. The maximum difference in this case was 11.8%.

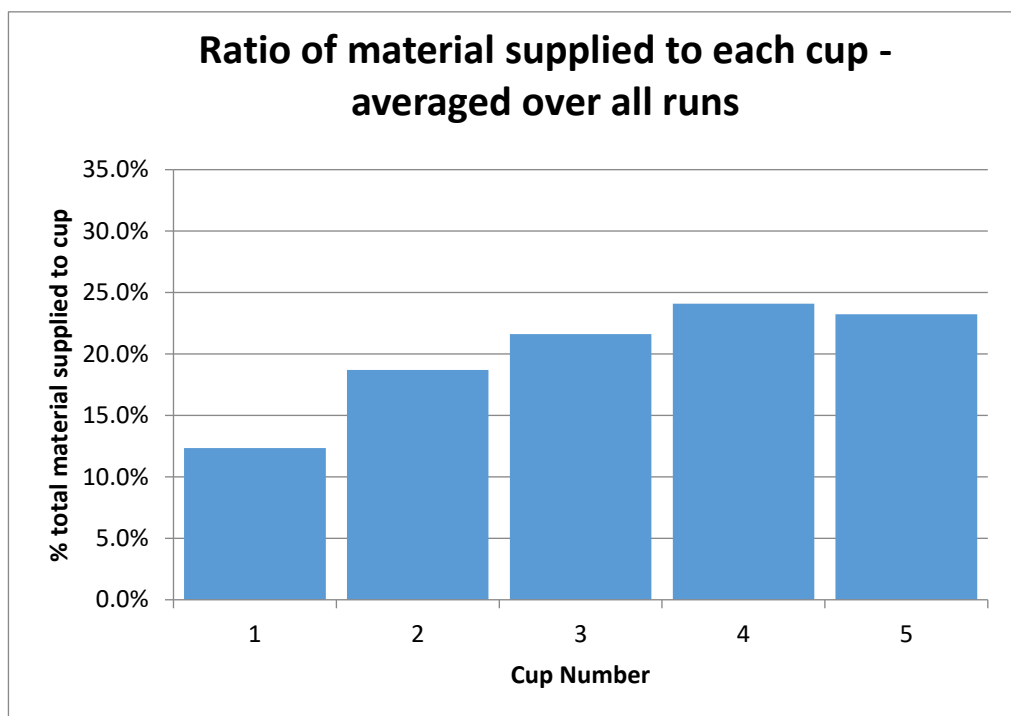


FIGURE 8.5 - AUGER RIG HILLS REMOVED TEST RESULTS GRAPH 2

8.6.2 MEASURING FRONT AND REAR HALVES OF BED INDEPENDENTLY

The same effect was observed here where there was much less powder in Cups 1 and 2, but the front/rear ratio continued to favour the front half with an average of 60%. The maximum difference between cups was 10.7%. This can be seen in Figure 8.6.

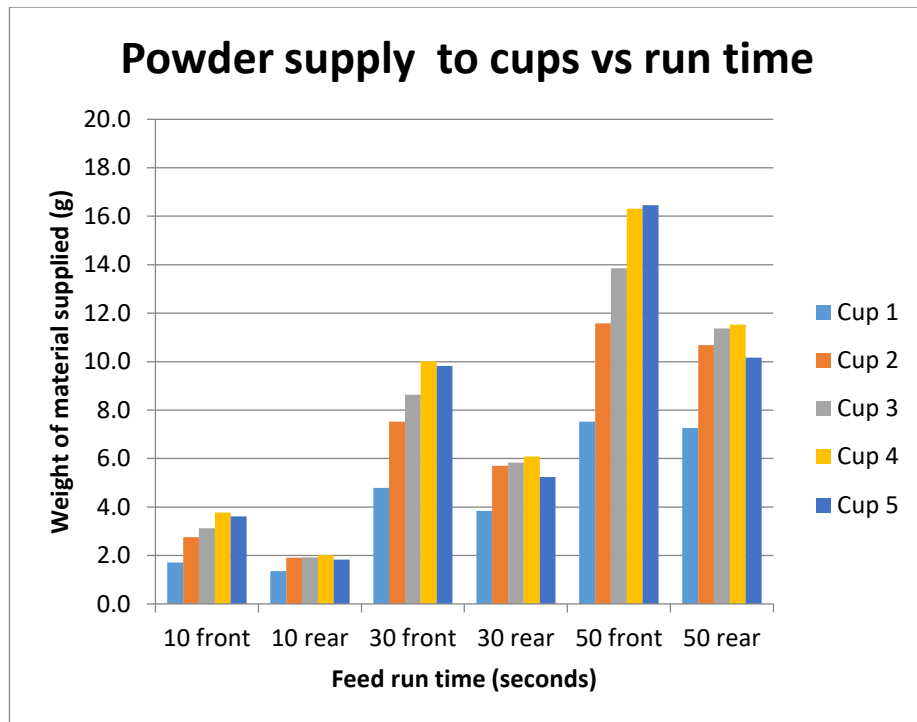


FIGURE 8.6 - AUGER RIG HILLS REMOVED FRONT/REAR TEST RESULTS GRAPH 1

8.7 LOOSENING AUGERS IN TURN

It was useful to observe the amount of powder delivered by each auger and where on the output tray each auger delivered its powder to, because this allowed verification of whether or not powder in the output tray rose vertically from the auger, or 'drifted' to one side of the tray due to the rotation of the auger. It also helped to quantify the effectiveness of each auger, ruling out any mechanical inconsistencies reducing powder delivery to Cups 1 and 2. To this end, various combinations of augers were mechanically loosened so that their timing wheels slipped leaving the shaft and auger stationary, and several more experiments were performed.

8.7.1 AUGER 1 LOOSE

The timing wheel driving auger 1 (LHS, closest to Cup 1) was loosened from its shaft, allowing Auger 1 to remain stationary while Augers 2 and 3 turned as normal. Results are shown in Figure 8.7.

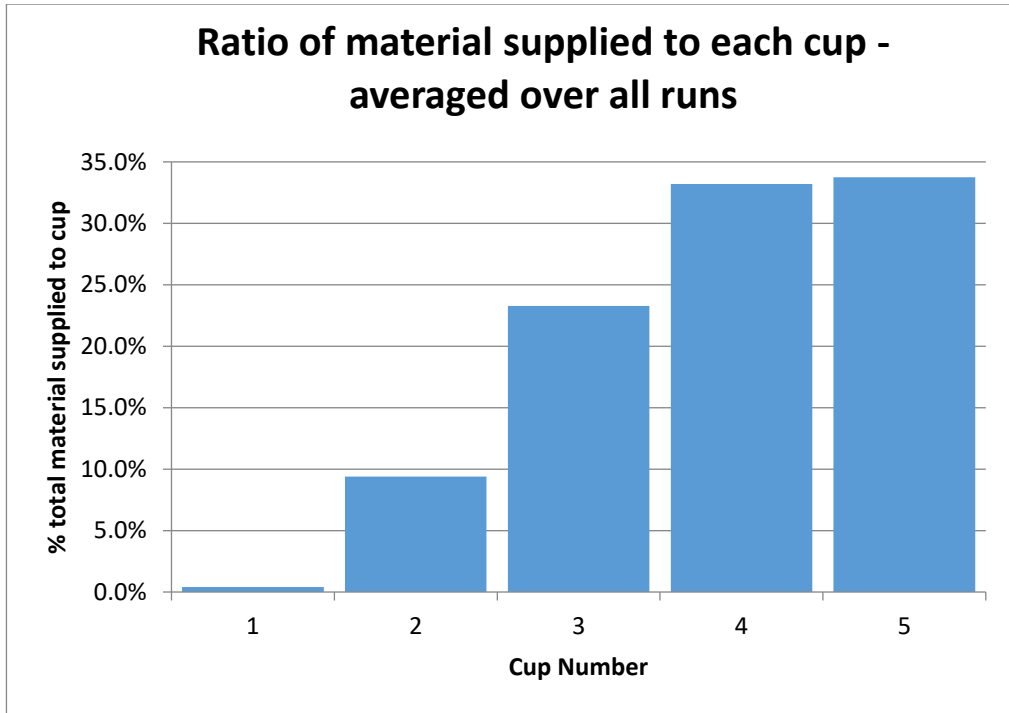


FIGURE 8.7 - AUGER 1 LOOSE TEST RESULTS GRAPH 2

These results show that the majority of powder from Auger 1 was delivered to Cup 1 and to a lesser extent Cup 2. It also shows that some of the powder from the other two augers was delivered to Cup 2, though this effect could be symmetrical, with some powder from Auger 2 also arriving in Cup 4.

8.7.2 AUGER 2 LOOSE

The timing wheel driving Auger 2 (centre, closest to Cup 3) was loosened from its shaft, allowing Auger 2 to remain stationary whilst Augers 1 and 3 turned as normal. Results are shown in Figure 8.8.

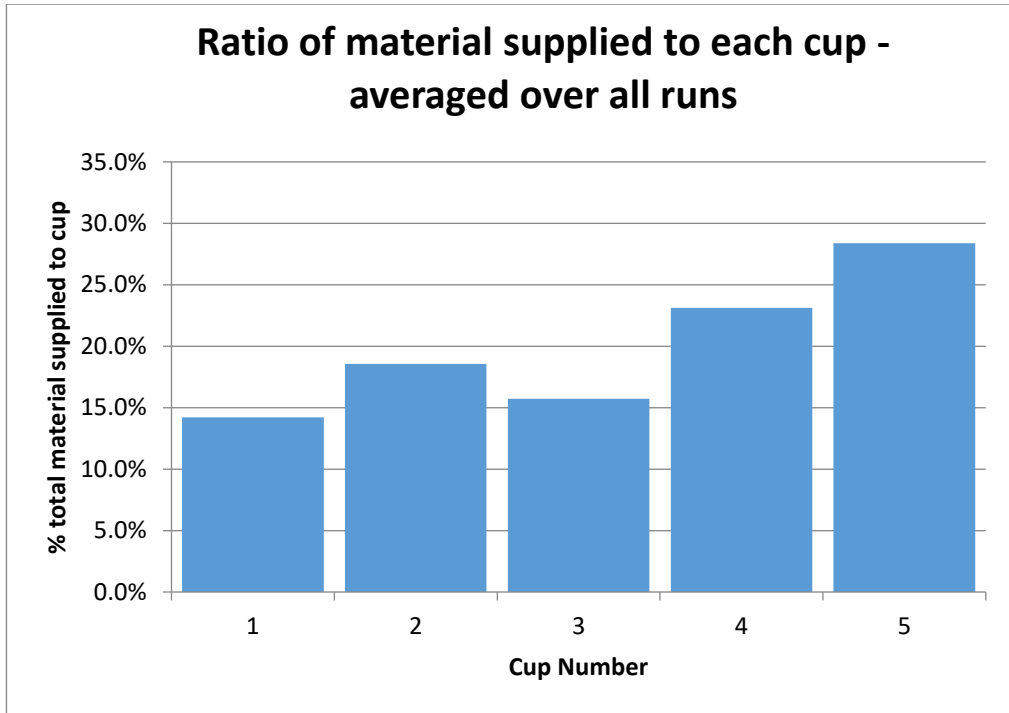


FIGURE 8.8 - AUGER 2 LOOSE TEST RESULTS GRAPH 2

These results show a clear reduction in powder delivered to Cups 2, 3 and 4, though interestingly the profile was not symmetrical as could be expected; the powder in Cups 1 and 2 was still much less than the powder in Cups 4 and 5. It also appears that a significant amount of powder from Augers 1 and 3 was delivered to Cup 3, which represents the section of the output tray directly above the 'loosened' Auger 2. This shows that while the powder rose in the output tray, it spread to fill any available space.

8.7.3 AUGER 3 LOOSE

The timing wheel driving Auger 3 (RHS, closest to Cup 5) was loosened from its shaft, allowing Auger 3 to remain stationary while Augers 1 and 2 turned as normal. Results are shown in Figure 8.9.

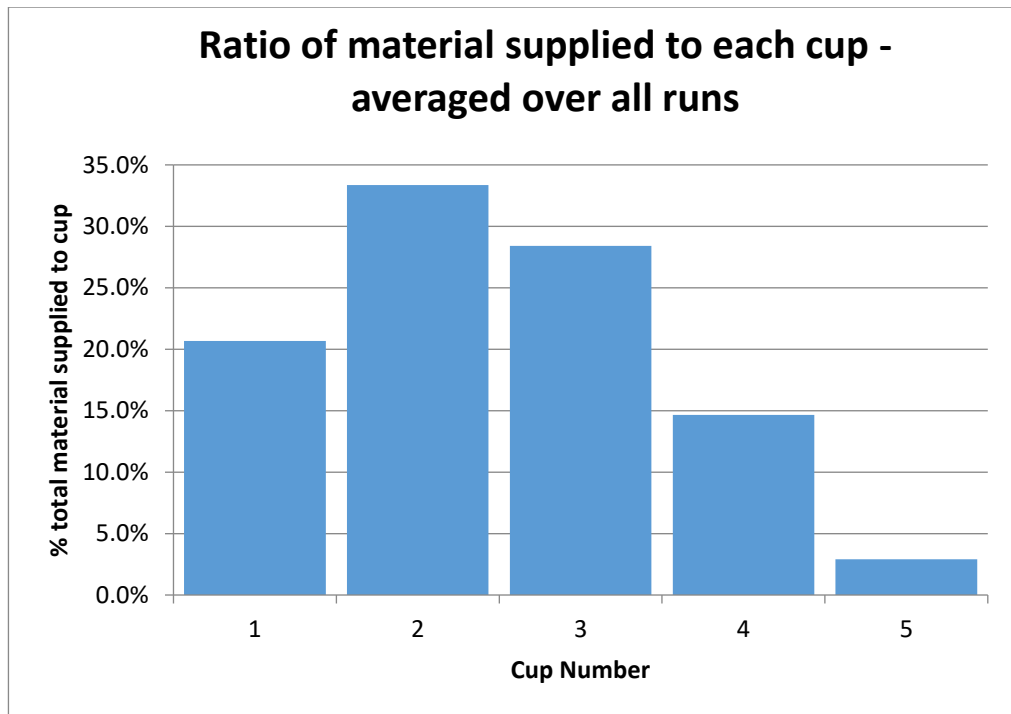


FIGURE 8.9 - AUGER 3 LOOSE TEST RESULTS GRAPH 2

These results are the approximate mirror image of those obtained in Auger 1 Loose, though there was notably less powder in Cup 1 than would be expected. If Augers 1 and 3 were performing symmetrically, it would be expected to see 35% of powder delivered to Cup 1 and 35% to Cup 2 as in Auger 1 Loose. Instead, approximately 21% of powder is delivered to Cup 1. This suggests that either there was some mechanical inconsistency preventing Auger 1 from functioning properly, or there exists some ‘drift’ phenomenon whereby powder ‘flowed’ laterally according to the rotation of the augers.

A lateral flow phenomenon is the most likely candidate at this stage, because it can be observed that the powder delivered to Cup 4 in this experiment was approximately 14%, where the powder delivered to Cup 2 in Figure 8.7 is approximately 9%. In both cases the powder in these cups is most likely delivered from the centre auger, which was configured identically for both tests.

8.8 ALTERNATE TIMING WHEELS

Working under the assumption that a lateral flow phenomenon has been observed, it needed to be determined whether such an effect could be countered such that an equal

amount of powder is delivered to each cup to minimise powder wastage were this method to be used in a production environment.

The first potential solution was to alter the speed of the augers such that Auger 1 rotated slightly faster, delivering more powder than it otherwise would. Up to this point the timing wheels which transfer power to the augers through a toothed belt were all sized at 26 teeth, 50mm diameter. Alternative timing wheels with 20 and 24 teeth were obtained, and experiments run.

8.8.1 AUGER 1 – 20 TEETH

The timing wheel from Auger 1 was replaced with a 20-tooth wheel. All other timing wheels, including the motor driving timing wheel were 26 teeth. The calculations in chapter 8 show all the augers initially spun at 4 rpm, with the new 20 tooth wheel on Auger 1 providing a ratio of 1:1.3, Auger 1 would theoretically spin at 5.2 rpm, 30% faster than previously, delivering 30% more powder. Results are shown in Figure 8.10.

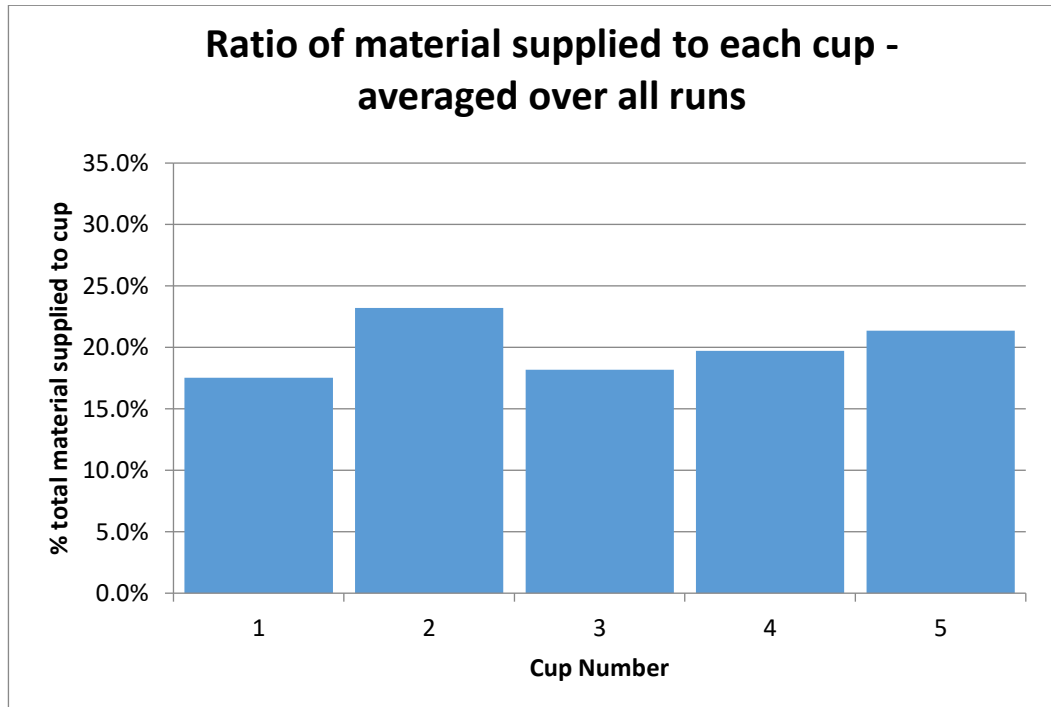


FIGURE 8.10 - AUGER 1 AT 5.2 RPM TEST RESULTS GRAPH 2

As compared with the baseline tests in chapter 8.2 it can be seen here that significantly more powder was delivered to Cup 2, though there was still less powder being delivered to Cup 1 than all other cups. It could be said that this was due to the continuing lateral drift effect as the extra powder from the faster Auger 1 was accounted for but had spread towards the higher numbered cups as opposed to Cup 1.

8.8.2 AUGER 1 – 24 TEETH

The previous experiment in sub-chapter 8.8.1 was repeated with Auger 1 using a 24 tooth timing wheel, giving it a speed of 4.3 rpm, 7.5% faster than Augers 2 and 3. Results can be seen in Figure 8.11.

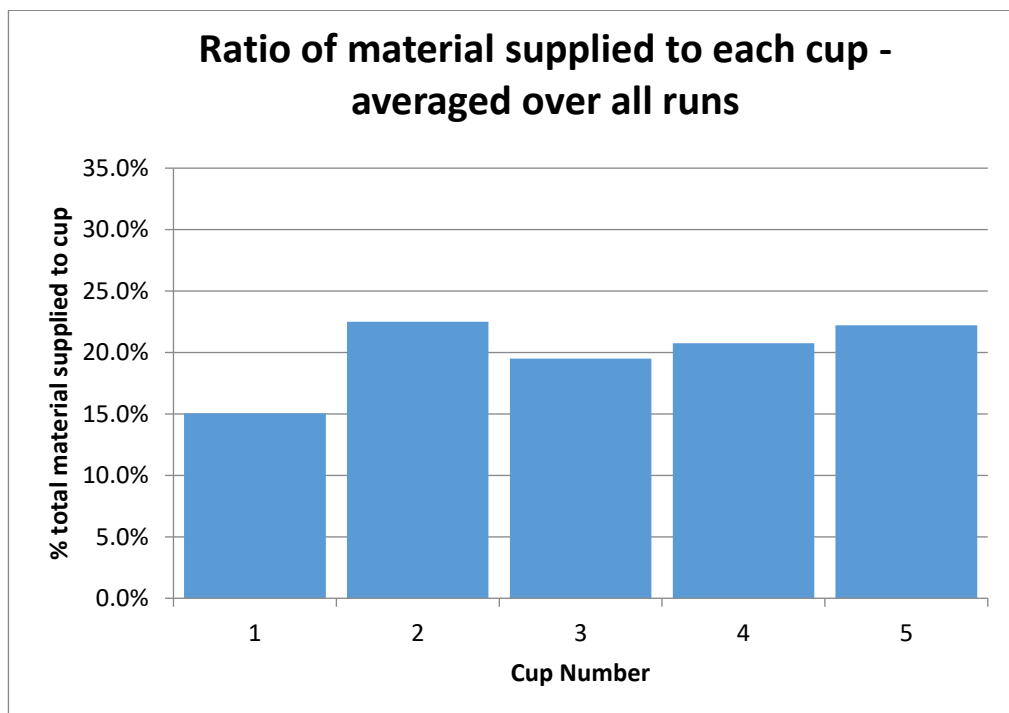


FIGURE 8.11 - AUGER 1 AT 4.3 RPM TEST RESULTS GRAPH 2

Here we see the same result as in the previous sub-chapter, but with a slightly less pronounced difference from the baseline. It is clear that this method did not produce the desired even profile of powder across the output tray, potentially due to the lateral drift phenomenon.

8.9 REPLACEMENT OUTPUT TRAY

A new design for the output tray was produced at this stage. As the original was produced using AM, it is possible that slight warping could have meant that the tray was not perfectly square. The new design also allowed for insertion of a 'baffle' arrangement which added guiding 'fins' to the output tray which, in theory, directed rising powder back towards Cup 1, negating the observed lateral drift effect. The new tray was also much shallower, allowing observation of what happened to powder immediately above the augers. The new tray was produced and on arrival was measured to ensure all dimensions are square and as accurate to the initial design as possible. Once this was verified, the new tray was fitted and another set of experiments performed, assessing the effectiveness of the new tray with and without the baffles and/or 'hills' in the base of the tray.

Note the timing wheels were returned to their original configuration of 26 teeth, 4 rpm at this stage and for the rest of the work on this rig, as differing auger speeds was determined to be an ineffective method of smoothing output powder profile.

8.9.1 WITHOUT HILLS, WITHOUT BAFFLES

Interestingly the results, shown in Figure 8.12, show the powder profile as being even less consistent than in the baseline test with the original output tray. Though the effect of the new 'baffles' had not been employed yet, this shows that manufacturing inaccuracies in the original output tray were likely not the cause of this. This could also be explained by the reduced depth of the output tray and would suggest that while rising the powder mixes and spreads across the five cups. The effect of output tray height is discussed in Chapter 8.10.

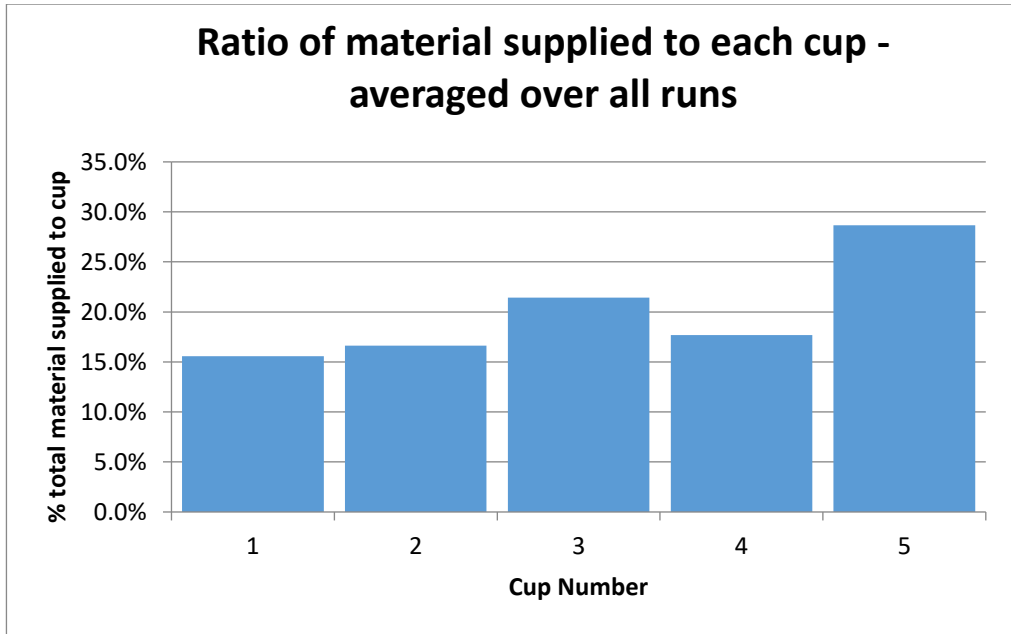


FIGURE 8.12 - NEW TRAY NO HILLS NO BAFFLES TEST RESULTS GRAPH 2

8.9.2 WITHOUT HILLS, WITH BAFFLES

The baffles were added to the output tray for the first time. These consisted of four equidistant 'fins' near the top of the output tray, tilted at 2° such that the tops were closer to Cup 1. Results are shown in Figure 8.13.

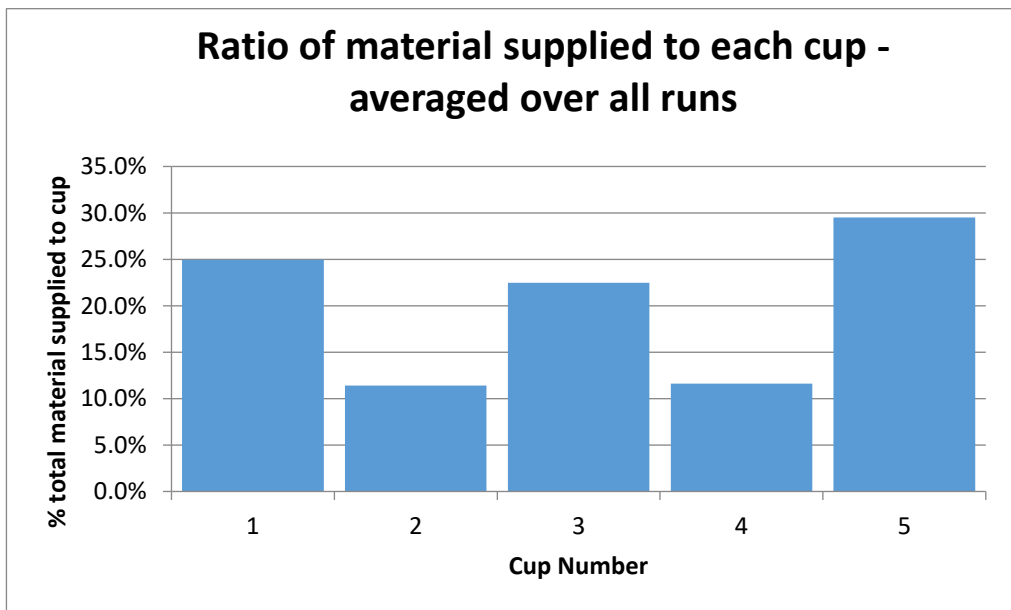


FIGURE 8.13 - NEW TRAY NO HILLS BAFFLES TEST RESULTS GRAPH 2

The immediately obvious effect of the baffles was to make the powder rise in three distinct mounds, in the gaps between the fins of the baffle, directly above each auger. This appeared to make more powder available at Cup 1, but had the extra undesirable effect that Cups 2 and 4 received very little powder in comparison.

Importantly at this stage, it was identified that adding barriers to the output tray can significantly change the output profile. If this could be altered, then in theory a baffle could be designed which produces a much more even output profile. This effect is investigated further in Chapter 8.14.

8.9.3 WITH HILLS, WITHOUT BAFFLES

The baffle was removed and the shaped 'hills' in the base of the output tray were returned to their original position in order to assess their effect on the new output tray. Results are shown in Figure 8.14.

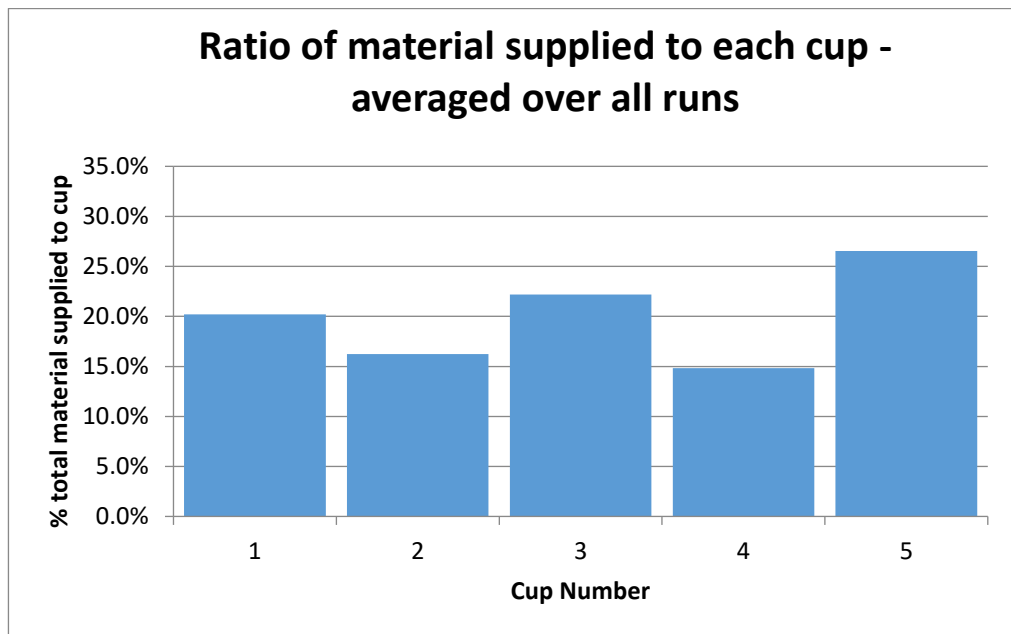


FIGURE 8.14 - NEW TRAY HILLS NO BAFFLES TEST RESULTS GRAPH 2

The same effect of distant mounds can be seen here, though it is less pronounced than in the previous experiment with baffles and no hills. It is suggested that, as earlier, the reduced depth of the new output tray reduced the powder's ability to spread into Cups

2 and 4. This is an effect which was likely exasperated by the presence of the hills, which significantly reduced the space available in the output tray.

8.9.4 WITH HILLS, WITH BAFFLES

Both the hills and baffles were added to the rig, and the experiment run once again. Results are shown in Figure 8.15.

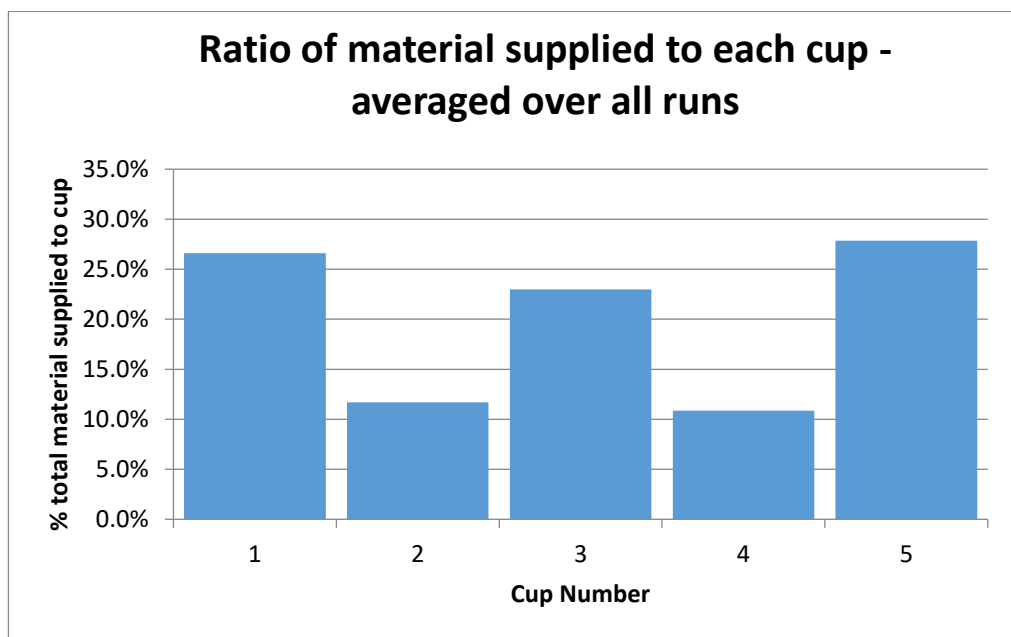


FIGURE 8.15 - NEW TRAY HILLS BAFFLES TEST RESULTS GRAPH 2

This experiment shows the most pronounced occurrence yet of the effect of the shallow tray and baffles. It has been clear from this set of experiments that the powder output profile could be manipulated through barriers in the tray, though clearly this particular configuration was not ideal for the purpose of creating an even profile.

8.9.5 TILTING MACHINE BASE

An extremely simple, cheap solution to the problem may have been to use gravity to tip powder back towards Cup 1, hopefully evening out the powder profile. To this end the entire auger rig was tilted 1° towards Cup 1 and the results recorded as follows. Results are shown in Figure 8.16.

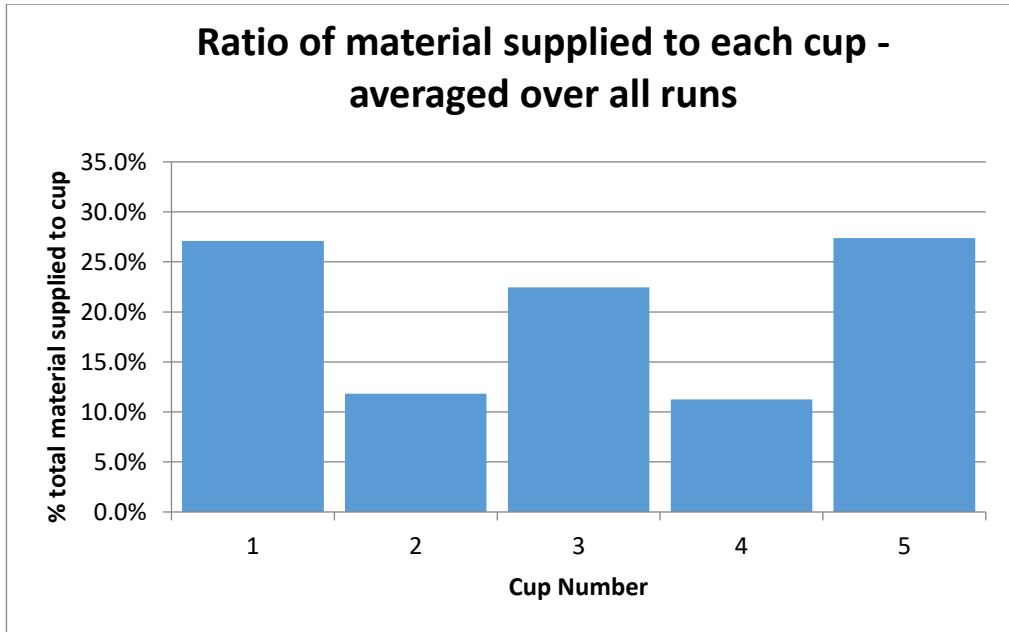


FIGURE 8.16 - RIG TILTED 1 DEGREE TEST RESULTS GRAPH 2

As compared with the results from the previous experiment (sub-chapter 8.9.4) it can be seen that gravity had indeed evened out the profile, though this would not be a practical solution in the case of a powder delivery system for an AM machine as these often require a perfectly level surface in order to manufacture parts correctly.

8.10 TALL OUTPUT TRAY

In sub-chapter 8.9.1 it was suggested that the shallower alternative output tray used may have reduced the powder's ability to mix and spread towards the areas of the tray between the augers. In order to investigate this effect, a 300mm collar was produced which sat between the machine's base and the output tray, thus increasing the distance by which the powder rose before reaching the surface.

8.10.1 BASELINE TEST

This experiment was performed using the shallow output tray with hills installed but no baffles. Results are shown in Figure 8.17.

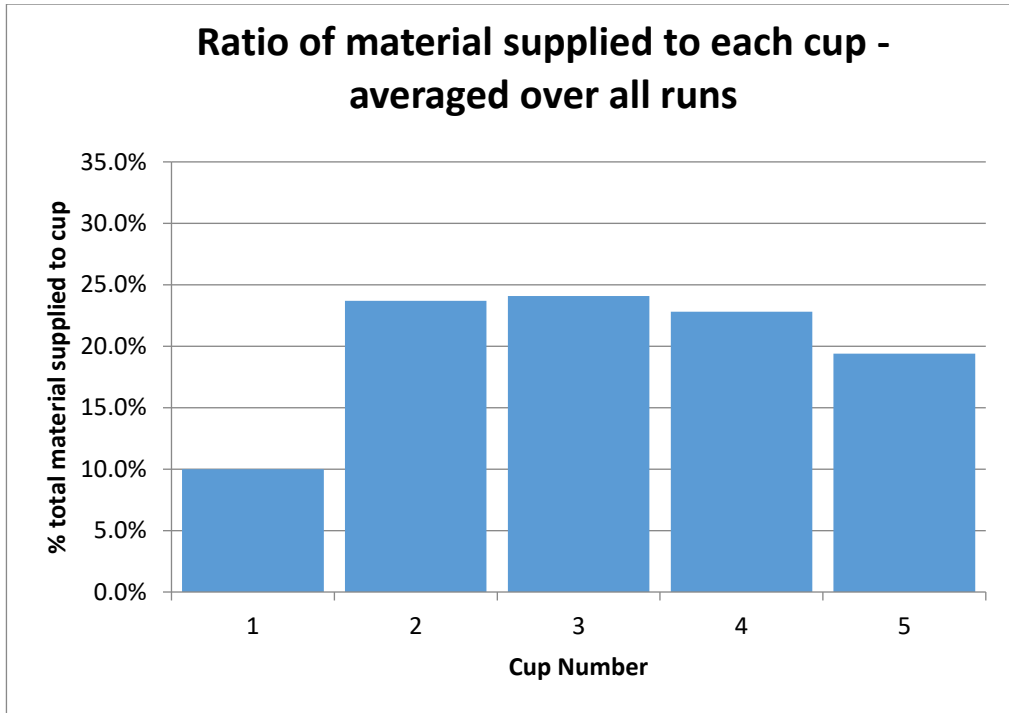


FIGURE 8.17 - 300MM COLLAR TEST RESULTS GRAPH 2

It can be seen from these results that the collar had negated the effect of the shallow tray, allowing powder to spread more freely while rising in the output tray. However, the initially observed effect of reduced powder in Cup 1 can still be clearly seen.

8.10.2 FRONT AND REAR HALVES MEASURED INDEPENDENTLY

This experiment was also repeated for measuring front and rear halves of the tray independently. Results are shown in Figure 8.18.

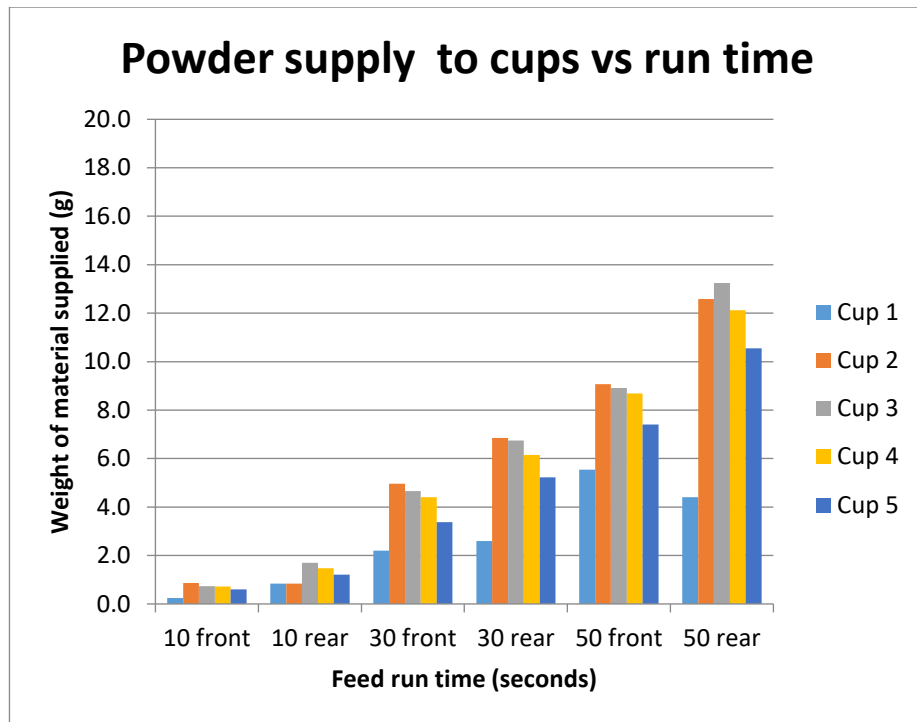


FIGURE 8.18 - 300MM COLLAR FRONT/REAR TEST RESULTS GRAPH 1

Measuring front and rear halves of the tray independently shows that in this case where the 300mm collar was present, more powder rose in the rear half of the tray (furthest from cups) in contrast to earlier experiments where more powder rose on the front half of the tray (closest to cups). This could be attributed to the ‘mixing’ effect of the taller output tray with collar, though due to the lack of powder still observed in Cup 1 and the fact that moving a much larger mass of powder required much more torque on the mechanism, this may not be a practical solution.

8.11 NEW BAFFLE DESIGN

After the previous baffle design failed to deliver the predicted results, a new baffle was designed where the angle of each baffle was adjusted in an attempt to ‘steer’ powder towards Cups 2 and 4, thus evening out the powder profile. This experiment was performed with the newer output tray, no collar, with hills and new baffle. Results are shown in Figure 8.19.

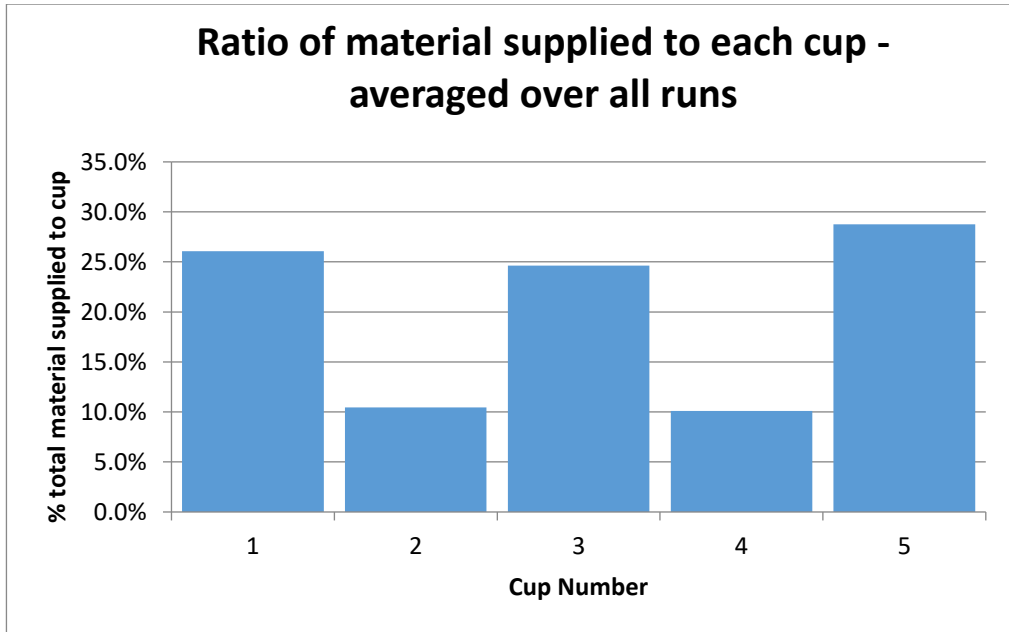


FIGURE 8.19 - SECOND BAFFLE DESIGN TEST RESULTS GRAPH 2

It can be clearly seen that the new baffle design had no significant effect on smoothing the powder profile as there is no significant change in the amount of powder in Cups 2 and 4. This shows that if an output tray baffle is to be used; in order to create an output profile which is acceptable for production use it would need to be significantly redesigned.

8.12 RUNNING AUGERS INDIVIDUALLY

In sub-chapter 8.7, each auger's driving pulley was loosened in turn giving the output profile for the other two running augers. This sub-chapter takes the opposite approach of running a single auger at a time, locking the other two in place. This gave a much more accurate idea of the powder delivered by each auger.

The results from these experiments are shown in figures 8.20, 8.21 & 8.22. The most notable point across the three sets of results was that while running Auger 1 only, Cup 1 contained 55% of the powder delivered and Cup 2 contained 41%. In contrast when running Auger 3, only Cup 5 contained 69% of the powder delivered and Cup 4 contained 30%. If it were the case that the powder tended to move towards or away from the walls of the tray, these results would have been the mirror image of each other, but as it stands

it still appeared as though some kind of lateral drift phenomenon was causing all powder to move away from Cup 1 and towards Cup 5.

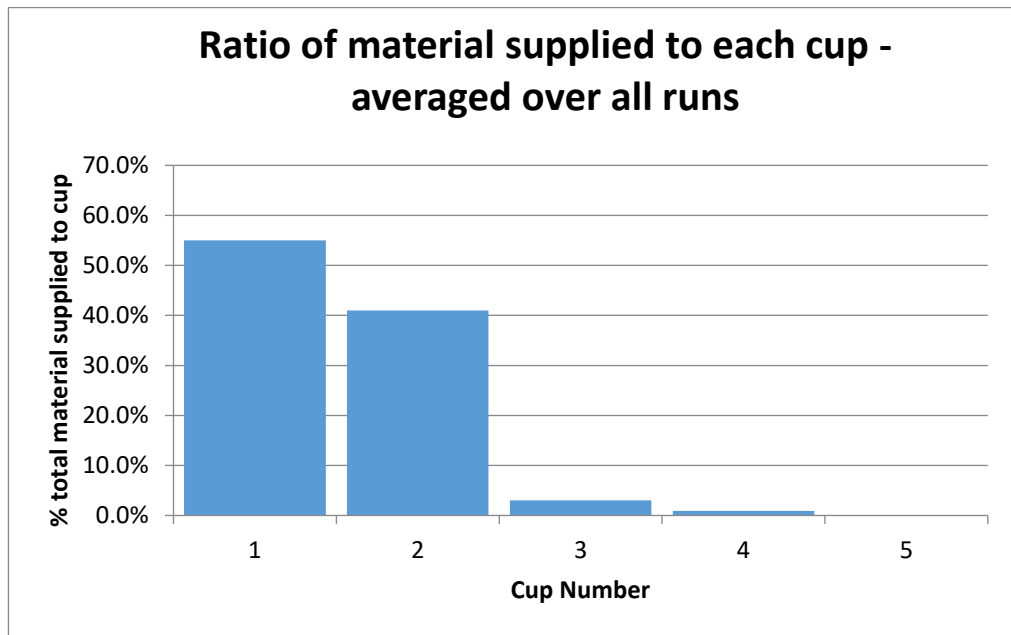


FIGURE 8.20 - AUGER 1 ONLY TEST RESULTS GRAPH 2

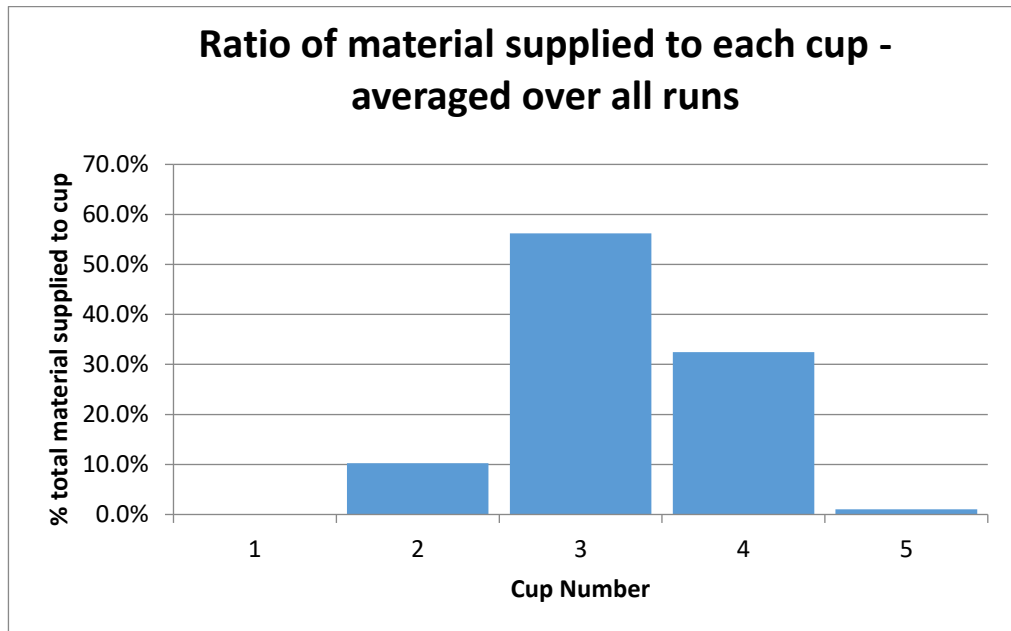


FIGURE 8.21 - AUGER 2 ONLY TEST RESULTS GRAPH 2

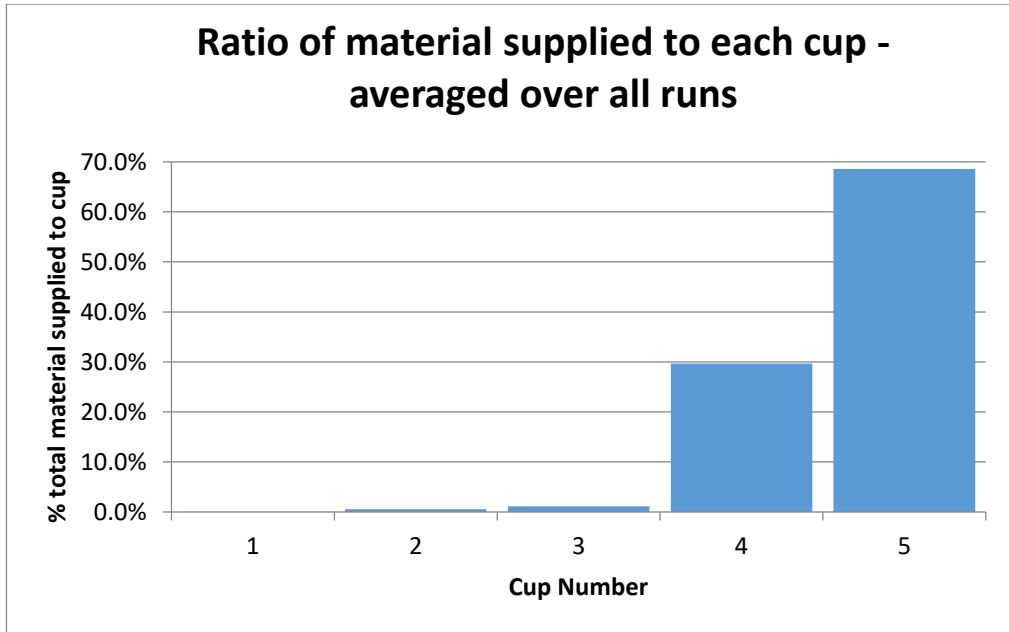


FIGURE 8.22 - AUGER 3 ONLY TEST RESULTS GRAPH 2

8.13 RUNNING AUGER 3 IN OPPOSITE DIRECTION

Up to this point all experiments had been performed with the augers rotating clockwise (when looking from input tray side, with Cup 1 on LHS) because augers by their construction cannot be reversed without also reversing the direction of powder travel. Once alternative augers were produced, experiments could be performed to determine the effect of counter-rotating Auger 3, which was selected due to the theorised drift effect moving powder towards this side of the tray. Results are shown in Figure 8.23.

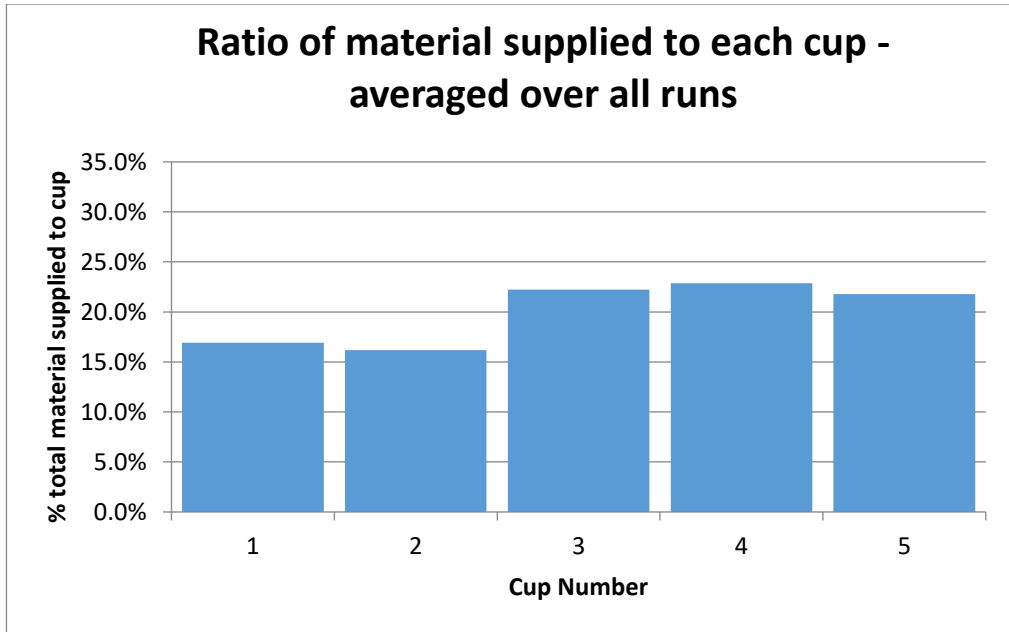


FIGURE 8.23 - AUGER 3 ANTI-CLOCKWISE TEST RESULTS GRAPH 2

The results here were slightly improved on previous experiments, though there was still more powder in Cups 3, 4 and 5 than in Cups 1 and 2. This may have been due to the fact that two augers were running clockwise and only one anti-clockwise. Unfortunately, due to the odd number of augers in the rig, it was not possible to create an entirely symmetrical configuration.

8.14 GRID BAFFLE

As described earlier it was established that adding physical barriers in the output tray had the ability to change the powder profile produced, though the four-baffle design previously seemed to serve only to divide the powder into three mounds, one above each auger. A third baffle design was produced in order to test this theory which took the form of a grid of rectangular spaces, into each of which a 'plug' could be placed to block or redirect the flow of powder depending on if the plug was flat or pointed on the bottom. An example of the grid baffle with plugs is shown in Figure 8.24 below.

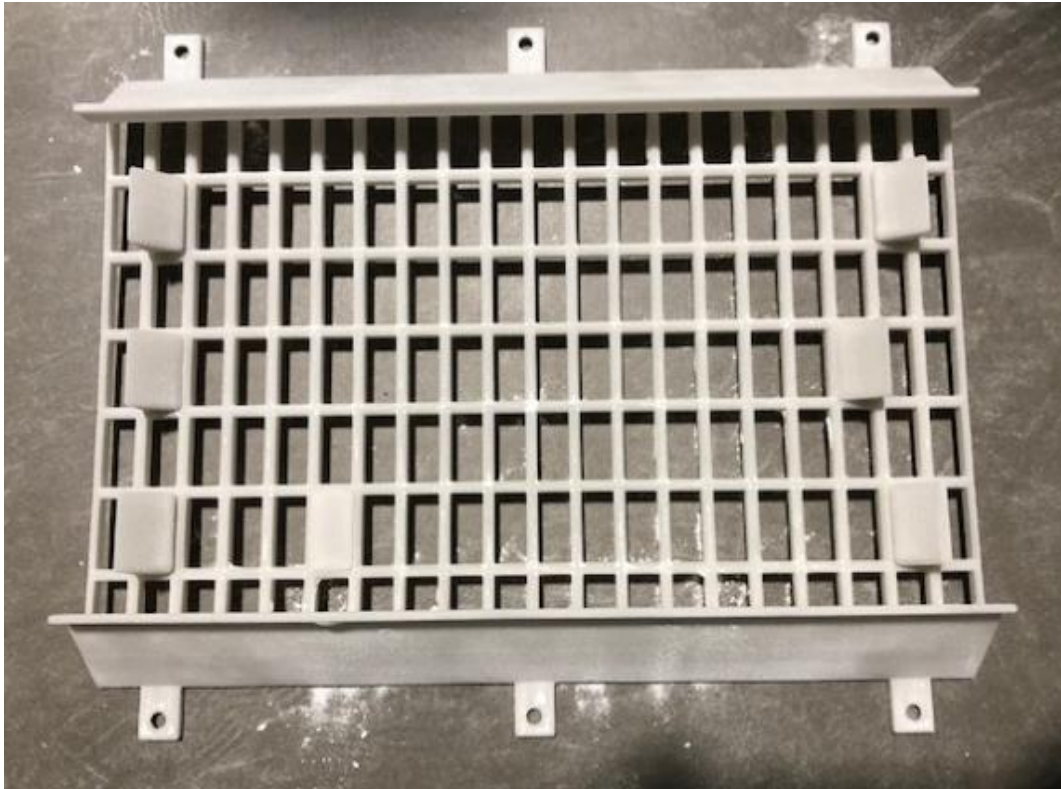


FIGURE 8.24 - GRID BAFFLE WITH PLUGS

The following describes the most significant stages in developing a level output using trial-and-error to determine the most effective arrangements of plug for the grid baffle. It is important to note all plug location figures 8.26, 8.28 & 8.30 are viewed from the bottom of the grid, where Cup 1 would be on the right and Cup 5 on the left. Plugs marked '1' are flat bottomed and simply block powder from rising at that spot. Plugs marked '2' are angled to send powder to either side depending on their orientation.

8.14.1 NO PLUGS

The initial results shown in Figure 8.25 seem to show a less pronounced version of the original straight baffles' results where there was more powder in Cups 1, 3 and 5, however the difference between those cups and Cups 2 and 4 was significantly less this time. This test would serve as a baseline by which different plug combinations could be compared and their effect determined.

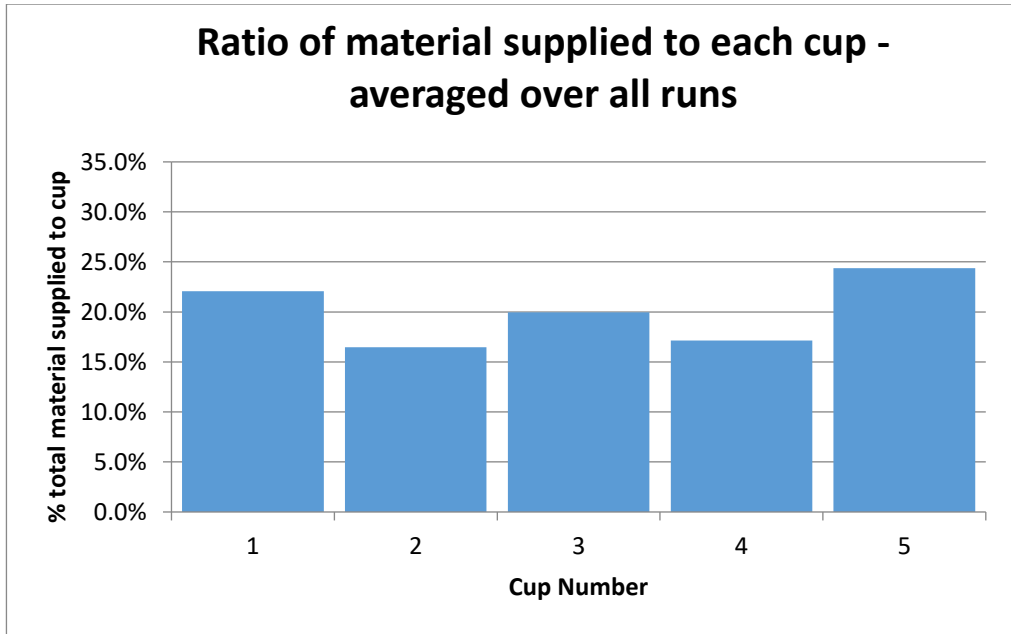


FIGURE 8.25 - GRID BAFFLE NO PLUGS TEST RESULTS GRAPH 2

8.14.2 PLUG ARRANGEMENT A

In this case, all plugs are angled to send powder towards the centre of the bed. Figure 8.26 shows the arrangement of plugs for this iteration, results are shown in Figure 8.27.

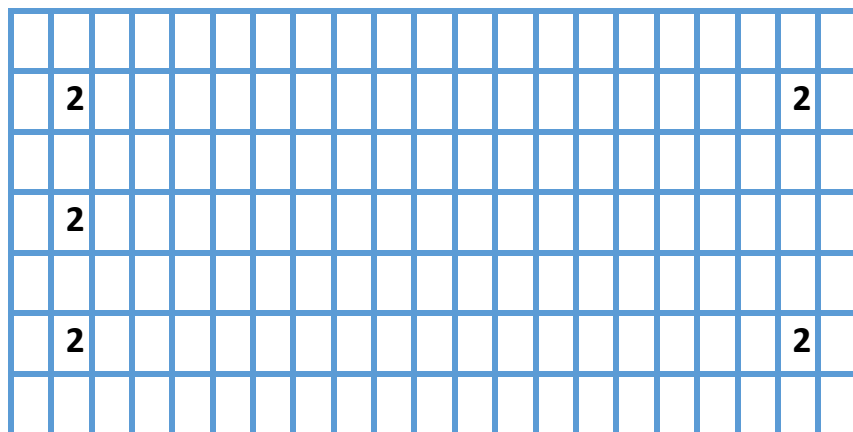


FIGURE 8.26 - GRID BAFFLE PLUG ARRANGEMENT A

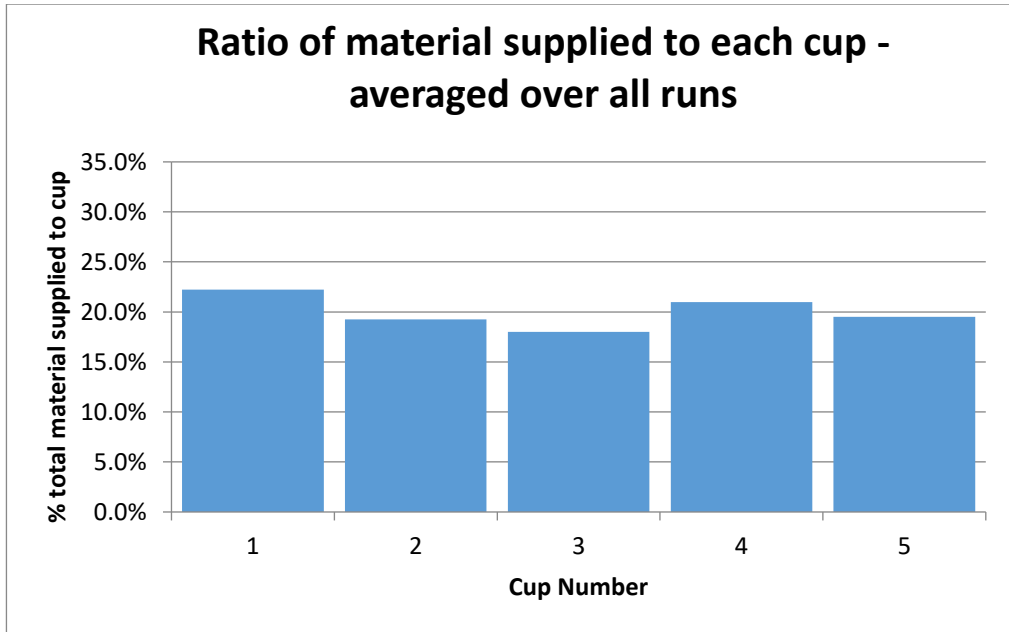


FIGURE 8.27 - GRID BAFFLE PLUG ARRANGEMENT A TEST RESULTS GRAPH 2

As compared with the grid baffle baseline test (no plugs), the response here was improved but more work was needed.

8.14.3 PLUG ARRANGEMENT B

Next, a flat plug was introduced in an attempt to limit the powder appearing in cup 4 as per the results from plug arrangement A above. Figure 8.28 shows the arrangement of plugs for this iteration, results are shown in Figure 8.29.

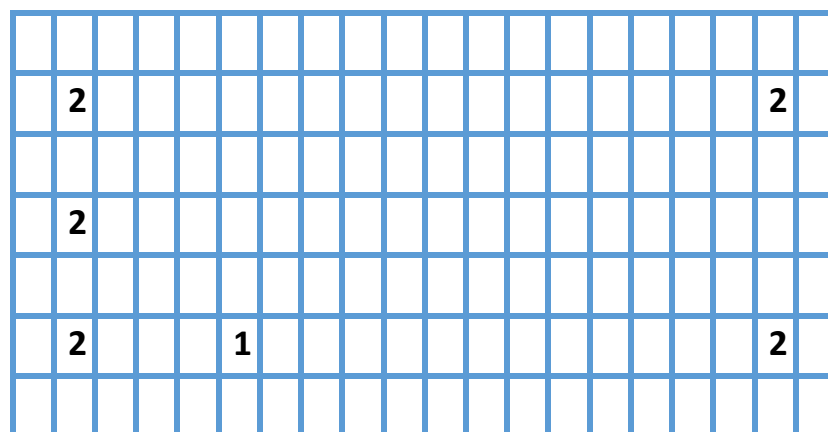


FIGURE 8.28 - GRID BAFFLE PLUG ARRANGEMENT B

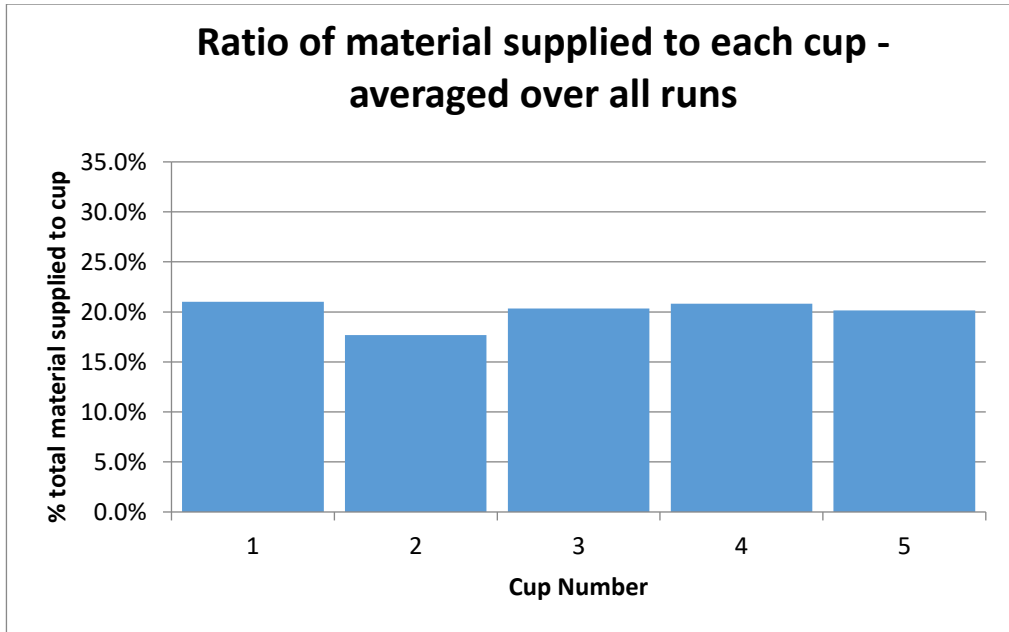


FIGURE 8.29 - GRID BAFFLE PLUG ARRANGEMENT B TEST RESULTS GRAPH 2

Once again, the response here was mostly improved from the baseline, with the notable exception of Cup 2, where much less powder was observed than would be expected.

8.14.4 PLUG ARRANGEMENT C

Finally, an extra sloped plug was added to persuade powder from cup one into Cup 2 and the experiment repeated. Figure 8.30 shows the arrangement of plugs for this iteration, results are shown in Figure 8.31.

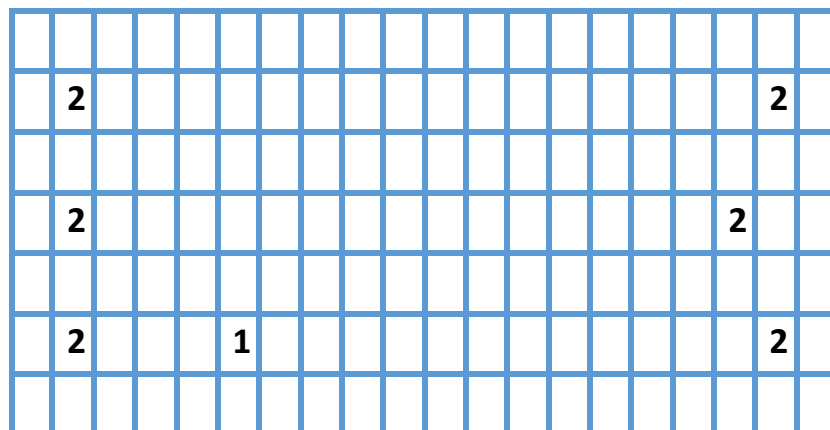


FIGURE 8.30 - GRID BAFFLE PLUG ARRANGEMENT C

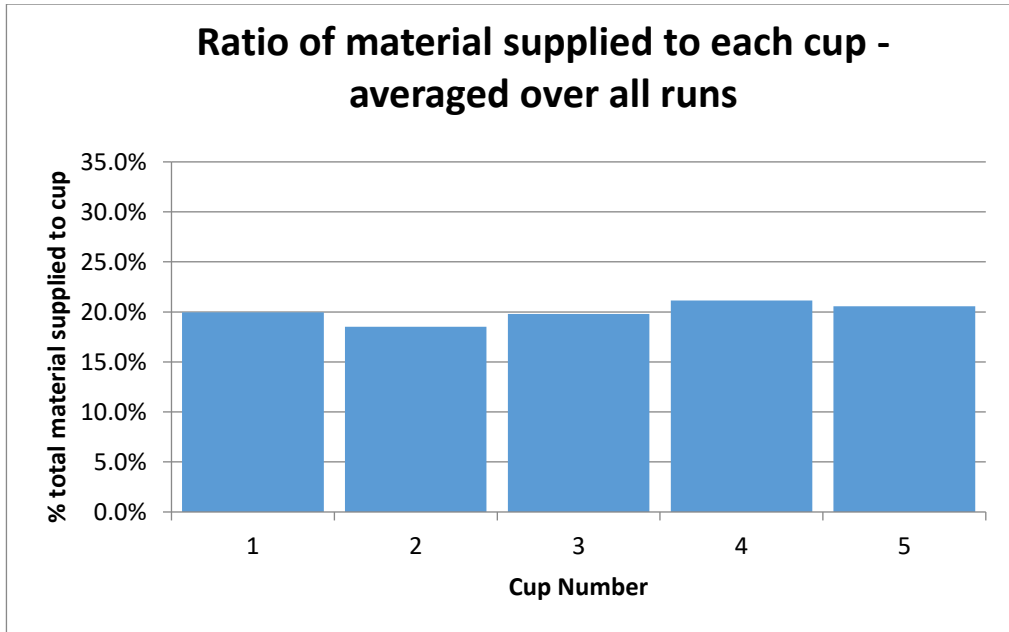


FIGURE 8.31 - GRID BAFFLE PLUG ARRANGEMENT C TEST RESULTS GRAPH 2

This was the best result achieved for the powder delivery rig and the target value of percentage difference of powder mass in each cup was met satisfactorily. Given the time spent on the experiment the decision was made to discontinue testing at this point. Results and analysis were then used in order to determine viability of the auger driven powder delivery system for full scale SLS machine use.

8.15 RESULTS & CONCLUSIONS

Table 8.1 below shows the summarised results across all of the experiments, showing the relative effectiveness of each change to the rig. This shows that many of the techniques used had a negative effect on the output powder profile, and the final arrangement of plugs in a grid baffle was the best result achieved in these experiments.

The column “Maximum % Average Difference Between Cups” was calculated as follows:

1. Find the net powder weight for each cup and each running time length.
2. Find the mean net weight of powder in each cup, as a percentage of the total net powder weight moved for each running time length.
3. Find the mean percentage for each cup across all running time lengths.
4. Subtract the smallest percentage cup from the largest.

TABLE 8.1 - AUGER DRIVEN POWDER DELIVERY RIG OVERALL RESULTS

Experiment	Sub-chapter	Maximum % Average Difference Between Cups
Baseline Test	8.2.	4.8
Alternate Operator	8.3.	4.8
Scraper Alterations	8.4.	4.9
Removing 'Hills' – Baseline	8.6.1.	11.8
Auger 1 Loose	8.7.1.	33.3
Auger 2 Loose	8.7.2.	14.2
Auger 3 Loose	8.7.3.	30.5
Auger 1 – 20 Teeth	8.8.1.	5.7
Auger 1 – 24 Teeth	8.8.2.	7.5
Replacement Output Tray – No Hills No Baffles	8.9.1.	13.1
Replacement Output Tray – No Hills With Baffles	8.9.2.	18.1
Replacement Output Tray – With Hills No Baffles	8.9.3.	11.7
Replacement Output Tray – With Hills With Baffles	8.9.4.	17.7
Replacement Output Tray - Tilting Machine Base	8.9.5.	16.2
Tall Output Tray – Baseline	8.10.1.	14.1
New Baffle Design	8.11.	18.7
Auger 1 Only	8.12.	55
Auger 2 Only	8.12.	56.2
Auger 3 Only	8.12.	68.6
Running Auger 3 in Opposite Direction	8.13.	6.7
Grid Baffle – No Plugs	8.14.1.	7.9
Grid Baffle – Plug Arrangement A	8.14.2.	4.2
Grid Baffle – Plug Arrangement B	8.14.3.	3.3
Grid Baffle – Plug Arrangement C	8.14.4.	2.6

Considerable time and effort was spent in determining the potential effectiveness of an auger driven powder delivery system for use in SLS type AM machines. This experiment ran for approximately eight months from start to finish and a large number of factors were examined in order to produce an even output powder profile.

The current methods use a pair of feed bins and pistons alternately feeding the roller mechanism, or a single feed bin and piston at the expense of build time due to the extra roller return time between layers. In either case this adds considerable size, cost and complexity to the machine. Additionally, it is not possible to add or remove powder from the machine during the build process as the chamber would have to be opened,

compromising the inert, heated atmosphere and cooling the unfinished build, which affects bonding between layers of a build (Walker Wroe, et al., 2016).

This novel, auger driven method would eliminate the need to open the machine to add powder as it could be fed from a hopper external to the machine. It also simplifies the production cycle of the machine by eliminating the need to remove and clean one or both feed pistons between builds. If leftover powder in the feed bin could not be used for the next build, the augers could be run at higher than usual speed and for an extended period so as to remove spent powder quickly and semi-automatically.

The auger method notably does not improve recoat time due to it still requiring either two feed bins or a single feed bin with extra roller travel time, though there is no detrimental effect to this either, the auger and feed piston methods both have the same recoat times depending on configuration.

A considerable disadvantage of the auger driven system is the need for calibration of the output tray, through a selectively plugged grid baffle as used here, or similar system. Comparatively, the feed piston system requires little to no calibration as the piston by its nature will raise the powder with an even profile. It is unclear at this time whether a selectively plugged grid baffle would need to be calibrated individually for each application or if a single plug layout could be used universally, though the variation in results from the previous experiments and overall sensitivity of the rig would suggest that the former may be more likely.

9 PROCESS SPEED & EFFICIENCY

Improving the length of time taken for one full cycle of an SLS machine is critical in making the technology commercially viable, as this affects both the cost of the process and the speed with which parts could be delivered. This required an examination of the cycle itself, in order to identify parts of the process which could be reduced in terms of time taken. This cycle was approximately as follows, but varied from machine to machine:

1. Clean all machine components which are exposed to powder
2. Load fresh powder into powder bins
3. Power on the machine
4. Configure the machine with the required settings and CAD files
5. Purge oxygen and bring machine up to temperature
6. Perform build layer by layer
7. Cool the machine
8. Power off the machine
9. Extract the build 'cake'
10. Clean excess powder from parts

This chapter addresses a selection of these steps, identified as being possible to improve while keeping cost to a minimum. These were the machine's power distribution system, the concept of a removable build cylinder and machine-to-operator informational feedback method. Other steps in the process were not considered for research due to time and funding availability.

9.1 POWER DISTRIBUTION SYSTEM

The process of switching on an SLS machine could in theory have been a simple as activating a single switch. However, this would be unsafe as there would be potential, in an error condition, for heaters to be active without nitrogen flow or with the door open. It was therefore decided that the machine should power up in steps, requiring verification from a human that the next stage of power is safe to activate. In order to simplify this process as much as possible, the operator was to be presented with two buttons to power

on the machine; green (advance power to next state if safe to do so) and red (stop everything/power off).

Additionally, it was useful to have an idea of how much power the machine would use at full load, as the availability of an appropriate electricity supply would partly determine which environments such a machine could be used in.

Initial calculations, based on datasheets of known components and estimates for unknown ones as shown in table 9.1, suggested that the machine would require a 32A 3-phase electricity supply. It would also require that each part of the machine be switched on in a sequence in order to avoid surges and maintain a safe working environment as the machine is being prepared. As such, a power distribution system was required to safely distribute power to all parts of the machine in a specific chronological order as follows:

1. PC and scanner controller
2. PLC, sensors and laser chiller
3. Motors, scanner and nitrogen
4. Heaters and laser

TABLE 9.1 - MACHINE POWER REQUIREMENT CALCULATIONS

Item	Max current (mA)	
PLC	750	
PC	4000	
Sensors	5000	Estimated
Laser	4167	
Chiller	4167	
Heaters	25000	
Motors	3750	
Scanner	5000	Estimated
Total	51834	
Per phase	17278	

Each power 'stage' was activated by button pushes, between which the user checked various safety considerations on the PC's user interface. If the safety parameters weren't met, the PLC did not allow power to that part of the machine.

Stage 1 was active when the machine was applied with power and the main power switch closed. This provided power to the PC, monitors and scanner controller card.

Stage 2 was activated by pressing the green button on the control panel. This provided power to the PLC, system sensors via DC power supplies and laser chiller.

Stage 3 was activated by pressing the green button on the control panel again, if the machine's chamber doors were shut this provided power to all motors including the laser scanner and the nitrogen flow control system.

Stage 4 was activated by pressing the green button on the control panel a third time, if the oxygen content within the machine's chamber was low enough, power was provided to all heaters and the laser. This was the fully powered state in which the machine would perform a build. Images of a partially constructed power distribution system can be found in appendix D.

9.2 REMOVABLE BUILD CYLINDER DOLLY

Possibly one of the most significant changes investigated by this dissertation in terms of minimising build turnaround time, was the removable build cylinder dolly which, upon its removal would allow the next to be started almost immediately with a different dolly, while the previous build was processed elsewhere. This could save something in the order of a few hours of turnaround time, as part extraction and cylinder cleaning could be performed concurrently with the start of the next build.

The first iteration of design and construction of removable build dolly was completed by the project sponsor, Euriscus Ltd of Chesham, England in 2016 and comprised simply of a trolley with a horizontal platform, driven vertically by a stepper motor via a gearbox. Three inductive proximity sensors registered the limits of travel for top, near bottom and bottom. These along with the stepper motor were connected to an Allen Bradley 1746-HSTP1 step motor control module via a Parker PDS15-2 step motor driver, through the use of several DIN type plugs, each of which had a different number of pins to prevent incorrect connection. More about this build dolly prototype can be found in Chapter 3.3.

As this initial version had been produced with only the testing of accurate piston control in mind, it was quickly established that another version would have to be constructed to include the following extra features:

- A build cylinder
- Build cylinder heater
- Piston heater
- Single dolly interconnect including trolley type identification pins

More about potential subsequent versions of the build dolly is discussed in Chapter 11.

In order for any build dolly to be successfully paired with the SLS machine, great care had to be taken to ensure the dolly and its receiving hole met properly aligned, such that the piston could be brought flush with the internal base of the machine with as little gap around the edges and cylinder top as possible. If the dolly is not aligned properly gas and powder could escape through the gap, potentially causing a build to fail completely should it have been allowed to start. To this end the machine frame was designed to incorporate inductive proximity sensors, to meet with specific metal faces on the build dolly. Once these sensors were triggered, a pair of electrically actuated lifting jacks engaged either side of the dolly raising it toward the receiving hole in the machine. As the dolly rose a number of protruding cones on the top of the dolly met with counterpart holes in the underside of the machine, guiding it as accurately as practicable into place.

9.3 PROCESS STATUS VISIBILITY

A relatively cheap and easy method for ensuring nearby machine operators were aware of the machine's current status was through the use of a beacon stack. These were commonly used in an industrial setting and could be configured for a range of different colours with solid or flashing lights, and often included an audible alert in the form of a buzzer.

The lamp stack chosen for use in this research was a Kompakt 37 (Werma Signaltechnik, Wellingborough, England). It featured three separate LEDs with red, amber and green lenses and an audible alert buzzer. Its 24VDC inputs allowed it to be directly driven by

four channels from one of the PLC's 24VDC digital output modules. It can be seen in Figure 9.1.



FIGURE 9.1 - LAMP STACK

The indications given by the lamp stack should be as intuitive as possible so as to be easily interpretable at a glance. This should help to minimise the time between any error occurring and human intervention, resulting in recovery of a build process if possible. As such the PLC's four digital outputs were configured as follows:

Solid green lamp – Machine idle and ready

Flashing green lamp – Machine idle and finished

Solid amber lamp – Machine running and nominal

Flashing amber lamp – Machine running with warning(s)

Solid red lamp – Build paused due to error

Flashing red lamp – Build stopped due to error

Buzzer – Immediate attention required/critical error

This configuration meant that in order for an operator to have an idea of what state a machine (or a number of machines) was currently in, they would simply have to look up at the lamp(s), which were mounted to the top of the machine(s) for this purpose. Other methods such as internet connectivity with mobile phone notifications could have also been effective but this would have cost more, been more complicated (and therefore more susceptible to failure) and required an operator to remove their phone from their pocket which generally took longer than to simply look upwards.

10 CONCLUSIONS

The examination of each of the system elements looked at during this dissertation has provided a number of insights into potential improvements to the SPLS build process in terms of build speed and part integrity. The following is a summary of the findings from each set of experiments.

Using ASCII over RS232 provided an extremely cheap and reliable way to maintain a link between PC and PLC, capable of updating hundreds of system parameters every second. While other methods could have provided more bandwidth, they also required proprietary hardware and software licenses at significant cost. RS232 and ASCII's well-established standards, low cost and wide availability mean future maintenance of its application in this context should be relatively simple. While unlikely to provide time savings in terms of the length of the build cycle, a good link here should reduce the likelihood of certain types of breakdown where the PLC is unable to communicate with the user and wider system, causing significant machine down time.

A single PID control loop triggering a number of infrared lamps was sufficient for creating a powder bed surface temperature distribution consistent enough with which to effectively sinter parts, without the risk of parts being partially un-sintered or melted. The experiments showed that moving the heat source upwards in the chamber, away from the powder surface appeared to have a defocussing effect which created a more consistent temperature profile. In the context of a working machine this would hypothetically reduce time spent by decreasing the number of failed or inadequate quality builds which require the build cycle to be entirely repeated.

A closed loop feedback control system utilising a pair of solenoid valves provided an effective way to deoxygenate a chamber rapidly and provide fine control for the purpose of maintaining a safe atmosphere for the duration of a build process. The oxygen sensor feedback mechanism also would have allowed the system to take safety measures in the event that the chamber became prematurely re-oxygenated. Improvements here offer an opportunity to reduce build times by a number of minutes by de-oxygenating the build chamber as rapidly as possible and may reduce the number of failed builds from oxygenated air leaking into the chamber.

The step motor, controller and encoder combination used in these experiments were capable of movement accuracy far greater than that required for sintering PA12 powder. However, accuracy of the piston itself was limited by mechanical backlash introduced by the gearbox and lead screw comprising the connection between the motor and piston surface. Sintering of powders with smaller particle sizes at higher z-height resolution would require finely machined parts in order to significantly reduce this backlash. In terms of build times using smaller z-heights, while increasing part fine detail, may increase the length of a build by increasing the number of layer cycles.

A set of 4 augers was successfully used, in conjunction with a grid patterned output baffle to consistently provide an amount of powder, distributed evenly along the axis parallel with the roller of an SLS machine. This meant that powder could be loaded into an SLS machine from an external hopper, allowing build media to be added at any point during a build process. The grid baffle manufactured for the experiments was also successful in mitigating the effects of the spinning augers which appeared to cause the powder to rise non-linearly in the output side of the experimental rig. Using this novel technique would allow time savings between build cycles as powder can be loaded at any time during a build.

Distributing power to individual components of a complex system was achieved by using a staged power-up system, each stage of which was enabled manually for safety reasons. This prevented surges on the mains 3-phase circuit from multiple devices activating at once and allowed elements such as heaters and motor driven assemblies to be isolated. This maintained a safe working environment while allowing some sensors and sub-systems to remain active for monitoring purposes. This method does not offer direct time savings, however isolating machine component's power from each other means a machine could be partially shut down for maintenance, potentially reducing the amount of time required to fully re-power it for the next build.

The ability to remove the entire build cylinder and associated hardware easily from an SLS machine was examined as a possibility and it was established that this would reduce the turnaround time for such a machine by a number of hours in the event where an identical piston trolley were immediately available for the next build.

The use of easily visible beacon stacks combined with an easily interpretable system of coloured light & sound signals provided a way to rapidly attract the attention of machine operators in order to minimise downtime and failed build frequency through waiting for required human interaction. This method is also cost effective and does not require the use of peripheral hardware such as an HMI or remote interface software via a phone or tablet.

If an SLS machine was built which implemented each of these features, it would have significant advantages over currently available machines and would potentially be more competitive with other methods of manufacturing with the same materials such as injection moulding. While it is often difficult to quantify time savings though system improvements due to lack of available information it is clear that certain elements, for example the removable build cylinder, offer an opportunity to significantly reduce the time taken to prepare the machine for its next cycle.

11 FUTURE PROJECT WORK

During the progress of this research, many concepts have been examined for potential viability, that may have been used for later parts of the overall machine development. This dissertation covers a two-year portion of the collaborative project with the industrial sponsor and as such some of this work fell outside of its scope. Some of these concepts are examined in the following sub-chapter.

11.1 BUILD DOLLY DEVELOPMENT

The prototype build dolly constructed, which was discussed in Chapters 3.3 and 9.2, required a secondary version to provide necessary functions for the build process as well as a more convenient interface to the machine in terms of its physical alignment and electronic interconnects. This second iteration fell outside of the scope of this dissertation, but its details had been proposed as follows.

The mechanism on the first prototype dolly consisted of a horizontally mounted motor feeding a gearbox, which in turn fed a vertically mounted lead screw. This mechanism, while offering a great deal of accuracy through the gearbox's high ratio, suffered a significant amount of backlash as discussed in Chapter 7 which was a major barrier to its accuracy. One proposed solution considered that upon the addition of the build piston casing, the platform would be effectively locked in the two horizontal dimensions, due to the requirement of tight fitment for the platform within the casing to mitigate against egress of build media. An amount of mechanical backlash would remain in this case due to the imperfect nature of meshing gears, though this is unavoidable save for minimisation through the purchase of more expensive mechanical components. If the amount of backlash is known and relatively constant, this could theoretically be partially compensated for from within control software.

The addition of heating elements to the build piston surface and casing is typical of current generation SLS machines and assists in maintaining the core temperature of the build cake (The solid mass of powder and sintered parts comprising the raw output of an SLS machine), ensuring it stays within the correct range of temperatures so as to avoid

part curling or warping. This would almost certainly be added to newer versions of the dolly as without it heat is quickly wicked away from the build cake into the cold metal piston and casing. These heaters would likely be each controlled by a closed loop control system whereby each heater's power was switched via a PLC PID loop, informed by thermocouples mounted near to the centre of the targeted area of each heater. This method affords the best possible control and accuracy of targeted temperatures.

A method by which to identify the specific build dolly being used in the machine, without human input, would be useful as it is possible that alternative versions could be produced, with differently sized pistons or differently configured heaters. The proposed method to achieve this was to reserve a small number of pins, some of which would be wired to a common pin, to received 24VDC from the PLC. This would, depending on the configuration of pin connections, create a binary code which could be compared against a record within the PLC code to determine the exact specifications of the dolly being used, and alter its control accordingly.

The electrical interconnections between the build dolly and the machine itself are numerous and would include the following items assuming all additions proposed in this sub-chapter are made:

- Motor power – 3.4A at 2.1VDC per phase, 8 pins
- Limit sensors – x3, <200mA at 24VDC, 9 pins total
- Heater power – Exact number and configuration to be determined
- Thermocouples – Exact number and configuration to be determined
- Dolly identification pins – Exact number and configuration to be determined

It is likely that all of these would share a single connection, as using separate connections for each function while mitigating potential interference between power and data pins, would increase the amount of time taken in connecting and disconnecting the dolly from the machine. As such a connection is required that is capable of carrying enough current to drive the step motor while maintaining separation from sensitive control signals. One such example of a connector capable of this through its vast configurability, is Harting's 'Han' modular range, which offer great flexibility but suffer from being relatively expensive.

A potential improvement for the mid-to-long term future of the research would be automation of the build dolly such that it could navigate unassisted between the SLS machine, finishing stations and dolly storage locations. The technology currently exists in some modern warehouses, where autonomous robots move about the warehouse, and sorting inventory according to the command of a central control computer. This would require a means of locomotion and steering probably provided by electric motors and servos or linear actuators, a means of sensing location achieved perhaps by permanent environment markers or otherwise, and a means of communication with the central control system for which there are a great number of options.

11.2 THERMAL IMAGING

Even and consistent heating of the build area surface is critical to the viability of the build process as discussed previously in Chapters 2.2 and 5. An idea conceived early in the work was determined at the time to be too expensive and time consuming but may be a good option for later research. This idea involved the use of a thermal camera mounted above the build area, as close to the centre as possible without interfering with the path of the laser. The camera would capture images of the build area surface temperature, then using some unspecified image processing software determine the effect of each heater, assuming there was an array of heaters each heating its own 'zone'. This data could then be fed back to each heater's control loop in the PLC code, thereby in theory maintaining constant temperature across the build area.

One drawback to this proposed approach was that the areas heated by each lamp would not likely have discrete edges, rather they would overlap and bleed into each other as the radiation from the lamps diffuses in the distance between the build chamber ceiling and the build area. This would make processing the images extremely complicated, likely requiring proprietary software and months of testing and refinement. This effect may possibly be mitigated by having heater 'zones' manually specified to physical areas of the build platform and coding to assume there is no crossover in area heating, though the effectiveness of this exact approach has not been investigated at time of writing and is therefore not known.

11.3 HEATED ROLLER

The reheating process, which occurs for the purpose of heating the freshly applied top layer of powder up to the desired surface temperature between each layer of a build, takes a significant portion of the total build time as it must be performed once for each layer of the build. In order to reduce the time taken during this part of the build cycle, SLS machine powder feed mechanisms are generally heated near to the desired temperature, but not so close as to affect the powder's ability to be spread evenly across the build area. Those machines which use a roller mechanism to apply each layer of powder suffer from having an unheated roller which causes the powder surface temperature to drop as it is applied and flattened. This work considered two methods by which to heat the roller with the hope of mitigating this effect.

The first method considers using embedded cartridge style heaters inside the roller itself. This, while possibly being the simpler solution conceptually, would have required a mechanism by which to transfer heater power and thermocouple connections, whose wiring is well established to be very sensitive, into the rotating part of the roller. Such mechanisms could have included a slip ring, which are generally expensive, have limited life span, are temperature limited and current limited. Or this mechanism may have used cables on a spool attached to the back end of the roller, feeding the wires to a fixed set of glands in the chamber wall at one side. This second mechanism would have potentially been cheaper to produce, and perhaps more complicated to implement reliably.

An alternative to embedded cartridge heaters considered for the research was to use a shroud with infrared lamps positioned above the roller, mounted to the roller transit carriage. This would not require a slip ring, though would still need a method to get cables from the moving roller transit carriage to the side of the build chamber, such that it does not become entangled with the moving parts of the roller mechanism. A common method to achieve this is with a cable chain, which forces cables to follow a predetermined path as dictated by a number of hinged sections, similar to a tank track.

12 APPENDICES

A PID LOOP CONTROL EXPERIMENT PARAMETERS

Table 12.1 defines the control parameters used in the PID loop control experiment. Each parameter has an 'ID' of format X[y] where X is a character preceding each line of data; either "C" for 'configuration parameters' or "S" for 'status parameters'. y defines the parameter's location within that line. The permission column shows which serial interface commands can be used with the parameter, the "GET" command was later removed from the system in order to preserve memory as it was largely unused. The "Sent on change" column shows which parameters were sent immediately via the serial interface when their value is changed, as opposed to waiting until the next set of messages to be sent through.

TABLE 12.1 - PLC PARAMETERS

ID	Parameter name	Type	Units	Permission	Description	Sent On Change?
C[1]	block_temp_max	int	degCx10	GET, SET	Maximum temperature value we specify to PLC	
C[2]	block_temp_min	int	degCx10	GET, SET	Minimum temperature value we specify to PLC	
C[3]	block_temp_target	int	degCx10	GET, SET	Target temperature value we specify to PLC	
C[4]	block_temp_err	int	degCx10	GET, SET	Maximum difference between target and current temperatures for "block_temp_reached" to set	
C[5]	block_temp_max_adv_val	int	degCx10	GET, SET	Value at and above which "block_temp_max_adv" is set	
C[6]	block_temp_min_adv_val	int	degCx10	GET, SET	Value at and below which "block_temp_min_adv" is set	
C[7]	block_temp_max_ala_val	int	degCx10	GET, SET	Value at and above which "block_temp_max_ala" is set and system stops	
C[8]	block_temp_min_ala_val	int	degCx10	GET, SET	Value at and below which "block_temp_min_ala" is set and system stops	
C[9]	block_time_to_temp_adv_val	int	seconds	GET, SET	"block_time_to_temp_adv" is set if block does not reach target temperature (+/- error) within this time	
C[10]	block_time_to_temp_ala_val	int	seconds	GET, SET	"block_time_to_temp_ala" is set and system stops if block does not reach target temperature (+/- error) within this time	
C[11]	heat_load_max	int	%	GET, SET	Maximum percent load of heater	
C[12],S[18]	block_heat_enable	bool	yes/no	GET, SET	Engages relay which provides power to heater	
C[13],S[19]	system_ala_stop	bool	yes/no	GET, SET	System has stopped due to an alarm	Y
C[14],S[20]	recoat_pending	bool	yes/no	GET, SET	Request the PLC to perform a recoat, PLC clears this bit when recoat starts	Y
S[1]	block_time_to_temp	int	seconds	GET	Starts counting when a new target temperature is set, resets when it is reached	
S[2]	system_run_time	int	seconds	GET	Time since equipment switched on	
S[3]	block_temp_now	int	degCx10	GET	Reading from thermocouple	*
S[4]	heat_load_now	int	%	GET	Current percent load of heater from output of PID	
S[5]	start_button	bool	yes/no	GET	Indicates current state of heater "start" button	Y
S[6]	system_idle	bool	yes/no	GET	System is ready to run	Y
S[7]	system_running	bool	yes/no	GET	System is running (heater is on)	Y
S[8]	block_temp_reached	bool	yes/no	GET	"block_temp_now" = "block_temp_target" +/- "block_temp_err"	Y
S[9]	block_temp_max_adv	bool	yes/no	GET	"block_temp_now" >= "block_temp_max_adv_val"	Y
S[10]	block_temp_min_adv	bool	yes/no	GET	"block_temp_now" <= "block_temp_min_adv_val"	Y
S[11]	block_temp_max_ala	bool	yes/no	GET	"block_temp_now" >= "block_temp_max_ala_val"	Y
S[12]	block_temp_min_ala	bool	yes/no	GET	"block_temp_now" <= "block_temp_min_ala_val"	Y
S[13]	block_temp_sens_fail	bool	yes/no	GET	Sensor reading is massive indicating failure	Y
S[14]	block_time_to_temp_adv	bool	yes/no	GET	"block_time_to_temp" >= "block_time_to_temp_adv_val"	Y
S[15]	block_time_to_temp_ala	bool	yes/no	GET	"block_time_to_temp" >= "block_time_to_temp_ala_val"	Y
S[16]	recoat_running	bool	yes/no	GET	A recoat (10 second delay) is currently in progress	Y
S[17]	recoat_complete	bool	yes/no	GET	A recoat has been completed. Resets when "recoat_pending" is set.	Y
S[21]	dummy_interlock	bool	yes/no	GET	Simulating chamber door, 1 = closed, 0 = open	Y
N/A	com_port_mode	bool	SYSTEM/ USER	NONE	Sent ONLY when PLCs com port mode is changed. Cannot use GET or SET.	Y

* Sent when a temperature related alarm or advisory changes.



**MATERIAL DATA SHEET
LS – PA12GF**

A GLASS FILLED POLYAMIDE 12 MATERIAL USED WITH SELECTIVE LASER SINTERING

Background

Polyamide 12 (PA12) is a well known plastic normally used for the injection moulding of parts intended for engineering applications. By adding glass beads, a glass filled composite is produced. This LS-PA12GF material produces stiffer and stronger components than natural LS-PA12 although these advantages are gained at the expense of a reduction in the elongation to break.

Features

The LS-PA12GF material produces parts with excellent strength and stiffness. Components made in these materials exhibit similar properties to those which are injection moulded in glass filled polyamide. The material also gives a smoother surface finish than the natural LS-PA12 material. The presence of the glass fill material enables components made in LS-PA12GF to be operated at a higher temperature than LS-PA12.

Benefits

Parts are accurate and strong, and can be machined, for example parts can be tapped or can be fitted with metal inserts, and can generally be treated in a similar way to injection moulded polyamide components. They can also be finished in a variety of ways, including being painted and plated. Components made in LS-PA12GF offer a quick route to completely functional plastic parts.

Applications

LS-PA12GF finds a great many applications in both prototyping and production applications. A wide range of industries, including aerospace, automotive, medical, environmental, defence and electrical goods are already wide users of this material. A list is given below of a few of the many applications to which LS-PA12GF parts can be put.

Prototyping	Production
Enclosures	Clips and stands
Frames, handles and mechanisms	Enclosures
Plugs and sockets	Parts likely to experience wear
Fans, impellers	Jigs and fixtures e.g. for drilling
Parts to be used at elevated temperatures	Assembly aids
Product chassis, cases and housings	
Load bearing components	



C POWDER DELIVERY EXPERIMENT PHOTOS & DATA

C.1 PHOTOS

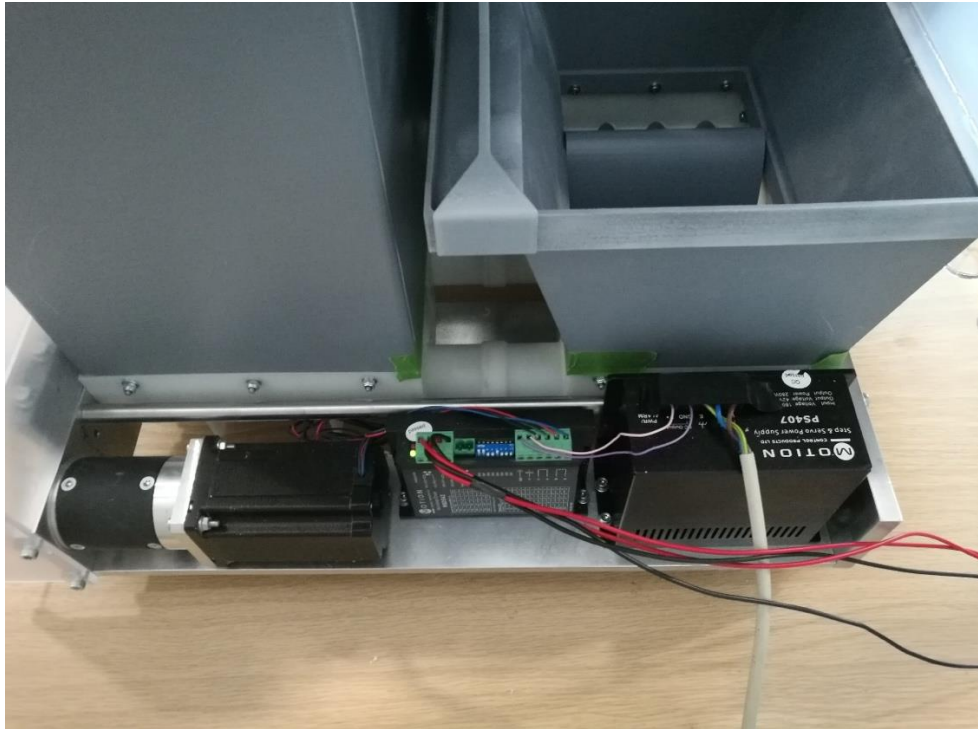


FIGURE 12.1 - POWDER DELIVERY TEST SYSTEM CONTROL ELECTRONICS



FIGURE 12.2 - FILLING POWDER DELIVERY TEST SYSTEM 1



FIGURE 12.3 - FILLING POWDER DELIVERY TEST SYSTEM 2



FIGURE 12.4 - FILLING POWDER DELIVERY TEST SYSTEM 3



FIGURE 12.5 - POWDER DELIVERY TEST SYSTEM FULL AND LEVEL



FIGURE 12.6 - POWDER DELIVERY TEST SYSTEM OUTLINE OF RISEN POWDER

C.2 BASELINE TEST

TABLE 12.2 - AUGER RIG BASELINE TEST RESULTS

	Cup 1	Cup 2	Cup 3	Cup 4	Cup 5
10	3.095	3.774	3.429	4.013	3.986
20	7.654	9.397	9.175	10.073	9.989
30	11.706	14.270	13.858	15.509	15.266
40	16.596	19.714	19.168	20.759	20.607
50	20.465	24.272	23.368	25.772	25.737

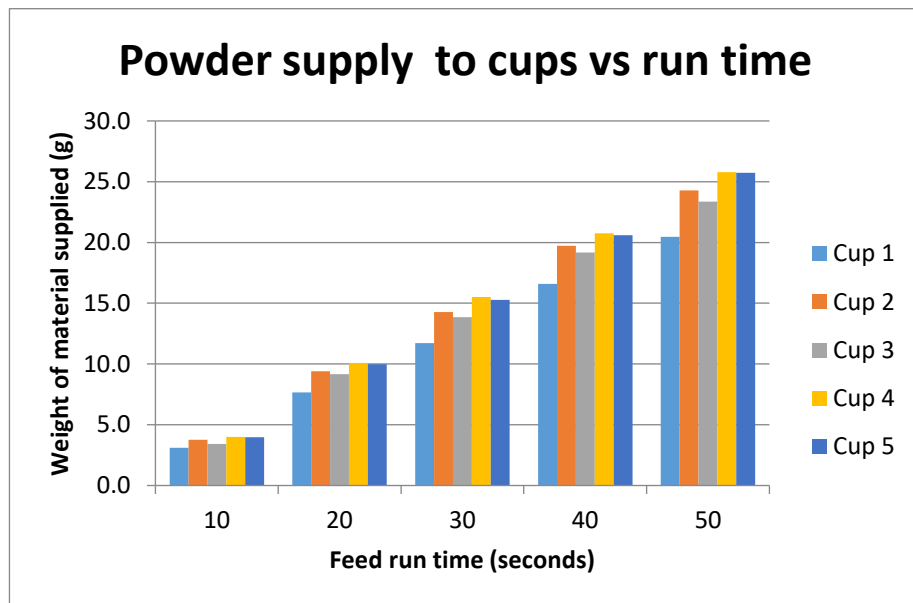


FIGURE 12.7 - AUGER RIG BASELINE TEST RESULTS GRAPH 1

C.3 ALTERNATIVE OPERATOR

TABLE 12.3 - AUGER RIG ALTERNATE OPERATOR TEST RESULTS

	Cup 1	Cup 2	Cup 3	Cup 4	Cup 5
10	3.832	4.584	4.167	4.822	4.567
20	7.689	9.728	9.224	10.083	10.215
30	12.454	14.932	14.082	15.611	15.638
40	15.944	19.405	18.642	20.638	20.864
50	19.932	24.803	24.283	26.349	26.787

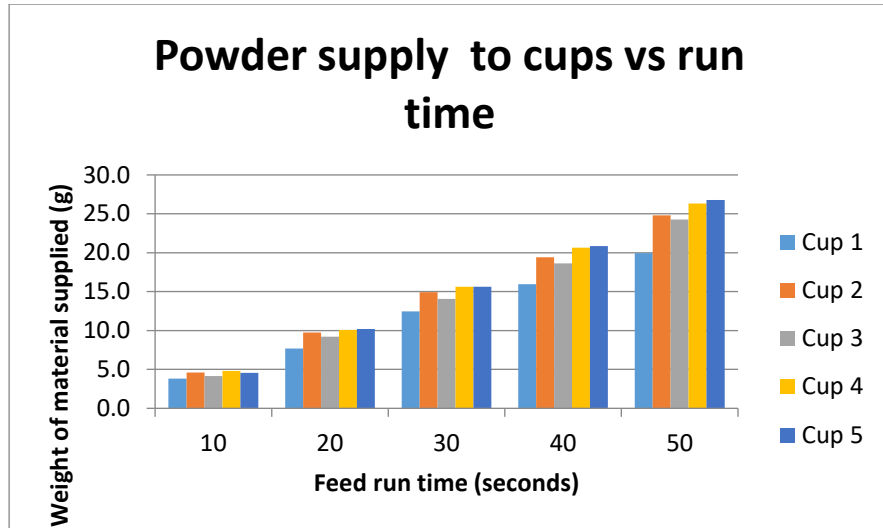


FIGURE 12.8 - AUGER RIG ALTERNATE OPERATOR TEST RESULTS GRAPH 1

C.4 SCRAPER ALTERATIONS

TABLE 12.4 - AUGER RIG ALTERED SCRAPER TEST RESULTS

	Cup 1	Cup 2	Cup 3	Cup 4	Cup 5
10	4.046	4.898	4.422	5.140	4.998
20	7.921	9.881	9.093	10.284	10.020
30	11.719	14.866	13.872	15.401	15.489
40	16.464	20.366	19.350	21.140	21.681
50	20.246	24.738	23.255	25.556	26.759

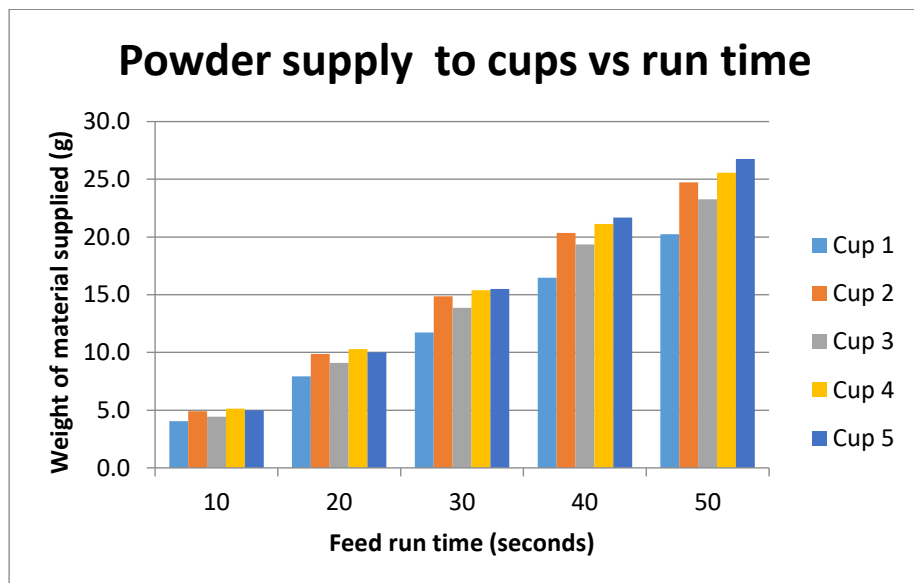


FIGURE 12.9 - AUGER RIG ALTERED SCRAPER TEST RESULTS GRAPH 1

C.5 MEASURING FRONT AND REAR HALVES OF BED INDEPENDENTLY

TABLE 12.5 - AUGER RIG FRONT/REAR TEST RESULTS

	Cup 1	Cup 2	Cup 3	Cup 4	Cup 5
10 front	2.223	2.620	2.201	2.913	3.026
10 rear	1.314	1.800	1.862	1.613	1.312
30 front	7.576	9.163	8.001	10.053	10.905
30 rear	4.088	5.689	5.373	5.364	4.555
50 front	12.165	14.600	13.206	16.021	17.155
50 rear	7.305	10.247	10.274	9.596	8.362

C.6 REMOVED HILLS BASELINE

TABLE 12.6 - AUGER RIG HILLS REMOVED TEST RESULTS

	Cup 1	Cup 2	Cup 3	Cup 4	Cup 5
10	1.374	2.229	2.690	3.426	3.416
20	5.763	8.601	9.917	10.679	9.714
30	8.572	13.315	14.960	15.861	14.981
40	11.800	17.358	20.167	21.847	21.325
50	15.232	22.187	25.337	27.472	27.282

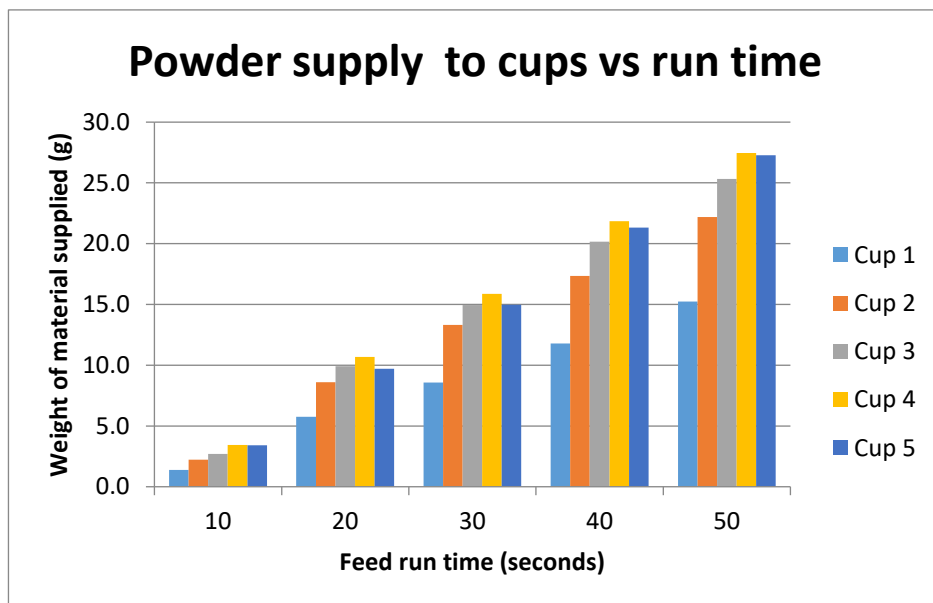


FIGURE 12.10 - AUGER RIG HILLS REMOVED TEST RESULTS GRAPH 1

C.7 REMOVED HILLS FRONT & REAR

TABLE 12.7 - AUGER RIG HILLS REMOVED FRONT/REAR TEST RESULTS

	Cup 1	Cup 2	Cup 3	Cup 4	Cup 5
10 front	1.713	2.753	3.124	3.766	3.613
10 rear	1.349	1.912	1.923	2.017	1.830
30 front	4.783	7.524	8.635	10.018	9.818
30 rear	3.832	5.702	5.832	6.080	5.240
50 front	7.529	11.575	13.849	16.309	16.461
50 rear	7.262	10.684	11.367	11.532	10.168

C.8 AUGER 1 LOOSE

TABLE 12.8 - AUGER 1 LOOSE TEST RESULTS

	Cup 1	Cup 2	Cup 3	Cup 4	Cup 5
10	0.006	0.950	2.893	4.542	4.610
20	0.139	2.798	6.752	9.889	10.192
30	0.198	4.751	11.317	15.694	15.817
40	0.303	6.311	14.748	20.375	20.763
50	0.474	8.297	19.720	26.405	26.675

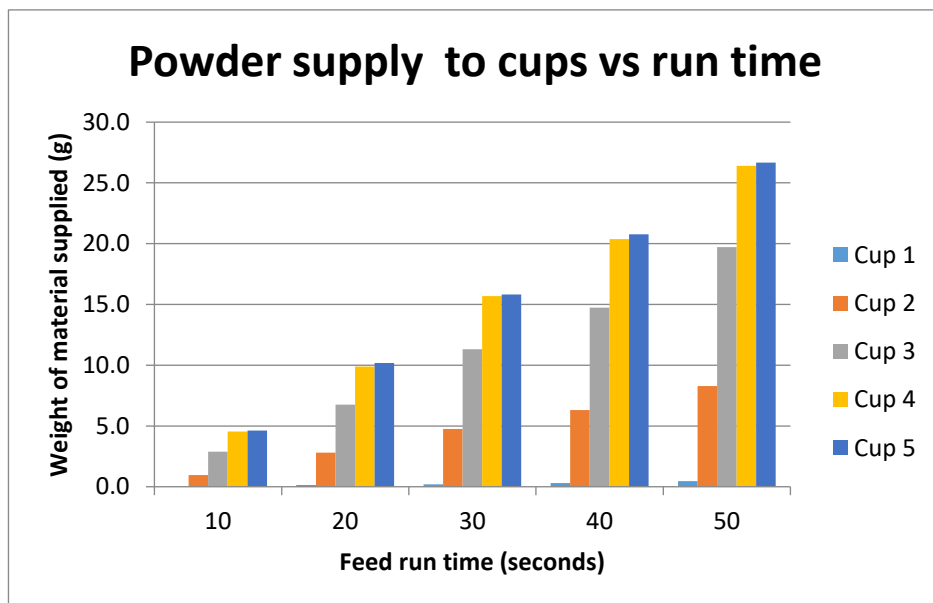


FIGURE 12.11 - AUGER 1 LOOSE TEST RESULTS GRAPH 1

C.9 AUGER 2 LOOSE

TABLE 12.9 - AUGER 2 LOOSE TEST RESULTS

	Cup 1	Cup 2	Cup 3	Cup 4	Cup 5
10	2.114	2.575	1.987	3.095	3.568
20	4.379	6.083	5.275	7.672	8.493
30	6.989	8.953	7.628	11.191	14.165
40	8.886	11.637	9.633	14.677	19.949
50	11.823	16.000	14.653	20.063	25.367

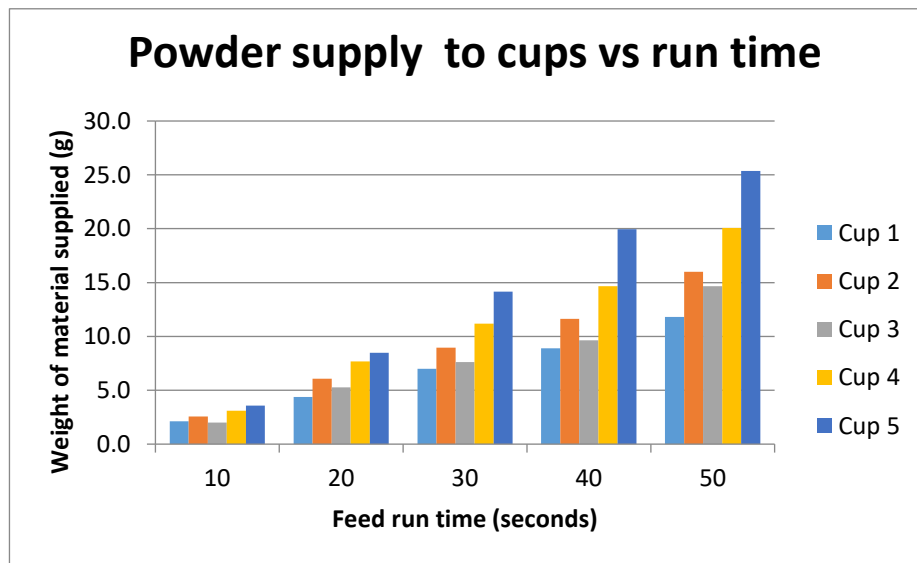


FIGURE 12.12 - AUGER 2 LOOSE TEST RESULTS GRAPH 1

C.10 AUGER 3 LOOSE

TABLE 12.10 - AUGER 3 LOOSE TEST RESULTS

	Cup 1	Cup 2	Cup 3	Cup 4	Cup 5
10	2.409	4.128	2.992	1.073	0.069
20	5.217	9.338	7.766	3.839	0.547
30	8.644	14.310	12.587	6.883	1.889
40	13.116	19.485	18.158	10.185	2.092
50	17.259	24.656	22.789	14.153	3.457

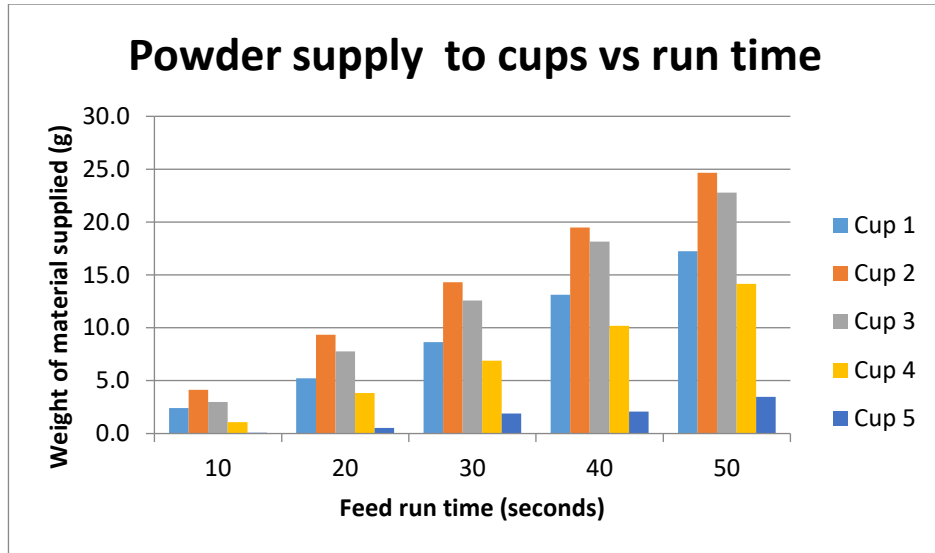


FIGURE 12.13 - AUGER 3 LOOSE TEST RESULTS GRAPH 1

C.11 20 TOOTH TIMING WHEEL

TABLE 12.11 - AUGER 1 AT 5.2 RPM TEST RESULTS

	Cup 1	Cup 2	Cup 3	Cup 4	Cup 5
10	3.976	5.517	3.798	4.365	4.819
20	9.621	13.306	10.184	11.324	11.608
30	13.727	18.656	14.739	15.667	17.179
40	18.628	23.891	19.270	20.221	22.834
50	23.570	28.662	25.152	26.623	28.288

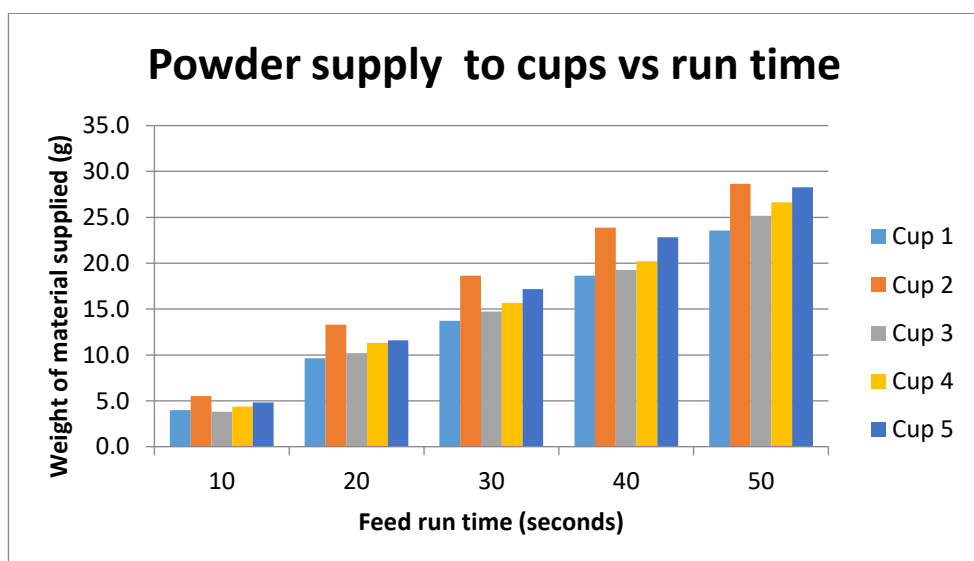


FIGURE 12.14 - AUGER 1 AT 5.2 RPM TEST RESULTS GRAPH 1

C.12 24 TOOTH TIMING WHEEL

TABLE 12.12 - AUGER 1 AT 4.3 RPM TEST RESULTS

	Cup 1	Cup 2	Cup 3	Cup 4	Cup 5
10	3.488	5.226	4.137	4.631	5.191
20	6.963	11.253	9.694	10.261	10.573
30	11.270	16.292	14.232	15.219	16.289
40	14.620	21.683	19.934	20.220	21.625
50	18.882	27.306	24.338	25.934	27.427

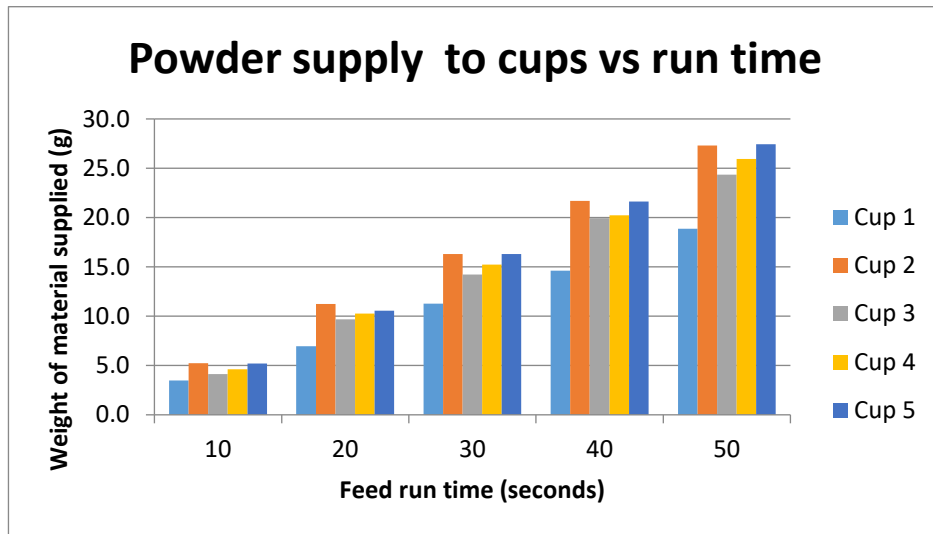


FIGURE 12.15 - AUGER 1 AT 4.3 RPM TEST RESULTS GRAPH 1

C.13 NEW OUTPUT TRAY – NO HILLS, NO BAFFLES

TABLE 12.13 - NEW TRAY NO HILLS NO BAFFLES TEST RESULTS

	Cup 1	Cup 2	Cup 3	Cup 4	Cup 5
10	3.769	3.602	5.020	2.875	5.907
20	6.756	7.151	9.169	8.093	12.884
30	9.992	11.070	13.895	12.496	19.436
40	13.178	15.482	18.807	18.604	26.240

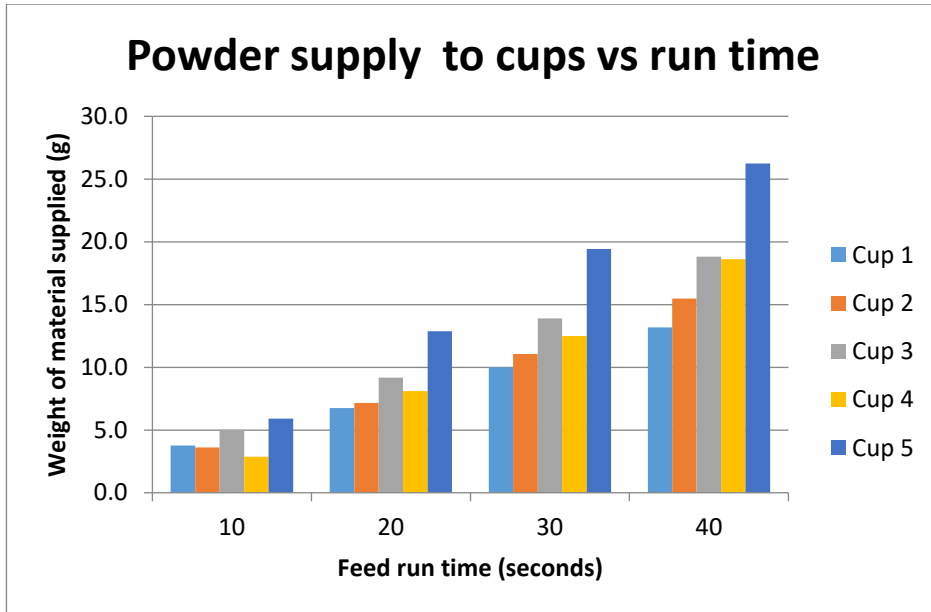


FIGURE 12.16 - NEW TRAY NO HILLS NO BAFFLES TEST RESULTS GRAPH 1

C.14 NEW OUTPUT TRAY – NO HILLS, BAFFLES

TABLE 12.14 - NEW TRAY NO HILLS BAFFLES TEST RESULTS

	Cup 1	Cup 2	Cup 3	Cup 4	Cup 5
10	5.566	1.915	5.515	2.044	6.857
20	11.670	5.247	10.308	5.292	13.246
30	17.116	8.608	14.868	8.976	20.456
40	23.564	12.654	20.155	12.267	27.479

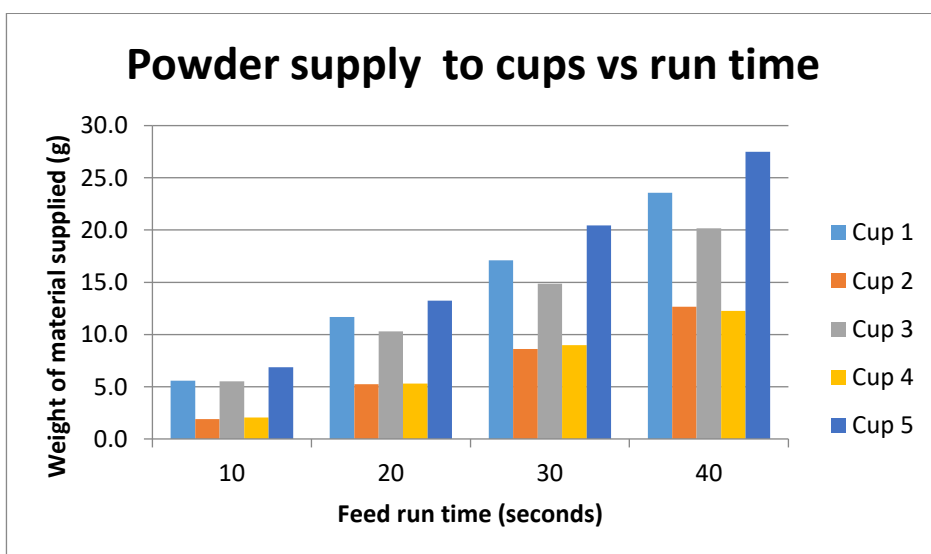


FIGURE 12.17 - NEW TRAY NO HILLS BAFFLES TEST RESULTS GRAPH 1

C.15 NEW OUTPUT TRAY - HILLS, NO BAFFLES

TABLE 12.15 - NEW TRAY HILLS NO BAFFLES TEST RESULTS

	Cup 1	Cup 2	Cup 3	Cup 4	Cup 5
10	4.917	3.206	4.873	2.827	5.797
20	8.734	6.710	9.678	6.393	11.106
30	13.127	11.638	14.665	10.210	18.064
40	16.856	15.863	20.212	14.921	24.602

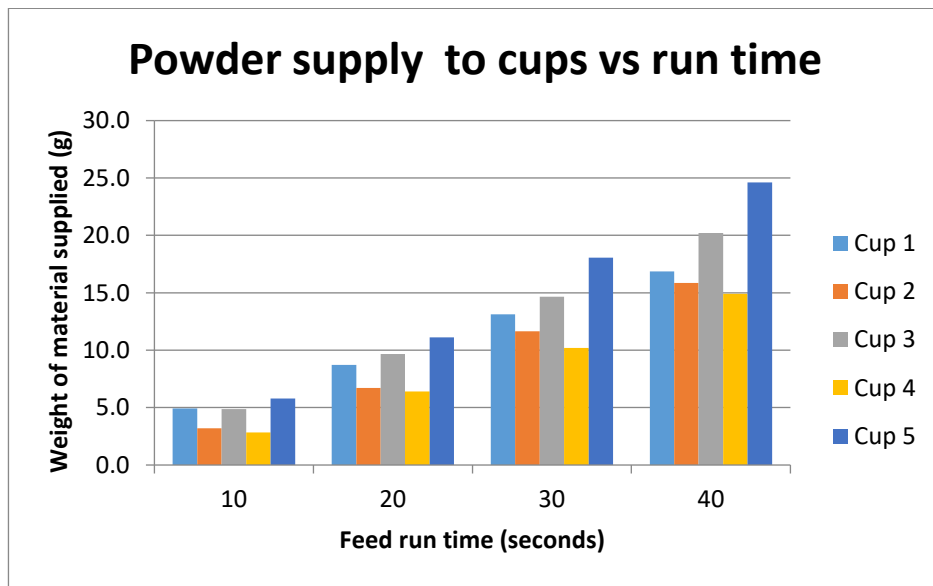


FIGURE 12.18 - NEW TRAY HILLS NO BAFFLES TEST RESULTS GRAPH 1

C.16 NEW OUTPUT TRAY – HILLS, BAFFLES

TABLE 12.16 - NEW TRAY HILLS BAFFLES TEST RESULTS

	Cup 1	Cup 2	Cup 3	Cup 4	Cup 5
10	7.014	2.071	5.931	1.902	6.968
20	12.080	5.403	10.431	4.670	12.983
30	18.270	9.013	15.883	8.667	19.334
40	23.779	13.003	21.004	12.422	25.486

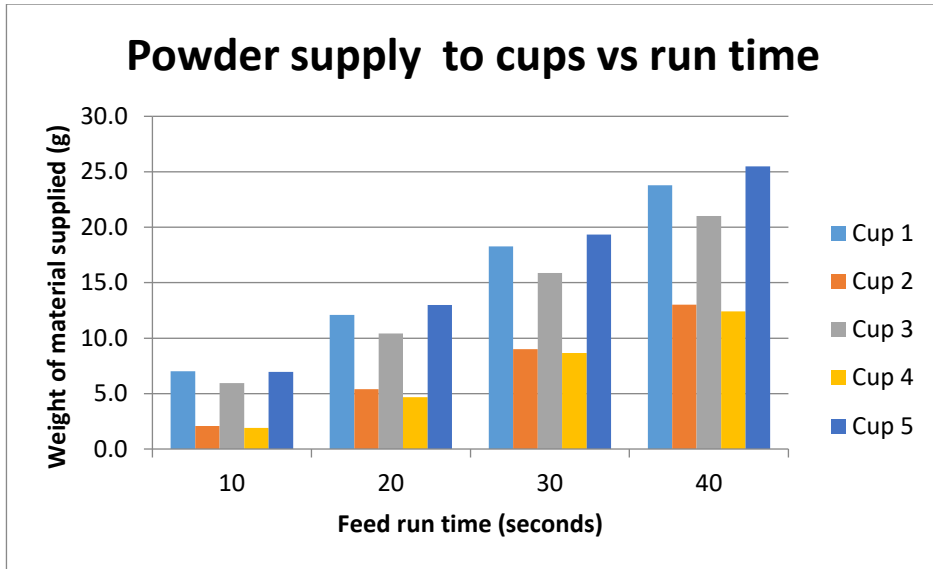


FIGURE 12.19 - NEW TRAY HILLS BAFFLES TEST RESULTS GRAPH 1

C.17 NEW OUTPUT TRAY – TILTED BASE

TABLE 12.17 - RIG TILTED 1 DEGREE TEST RESULTS

	Cup 1	Cup 2	Cup 3	Cup 4	Cup 5
10	6.347	1.939	5.317	1.801	6.373
20	12.363	5.228	9.904	5.011	12.349
30	18.314	9.368	15.439	9.071	18.790
40	25.198	13.214	20.975	12.423	25.606

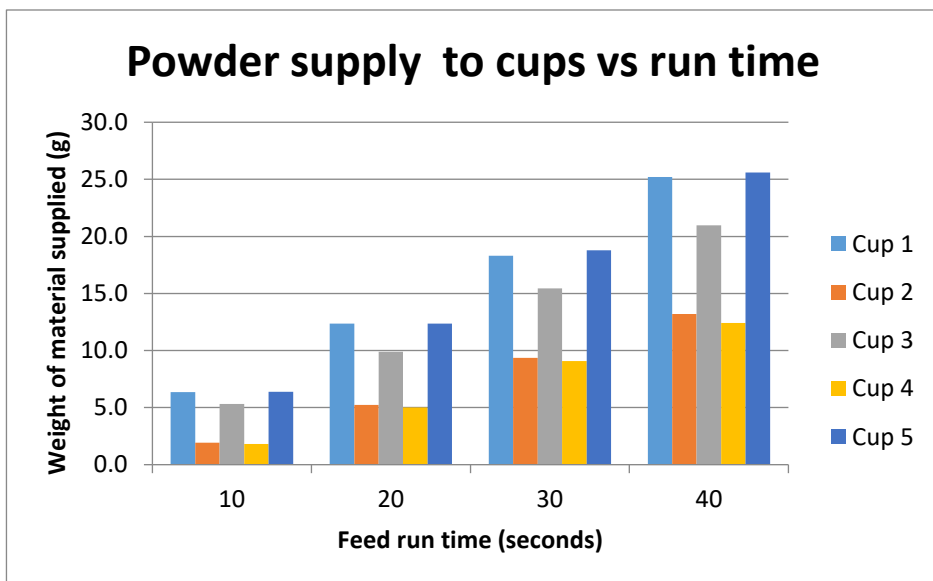


FIGURE 12.20 - RIG TILTED 1 DEGREE TEST RESULTS GRAPH 1

C.18 TALL OUTPUT TRAY BASELINE

TABLE 12.18 - 300MM COLLAR TEST RESULTS

	Cup 1	Cup 2	Cup 3	Cup 4	Cup 5
10	1.428	3.562	3.451	3.313	2.870
20	3.095	8.592	8.671	8.400	6.800
30	5.321	12.971	13.198	12.467	10.697
40	8.626	18.890	19.676	18.381	15.613
50	11.076	22.972	24.084	22.327	19.380

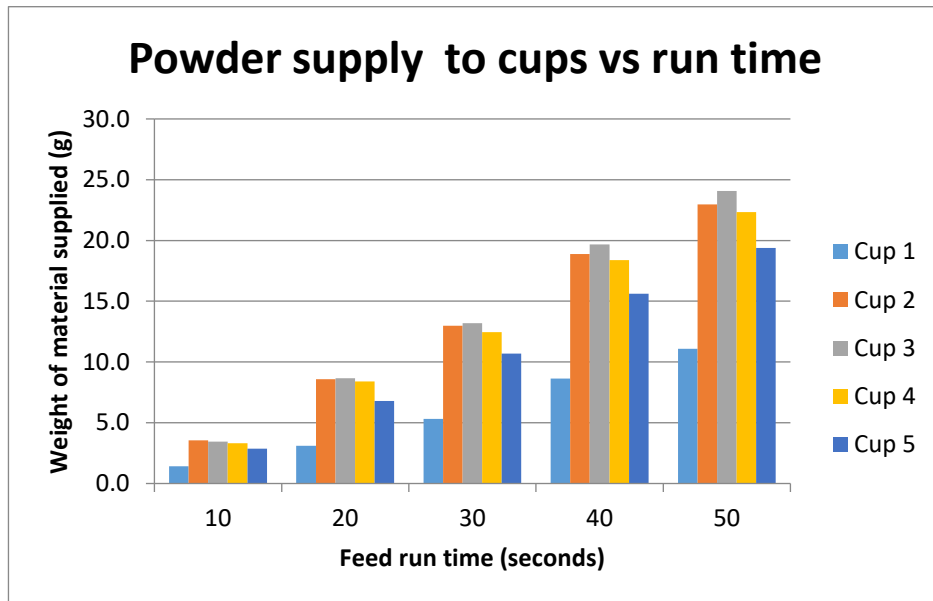


FIGURE 12.21 - 300MM COLLAR TEST RESULTS GRAPH 1

C.19 TALL OUTPUT TRAY FRONT & REAR

TABLE 12.19 - 300MM COLLAR FRONT/REAR TEST RESULTS

	Cup 1	Cup 2	Cup 3	Cup 4	Cup 5
10 front	7.6%	27.4%	23.2%	22.7%	19.1%
10 rear	13.8%	13.9%	28.1%	24.2%	20.1%
30 front	11.3%	25.3%	23.7%	22.5%	17.2%
30 rear	9.4%	24.9%	24.5%	22.3%	19.0%
50 front	14.0%	22.9%	22.5%	21.9%	18.7%
50 rear	8.3%	23.8%	25.0%	22.9%	19.9%
Ave	10.7%	23.0%	24.5%	22.8%	19.0%

C.20 NEW BAFFLE DESIGN

TABLE 12.20 - SECOND BAFFLE DESIGN EXPERIMENT RESULTS

	Cup 1	Cup 2	Cup 3	Cup 4	Cup 5
10	5.688	1.321	6.291	1.282	6.354
20	11.482	4.456	10.619	4.567	13.511
30	16.087	8.126	14.891	7.453	17.859
40	23.227	11.284	18.893	10.986	23.454

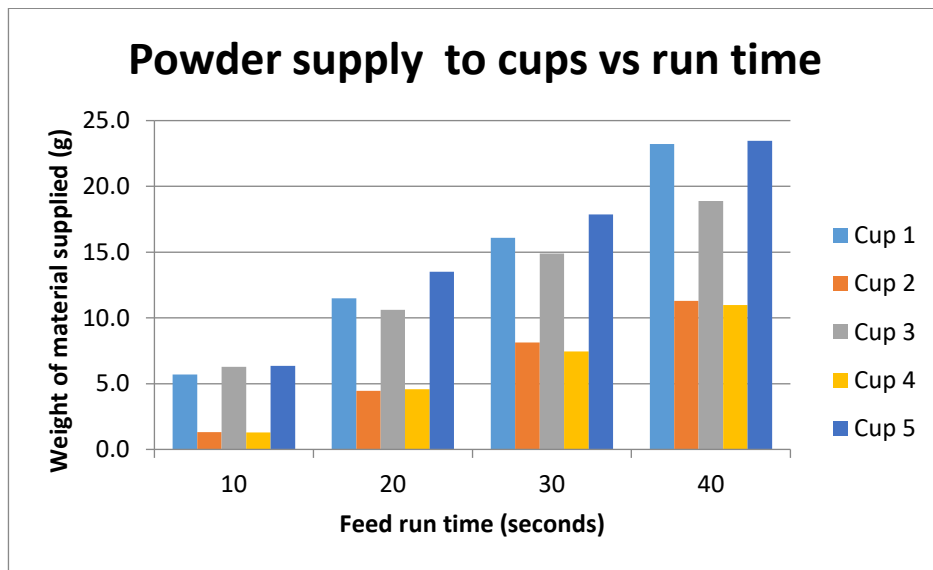


FIGURE 12.22 - SECOND BAFFLE DESIGN TEST RESULTS GRAPH 1

C.21 AUGER 1 ONLY

TABLE 12.21 - AUGER 1 ONLY TEST RESULTS

	Cup 1	Cup 2	Cup 3	Cup 4	Cup 5
10	4.750	2.806	0.286	0.292	0.007
20	8.211	6.327	0.231	0.005	0.011
30	12.290	10.018	0.699	0.008	0.001
40	16.339	13.385	1.275	0.011	0.002

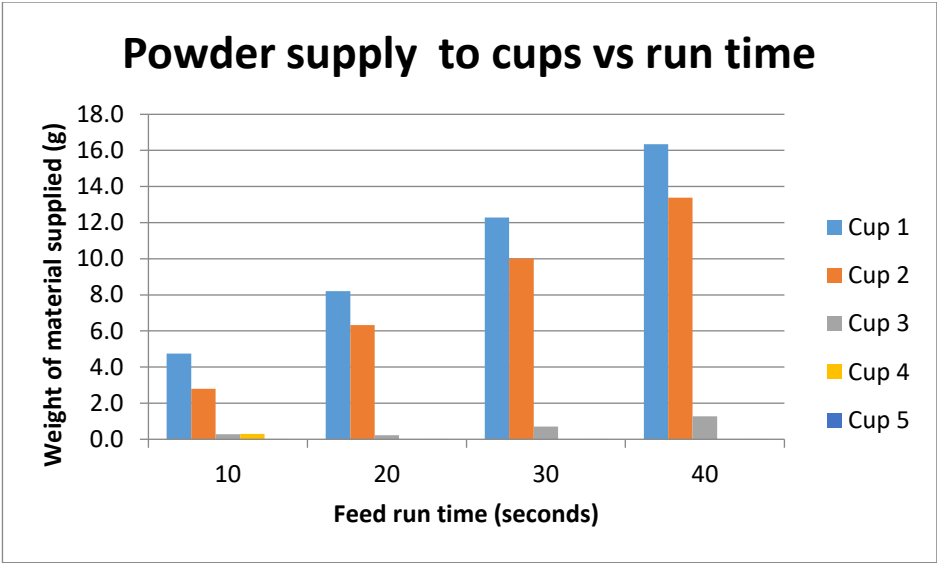


FIGURE 12.23 - AUGER 1 ONLY TEST RESULTS GRAPH 1

C.22 AUGER 2 ONLY

TABLE 12.22 - AUGER 2 ONLY TEST RESULTS

	Cup 1	Cup 2	Cup 3	Cup 4	Cup 5
10	0.005	0.863	5.481	2.791	0.086
20	0.000	1.438	8.929	4.642	-0.002
30	0.012	2.436	13.250	7.954	0.164
40	0.024	3.792	16.082	11.327	0.785

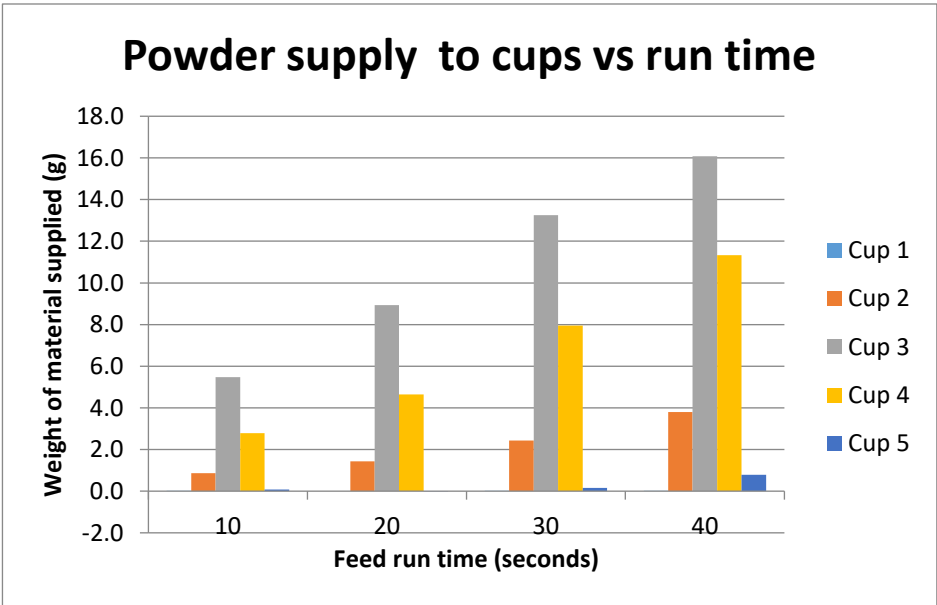


FIGURE 12.24 - AUGER 2 ONLY TEST RESULTS GRAPH 1

C.23 AUGER 3 ONLY

TABLE 12.23 - AUGER 3 ONLY TEST RESULTS

	Cup 1	Cup 2	Cup 3	Cup 4	Cup 5
10	0.003	0.081	0.139	1.998	3.315
20	0.005	0.041	0.070	3.915	9.702
30	0.032	0.081	0.277	5.907	15.867
40	0.010	0.025	0.086	8.259	21.689

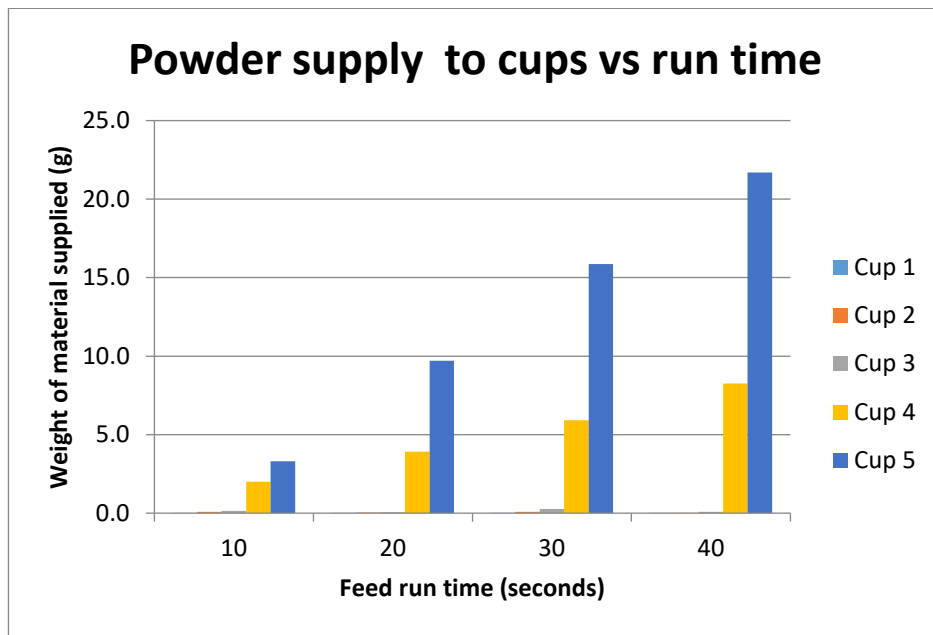


FIGURE 12.25 - AUGER 3 ONLY TEST RESULTS GRAPH 1

C.24 AUGER 3 OPPOSITE DIRECTION

TABLE 12.24 - AUGER 3 ANTI-CLOCKWISE TEST RESULTS

	Cup 1	Cup 2	Cup 3	Cup 4	Cup 5
10	4.290	3.313	4.524	5.117	4.707
20	7.684	7.429	10.954	10.314	10.508
30	10.751	11.149	14.975	15.422	14.378
40	14.391	15.692	20.754	21.226	20.023

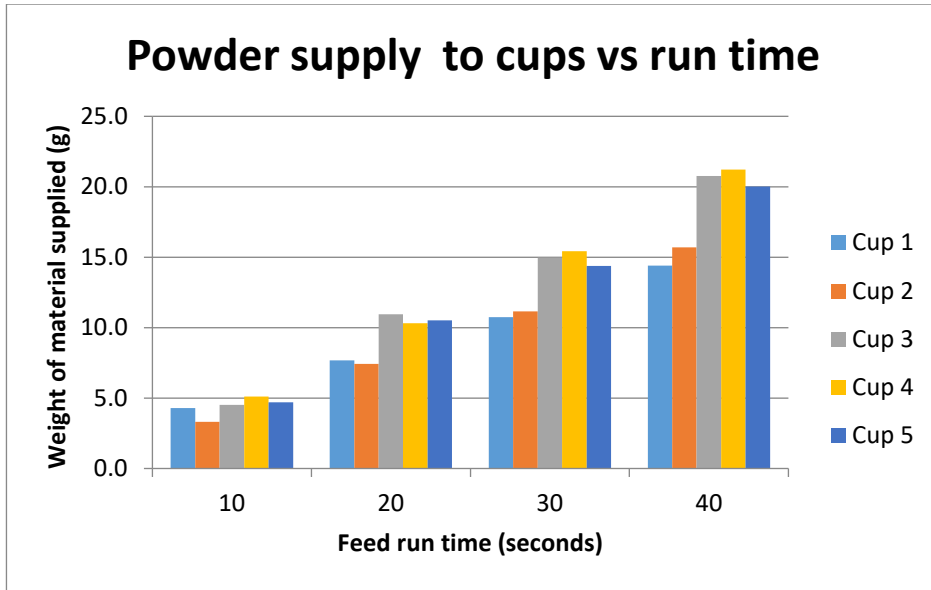


FIGURE 12.26 - AUGER 3 ANTI-CLOCKWISE TEST RESULTS GRAPH 1

C.25 GRID BAFFLE NO PLUGS

TABLE 12.25 - GRID BAFFLE NO PLUGS TEST RESULTS

	Cup 1	Cup 2	Cup 3	Cup 4	Cup 5
10	5.559	3.620	4.770	3.663	4.469
20	7.686	6.239	7.525	6.651	10.674
30	13.804	10.622	12.229	10.936	15.530
40	16.199	12.525	14.690	13.209	18.991

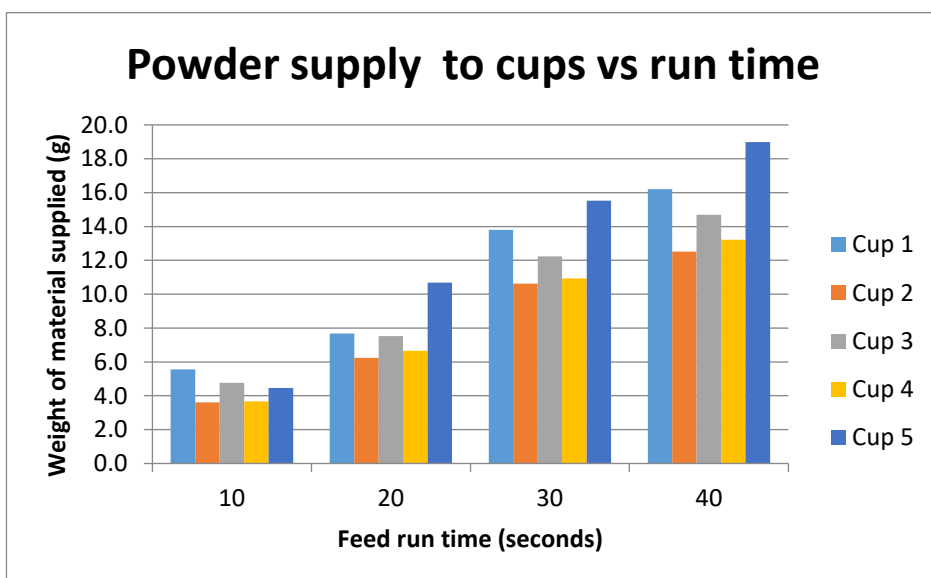


FIGURE 12.27 - GRID BAFFLE NO PLUGS TEST RESULTS GRAPH 1

C.26 GRID BAFFLE A

TABLE 12.26 - GRID BAFFLE PLUG ARRANGEMENT A TEST RESULTS

	Cup 1	Cup 2	Cup 3	Cup 4	Cup 5
10	5.497	4.644	4.928	5.452	4.590
20	8.684	7.083	6.095	8.357	8.387
30	12.157	11.189	10.878	12.063	11.073
40	16.292	14.388	12.280	13.602	13.068

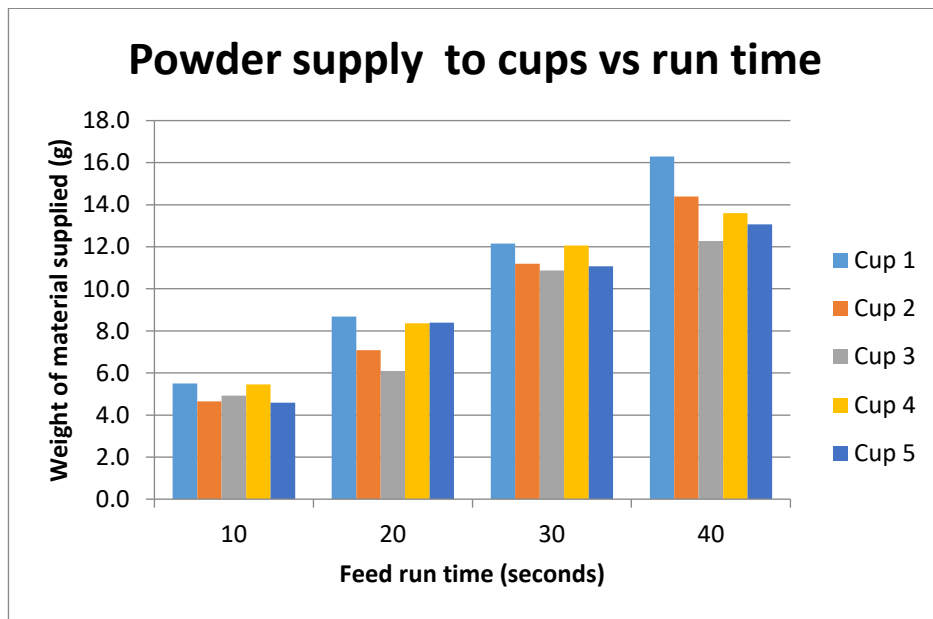


FIGURE 12.28 - GRID BAFFLE PLUG ARRANGEMENT A TEST RESULTS GRAPH 1

C.27 GRID BAFFLE B

TABLE 12.27 - GRID BAFFLE PLUG ARRANGEMENT B TEST RESULTS

	Cup 1	Cup 2	Cup 3	Cup 4	Cup 5
10	5.787	4.251	5.470	5.213	4.912
20	9.393	7.780	8.816	9.273	9.225
30	13.476	12.192	13.607	14.194	13.665
40	18.301	16.643	17.978	18.832	18.305

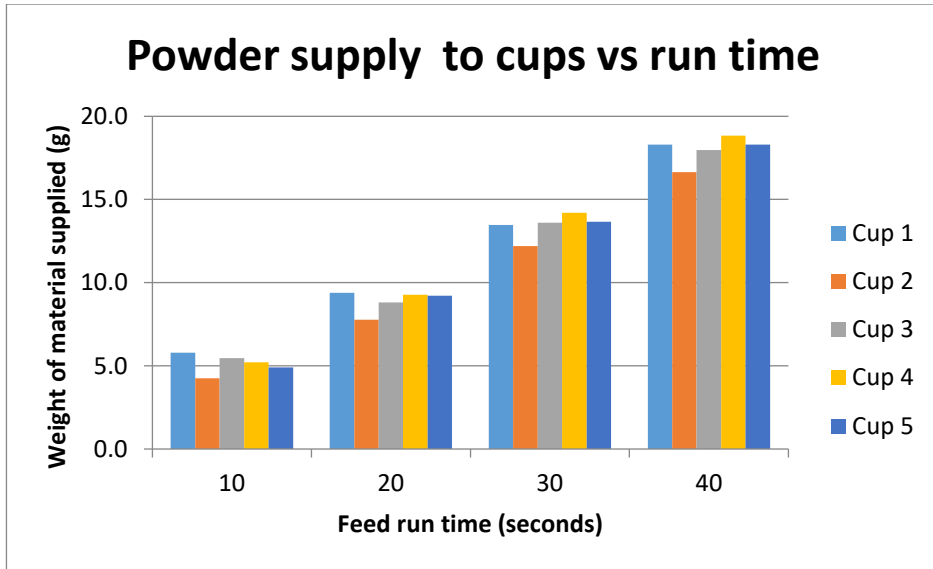


FIGURE 12.29 - GRID BAFFLE PLUG ARRANGEMENT B TEST RESULTS GRAPH 1

C.28 GRID BAFFLE C

TABLE 12.28 - GRID BAFFLE PLUG ARRANGEMENT C TEST RESULTS

	Cup 1	Cup 2	Cup 3	Cup 4	Cup 5
10	5.224	4.756	5.058	5.691	5.422
20	8.892	7.729	8.565	9.073	8.893
30	12.513	12.311	13.129	13.781	13.729
40	17.643	16.787	17.411	18.083	17.477

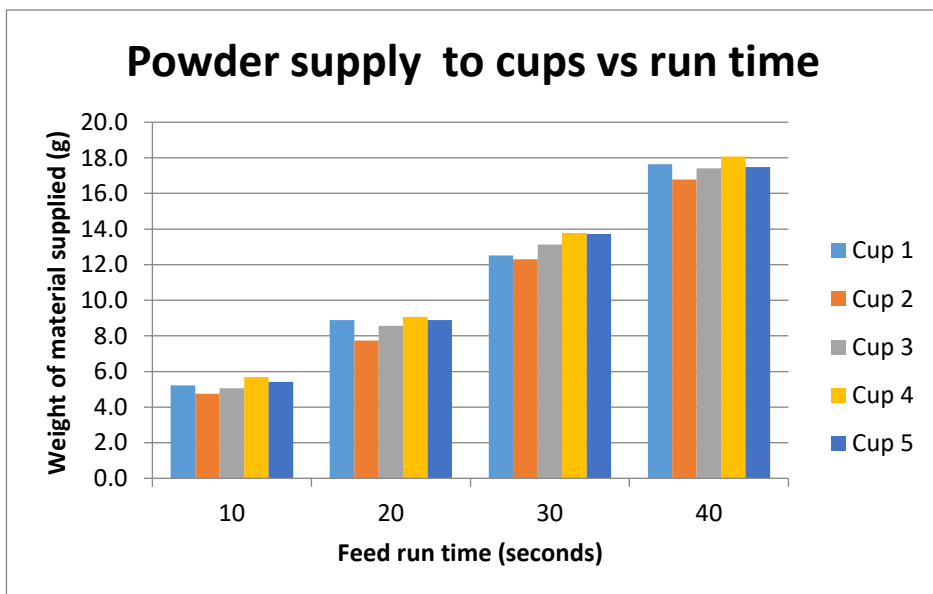


FIGURE 12.30 - GRID BAFFLE PLUG ARRANGEMENT C TEST RESULTS GRAPH 1

D POWER DISTRIBUTION SYSTEM IMAGES



FIGURE 12.31 - POWER DISTRIBUTION CABINET INPUT SIDE (LEFT)



FIGURE 12.32 - POWER DISTRIBUTION CABINET OUTPUT SIDE (RIGHT)

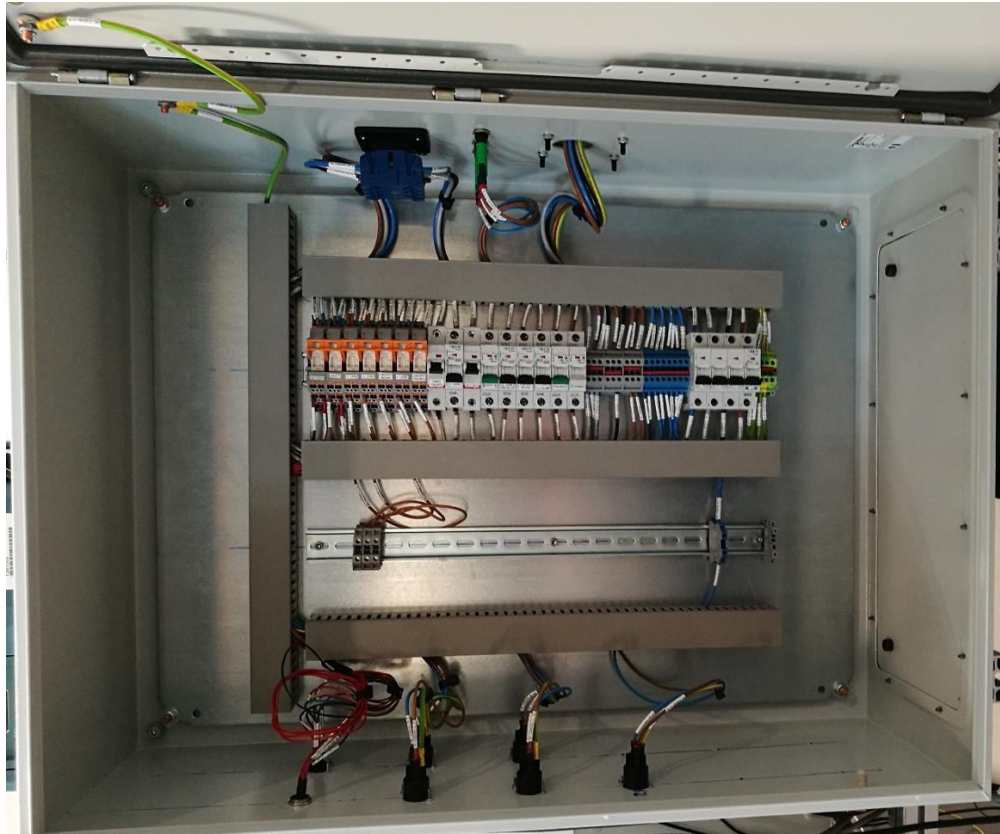


FIGURE 12.33 - POWER DISTRIBUTION CABINET INTERIOR

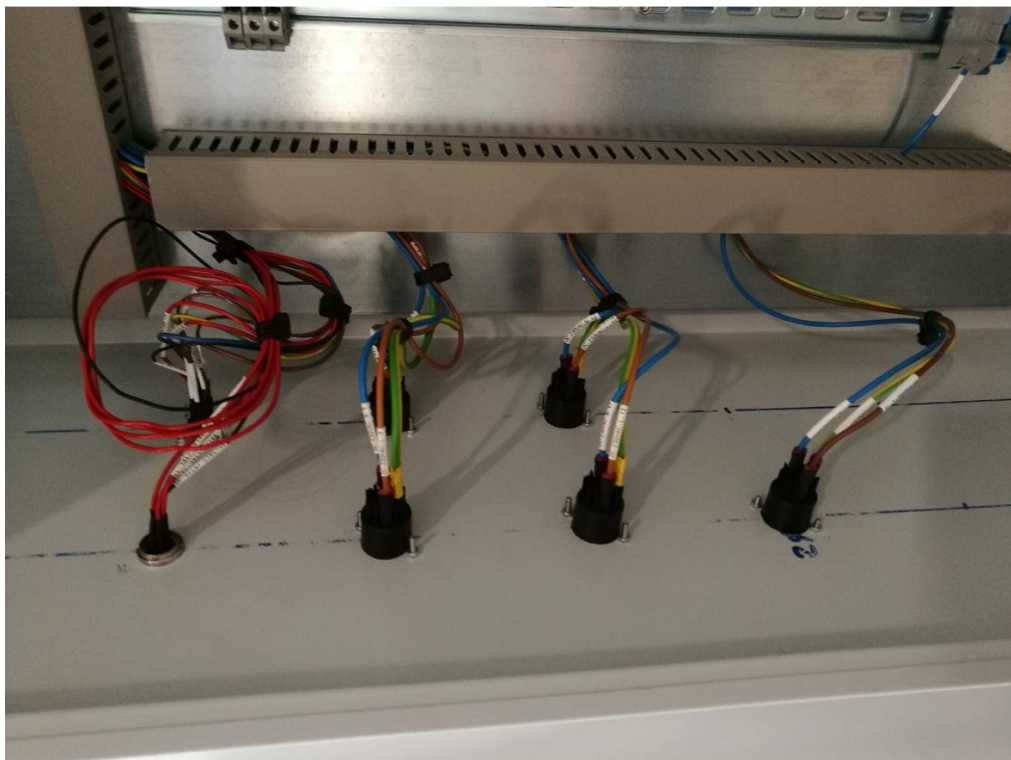


FIGURE 12.34 - POWER DISTRIBUTION CABINET OUTPUT WIRING

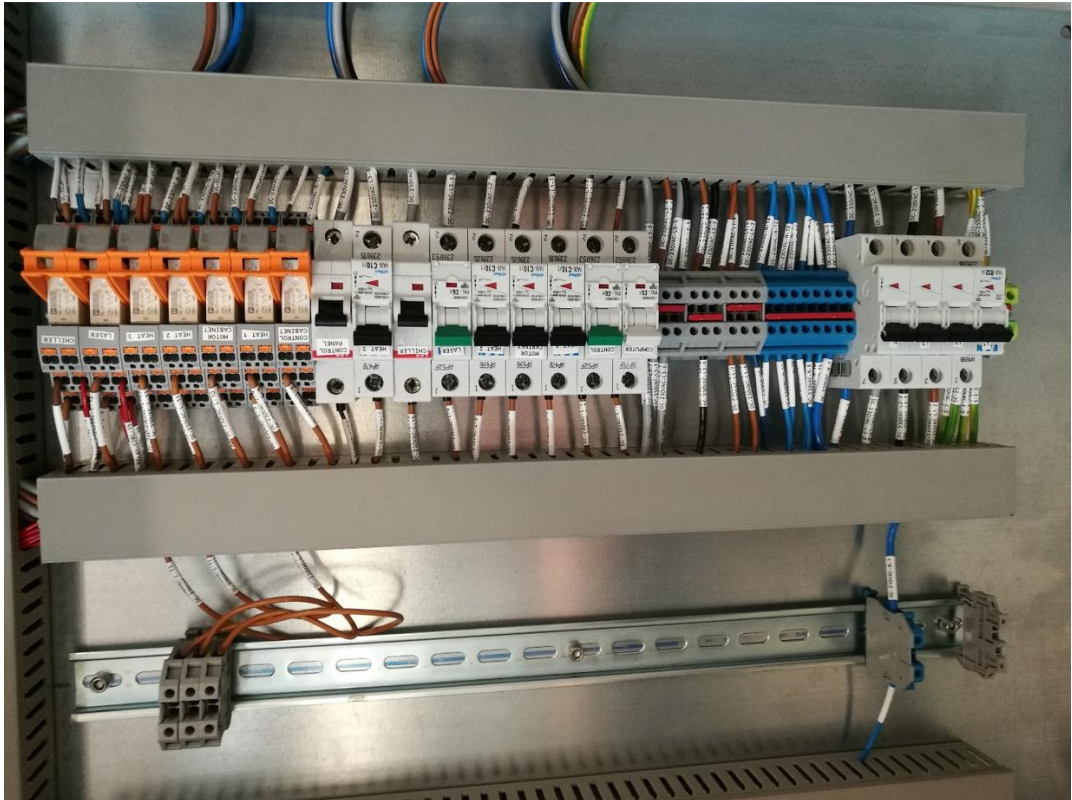


FIGURE 12.35 - POWER DISTRIBUTION CABINET CIRCUIT BREAKER AND RELAY WIRING

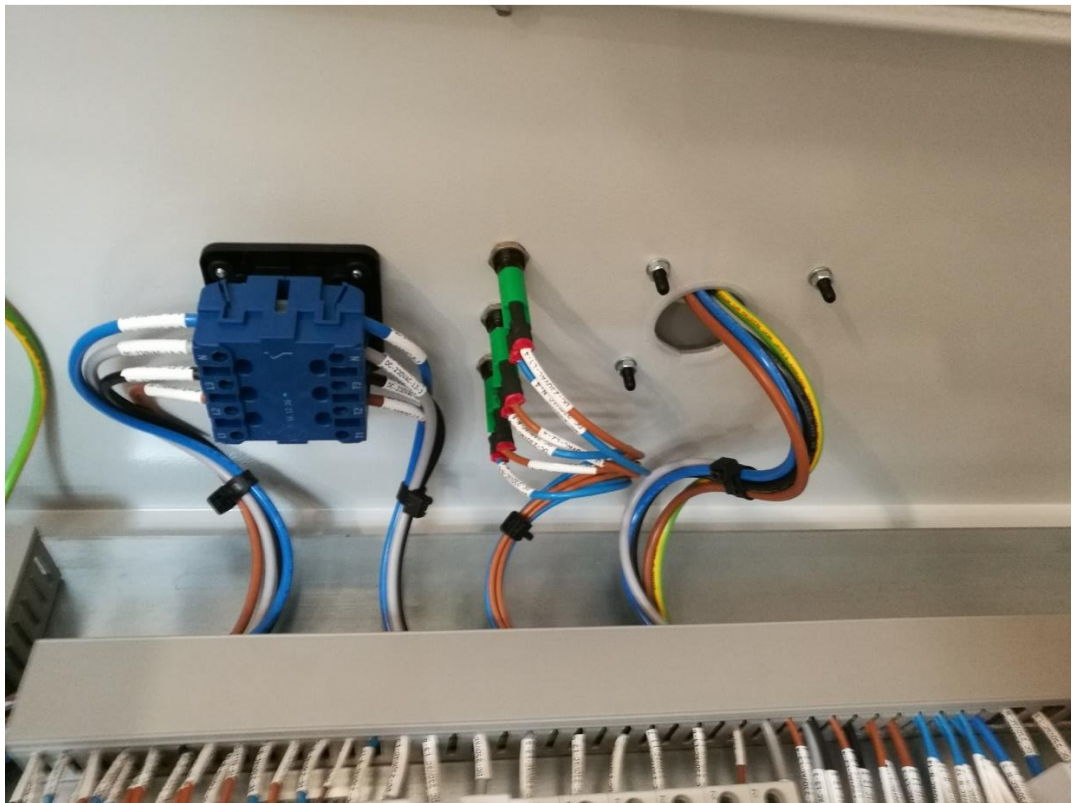


FIGURE 12.36 - POWER DISTRIBUTION CABINET INPUT WIRING



FIGURE 12.37 - CONTROL PANEL DOOR INTERIOR



FIGURE 12.38 - CONTROL PANEL DOOR EXTERIOR

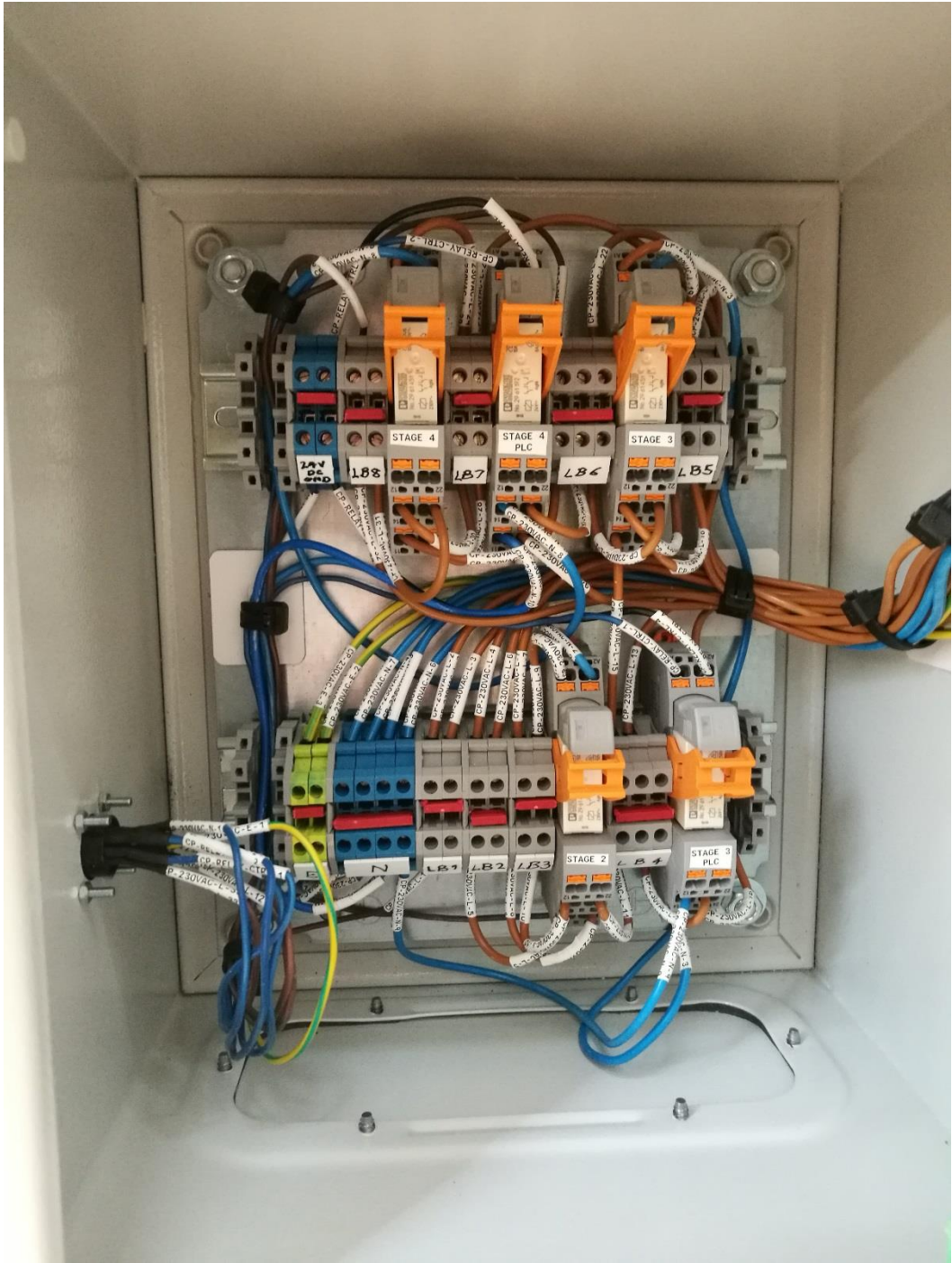


FIGURE 12.39 - CONTROL PANEL INTERIOR WIRING

13 REFERENCES

- Autonomous Manufacturing Ltd. (2019, January 28). Retrieved from amfg.ai:
<https://amfg.ai/2017/08/14/two-fundamental-types-sls-material/>
- Bourell, D. L., Watt, T. J., Leigh, D. K., & Fulcher, B. (2014). Performance Limitations in Polymer Laser Sintering. *Physics Procedia*, 147-156.
- Conner Seepersad, C., Govett, T., Kim, K., Lundin, M., & Pinero, D. (2012). A designer's guide for dimensioning and tolerancing SLS parts. *23rd Annual International Solid Freeform Fabrication Symposium* (pp. 921-931). Austin: Univeristy of Texas.
- Crawford, R. J., & Kearns, M. P. (2012). *Practical Guide to Rotational Moulding*. Shrewsbury: Smithers Rapra Technology Ltd.
- CRDM. (2019, 3 18). Retrieved from crdm.co.uk: <http://crdm.co.uk/pdf/LS-PA12.pdf>
- Espalin, D., Muse, D. W., MacDonald, E., & Wicker, R. B. (2014). 3D Printing multifunctionality: structures with electronics. *Int. J. Advanced Manufacturing Technology*, 963-978.
- Fitchett Jr, D. (2017, November 8). *Quora*. Retrieved from <https://www.quora.com/Is-the-Allen-Bradley-SLC500-PLC-worth-buying-in-2017>
- Folgado, R., Peças, P., & Henriques, E. (2010). Life cycle cost for technology selection: A Case study in the manufacturing of injection moulds. *Int. J. Production Economics*, 368-378.
- Formlabs. (2019, 4 8). *Guide to Manufacturing Processes for Plastics*. Retrieved from formlabs.com: <https://formlabs.com/blog/guide-to-manufacturing-processes-for-plastics/>
- Goodridge, R., Tuck, C., & Hague, R. (2012). Laser sintering of polyamides and other polymers. *Progress in Materials Science*, 57(2), 229-267.

- Grand View Research. (2019, January 24). Retrieved from grandviewresearch.com:
<https://www.grandviewresearch.com/press-release/global-injection-molded-plastics-market>
- Hager, I., Golonka, A., & Putanowicz, R. (2016). 3D printing of buildings and building components as the future of sustainable construction? *International Conference on Ecology and new Building materials and products* (pp. 31-155). Cracow: Procedia Engineering.
- Hardy, C. (2014, April 9). *The Basics of Tuning PID Loops*. Retrieved from Cross Co.:
<https://www.crossco.com/blog/basics-tuning-pid-loops>
- Hu, D., & Kovacevic, R. (2003). Sensing, modeling and control for laser-based additive manufacturing. *International Journal of Machine Tools and Manufacture*, 51-60.
- Industrial Heating Equipment Association. (2019, February 5). Retrieved from pro-therm.com: https://pro-therm.com/infrared_basics.php
- Integra. (2019, 3 18). Retrieved from integra-support.com: http://www.integra-support.com/docs/MultiZone_flyer_web.pdf
- Kress, C. (2015). *An experimental and theoretical analysis of additive manufacturing and injection moulding*. Toledo: The University of Toledo.
- Nan, W., & Ghadiri, M. (2019). Numerical simulation of powder flow during spreading in additive manufacturing. *Powder Technology*, 801-807.
- O'Brien, M. (2012, August). Retrieved from analog.com:
<https://www.analog.com/media/en/analog-dialogue/volume-46/number-3/articles/designing-robust-isolated-rs-232-data-interfaces.pdf>
- Petrick, I. J., & Simpson, T. W. (2015). 3D Printing Disrupts Manufacturing: How Economies of One Create New Rules of Competition. *Research-Technology Management*, 56(6), 12-16.

- Pham, D. T., Dotchev, K. D., & Yusoff, W. A. (2008). Deterioration of polyamide powder properties in the laser sintering process. *Proceedings of the Institution of Mechanical Engineers, Part C: Journal of Mechanical Engineering Science*. 222(11), pp. 2163-2176. Cardiff: Institution of Mechanical Engineers.
- Psarommatis Giannakopoulos, F. (2016). *Development of a Powder Management Mechanism for an SLS/SLM Machine*. (Masters Thesis). Athens: National Technical University of Athens.
- Puravent. (2019, 3 18). *puravent.co.uk*. Retrieved from <https://www.puravent.co.uk/blog/radiant-heaters/radiant-heating/>
- Qualman, D. (2019, April 4). *Global Plastics Production, 1917 to 2050*. Retrieved from [darrinqualman.com: https://www.darrinqualman.com/global-plastics-production/](https://www.darrinqualman.com/global-plastics-production/)
- Rockwell Automation. (2008, June). Retrieved from [literature.rockwellautomation.com: https://literature.rockwellautomation.com/idc/groups/literature/documents/um/1747-um011_-en-p.pdf](https://literature.rockwellautomation.com/idc/groups/literature/documents/um/1747-um011_-en-p.pdf)
- Schmid, M., Amado, A., & Wegener, K. (2015). *Polymer Powders for Selective Laser Sintering (SLS)*. AIP. AIC Publishing LLC.
- Science History Institute. (2019, April 4). *The History and Future of Plastics*. Retrieved from [sciencehistory.org: https://www.sciencehistory.org/the-history-and-future-of-plastics](https://www.sciencehistory.org/the-history-and-future-of-plastics)
- Sigma-Aldrich. (2019, January 24). Retrieved from [sigmaaldrich.com: https://www.sigmaaldrich.com/catalog/product/aldrich/gf33201098?lang=en®ion=GB](https://www.sigmaaldrich.com/catalog/product/aldrich/gf33201098?lang=en®ion=GB)
- SME. (2019, January 24). Retrieved from [energy.gov: https://www.energy.gov/sites/prod/files/2014/01/f6/sme_man_engineering.pdf](https://www.energy.gov/sites/prod/files/2014/01/f6/sme_man_engineering.pdf)

- Statum, R. (2016). Experimental Determination Of Uniform Heating In The Selective Laser Sintering Part Bed. *Proceedings of the National Conference On Undergraduate Research* (pp. 1678-1686). Asheville, North Carolina: The University of North Carolina, Asheville.
- Turner, B. N., & Gold, S. A. (2015). A review of melt extrusion additive manufacturing processes: II. Materials, dimensional accuracy, and surface roughness. *Rapid Prototyping Journal*, 21(3), 250-261.
- V.Wong, K., & Hernandez, A. (2012). A review of additive manufacturing. *ISRN Mechanical Engineering*, 2012(1).
- Vasquez, M., Haworth, B., & Hopkinson, B. (2011). Optimum Sintering Region for Laser Sintered Nylon-12. *Proceedings of the Institution of Mechanical Engineers, Part B: Journal of Engineering Manufacture*. 225(12), pp. 2240-2248. Sage Publications Ltd on behalf of the Institution of Mechanical Engineers.
- Walker Wroe, W., Gladstone, J., Phillips, T., Fish, S., Beaman, J., & McElroy, A. (2016). In-situ thermal image correlation with mechanical properties of nylon-12 in SLS. *Rapid Prototyping Journal*, 22(5), 794-800.
- Weller, C., Kleer, R., & Piller, F. T. (2015). Economic implications of 3D printing: Market structure models in light of additive manufacturing revisited. *Int. J. Production Economics*, 164(1), 43-56.
- Yang, S., & Evans, J. (2007). Metering and dispensing of powder; the quest for new solid freeforming techniques. *Powder Technology*, 178(1), 56-72.
- Zarringhalam, H. (2007). *Investigation into Crystallinity and Degree of Particle Melt in Selective Laser Sintering*. (Doctoral Thesis). Loughborough: Loughborough University.
- 许小曙. (2010). *China Patent No. CN102335741A*.